injection gas, and produces a gasifier product gas predicted by the kinetic and contacting relationships. In addition to the gas feed streams just mentioned, another gas stream may be fed at a specified height above the bottom of the bed. A final optional feed stream slot is available for the gasifier product gas calculated by the gas-phase equilibrium model block, allowing the product streams predicted by the two different methods to be compared.

The reactor model convergence routine is set up to calculate the value of any one of the following variables, with the others held constant:

- carbon conversion
- bed height
- bed diameter (or superficial velocity)
- coal rate

Thus, this fourth model block can be used to calculate the gasifier bed size (height and/or diameter) in the same computer run with the material and energy balance. Alternatively, the reactor model block will allow calculation of the predicted material and energy balance (carbon conversion or coal rate) for a given reactor size.

Initial validation runs for the overall model showed considerable savings in computer charges. For example, a run using the new tools to model a commercial gasifier with an integral steam reformer for heat input cost only half as much as the same case modeled using the old methods. In addition, the energy balance model block saved considerable engineering effort by eliminating development of a complex network of COPE computer operations to perform energy balance calculations for each different CCG case. The hand calculations previously required to complete the solids enthalpy balance were also eliminated.

This improved CCG reactor system material and energy balance model was used extensively in the laboratory guidance and process definition studies under the program. These included gasifier heat input studies and process variable screening studies. It is expected that the model will eventually need to be updated to some extent to reflect data from PDU operations and results from other laboratory and engineering studies.

5.3 Engineering Technology Studies

As part of the CCG Process Development Program, a coordinated set of engineering technology programs were conducted to develop fundamental process and equipment technology to support the overall laboratory and engineering process development effort. The work on these programs is described below.

5.3.1 Evaluation of Construction Materials for Catalytic Coal Gasification

The overall objective of this engineering technology program was to assemble a data base on materials performance for those plant sections which have materials considerations unique to catalytic coal gasification. A five-part in-situ materials testing/corrosion monitoring program was devised for the CCG PDU to identify problem areas and to assemble a data base for selecting materials for CCG process equipment. The program consisted of corrosion racks, corrosion probes, stream sampling, non-destructive testing inspection, and component examination. In a separate effort, materials screening tests in alkali-containing gasifier environments were instituted cooperatively with the Bureau of Mines. These separately-funded bench-scale tests were conducted at the Bureau of Mines Tuscaloosa Metallurgy Research Center.

Construction materials for the CCG Commercial Plant Study Design were specified conservatively, based heavily on limited materials data from earlier work on thermal gasification processes. Accordingly, materials test and development work was required for equipment exposed to conditions specific to the CCG process. These included equipment items in the gasification, raw gas heat exchange, wet scrubbing, sour water, char handling, and catalyst recovery systems. Potential materials problems identified in these areas were high temperature sulfidation, chloride and caustic stress corrosion cracking, sour water corrosion, and erosion in gas/solid and liquid/slurry services.

Materials Evaluation Program for the PDU

The major objective of the PDU materials evaluation program was to assemble a data base for design and scale-up of CCG equipment, with emphasis on hostile process environments. Specific objectives are listed below:

(1) Determine corrosion/erosion behavior of selected metals in the PDU via corrosion racks, corrosion probes, and non-destructive testing (NDT) inspection. Also evaluate chemical and erosion resistance of refractory specimens in the gasifier.

(2) Evaluate chloride and/or caustic induced stress corrosion cracking by means of U-bend specimens in the char digester.

(3) Relate process conditions to corrosion phenomena by chemical analyses of stream samples.

(4) Determine corrosion/failure mechanisms from analysis of failed equipment components. In addition, perform systematic metallurgical examination of critical working components to assess in-service deterioration.

An extensive program for materials evaluation in the PDU was developed. This program consisted of five interrelated elements:

- Corrosion racks
- Corrosion probes
- Stream sampling
- NDT inspection
- Component examination

Table 5.3-1 summarizes the five activities. Results for each activity are discussed individually below.

Corrosion Racks

Corrosion racks are devices on which small metal specimens (coupons) are assembled and secured for in-situ exposure inside operating equipment. Their purpose is to yield time-averaged corrosion rates based on weight loss measurements. The racks were designed, fabricated and assembled by the ER&E Corrosion Laboratory at Florham Park, New Jersey, which was responsible for pre- and post-exposure evaluations of specimens. All the racks were mounted on blind flanges (nozzles) or pipe plugs (couplings).

The locations of corrosion racks are indicated in Figure 5.3-1, a schematic process diagram of the PDU. Note that some of the test sites (TS) contain corrosion test devices other than racks. Only eight are active corrosion rack sites, as itemized in Table 5.3-2. Test Site 8 could not be fitted with a corrosion rack because of space limitations during stirrer operation, and was therefore abandoned. Nominal chemical compositions of test materials are shown in Table 5.3-3.

Results from the two exposure periods (Series I and Series II) are tabulated in Table 5.3-4. The corrosion rate of ordinary 18-8 stainless steel (304 SS) is over 30 mils/year at TS-1 but only about 7 mpy at TS-2. This lack of agreement cannot be explained on the basis of different environments since both racks are symmetrically installed at the same elevation. It may possibly be related to the geometry of the test coupons, since the disc shaped specimens at TS-1 are more prone to turbulence effects than the flush cylinder specimens at TS-2. Consequently, erosion may have played a part in the higher wastage rates measured at TS-2. Interestingly, the situation is reversed for HK-40 which appears to corrode faster at TS-2. This suggests that differences between TS-1 and TS-2 may not be real, but merely indicative of experimental error.

Corrosion rates for the sour water system Test Sites 4, 6 and 7 are low and are remarkably similar for both exposure periods. Of significance are the high corrosion rates observed on carbon steel (68.3 mpy) and 410 stainless steel (14.4 mpy) U-bends in the Char Digester. Visual examination showed generalized pitting on carbon steel, and localized pitting on 410 stainless steel. No cracking was observed in either case.

Table 5.3-1

PDU MATERIALS EVALUATION PROGRAM

Activity	Description	Purpose	Current Scope
Corrosion Racks	In-situ corrosion tests employing weight loss coupons and U-bend specimens	Determine average corrosion rates and stress corrosion cracking susceptibility	6 rack sites (9 racks); 15 test materials; 4 exposure cycles
Corrosion Probes	On-line corrosion monitoring employing electric resistance probes	Detect fluctuations in corrosion rate and supplement data base from racks	1 probe site
Stream Analysis	Quantitative chemical analysis of aggressive species in process streams	Relate corrosion/erosion experience to corrosive substances in environment	8 sampling points; liquids, gases, solids; H_2S, Cl, K, pH
NDT Inspection	Systematic program for measuring wall thickness of pressure equipment by non-destructive techniques	Monitor metal loss at critical locations and validate corrosion/erosion data from racks and probes	30-40 NDE points; supplemental visual inspection
Component Examination	Laboratory examination of failed or deteriorated equipment components	Determine cause and mode of attack or failure and establish materials related factors	Metallography; mechanical testing; chemical analysis

Figure 5.3-

PDU CORROSION TEST SITES

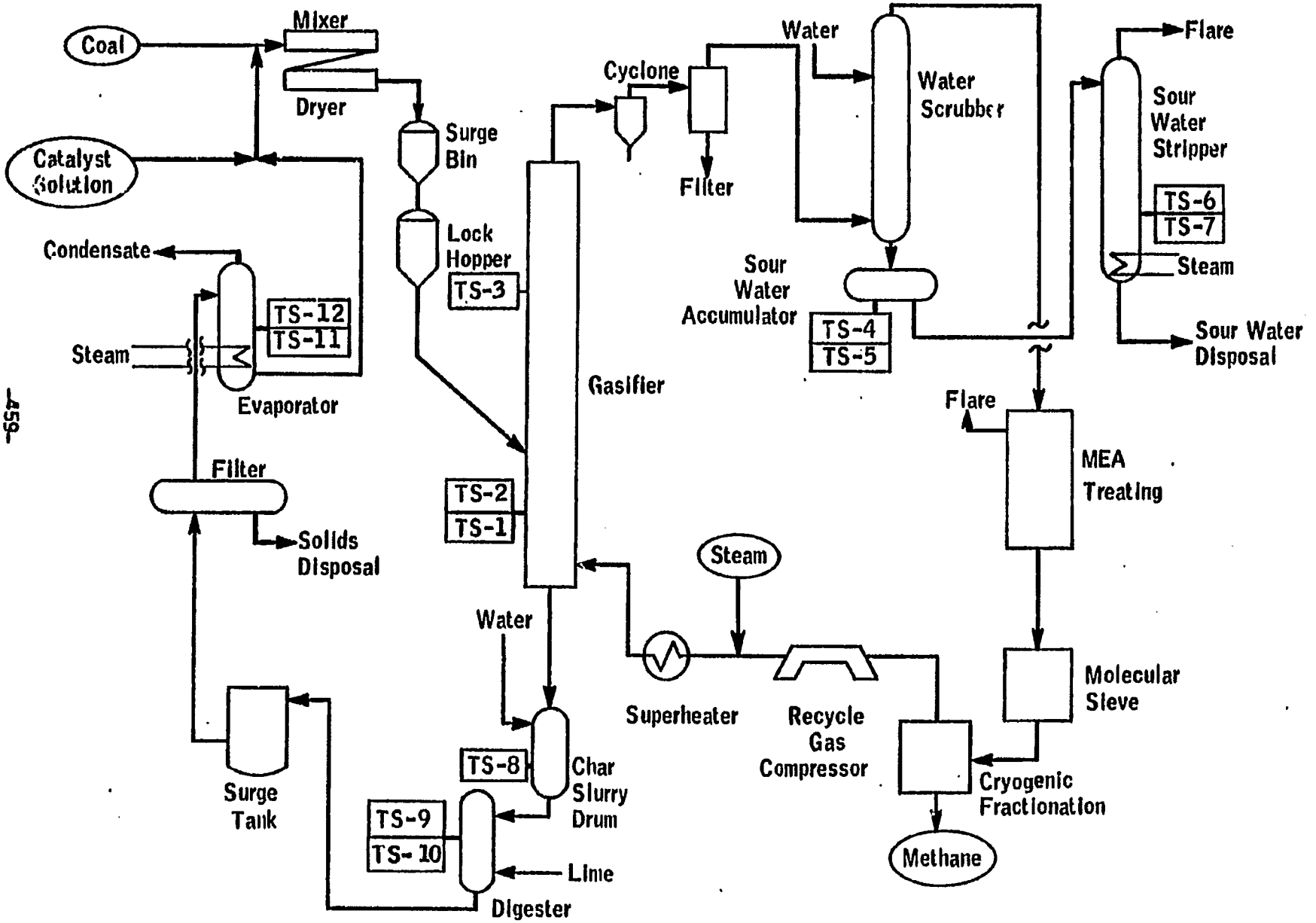

Table 5.3-2

CATALYTIC COAL GASIFICATION PDU
CORROSION RACKS AND PROBES -- SERIES I

Test Site	Equipment Item	Location	Type of Device	Specimen Type	Test Materials(1)
1	Gasifier (5' Level)	Dense phase	Rack	Refractory cylinders(3)	Kaiser Lo-Erode(2),(3)
2	Gasifier (5' Level)	Dense phase	Rack	Metal discs	HK-40, 304 SS, 309 SS
3	Gasifier (55' Level)	Dense/ dilute phase	Rack	Metal discs(3)	HK-40, 310 SS, 304 SS, 309 SS, 304 SS Alonized(3)
4	Sour water accumulator	Liquid	Rack	Metal discs	CS, 304 SS, 316 SS, Carpenter 20Cb3, Ti, Monel 400
5	Sour water accumulator	Liquid	Probe(4)	Wire element	CS
6	Sour water stripper	Packing	Rack	Metal discs	304 SS, 316 SS, CS
7	Sour water stripper	Packing	Rack	Metal discs	Carpenter 20Cb3, Monel 400, Ti
8(5)	Char slurry drum	Liquid	Rack	Metal discs	CS, 316 SS, Inconel 625
9	Char digestor	Liquid	Rack	Metal U-bends	CS, 316 SS, Monel 400, Inconel 600, Allegheny Ludlum 29-4
10	Char digestor	Liquid	Probe(4)	Wire element	CS
11	Evaporator	Liquid	Rack	Metal U-bends	CS, 316 SS, 410 SS, Monel 400, Inconel 600, E-Brite 26-1
12	Evaporator	Liquid	Steam coil	Metal tubing	Inconel 600, E-Brite 26-1

Notes:

(1) Abbreviations: CS - carbon steel; SS - stainless-steel.

(2) Kaiser Lo-Erode specimens, with and without 304 SS fiber reinforcement.

(3) During Series I, the racks for TS-1 and TS-3 were inadvertently interchanged, so that the metal specimens were exposed at TS-1 and the refractory specimens at TS-3.

(4) Non-retractable electric resistance probe

(5) Test Site 8 could not be used due to space limitations.

Table 5.3-3

NOMINAL CHEMICAL COMPOSITION PDU CORROSION TEST MATERIALS

Alloy Designation	Manufacturer	Major Elements, %				
		Fe	Cr	Ni	Mo	Cu
410 Stainless Steel	Many	Bal.	12	-	-	-
304 Stainless Steel	Many	Bal.	19	9	-	-
309 Stainless Steel	Many	Bal.	23	14	-	-
310 Stainless Steel	Many	Bal.	25	20	-	-
316 Stainless Steel	Many	Bal.	17	12	3	-
HK-40	Many	Bal.	26	20	-	-
Carpenter 20Cb3	Carpenter Technology	Bal.	20	34	3	4
Incoloy 800	Huntington Alloy	46	21	33	-	-
Inconel 600	Huntington Alloy	8	16	Bal.	-	-
Monel 400	Huntington Alloy	1	-	Bal.	-	32
E-Brite 26-1	Allegheny Ludlum	Bal.	26	-	1	-
Type 29-4	Allegheny Ludlum	Bal.	29	-	4	-

Table 5.3-4

CATALYTIC COAL GASIFICATION PDU
CORROSION RACK RESULTS

Test Site	Specimen Type	Location	Exposure Time (hrs) Series I	Exposure Time (hrs) Series II	Test Material (2)	Corrosion Rates(1)(mpy) Series I	Corrosion Rates(1)(mpy) Series II
1	Discs	Gasifier	2000	-	304 SS	33.3	
					304 SS, Alonized	38.4	
					309 SS	14.6	(3)
					310 SS	8.8	
					HK-40	6.7	
2	Cylinders	Gasifier	2000	-	304 SS	6.5	
					309 SS	4.7	(3)
					HK-40	12.8	
3	Cylinders	Gasifier	-	-	Lo-Erode	(4)	(3)
4	Discs	Sour water accumulator	2000	4160	CS	4.5	0.7
					304 SS	0.7	0.1
					316 SS	0.6	0.1
					Carpenter 20Cb3	0.4	0.1
					Ti	1.1	0.1
					Monel 400	1.1	0.3
6	Discs	Sour water stripper	2000	3350	CS	7.9	8.1
					304 SS	0.9	0.1
					316 SS	0.8	0.1
7	Discs	Sour water stripper	2000	3350	Carpenter 20Cb3	0.7	0.1
						3.6	3.1
						0.9	0.2
9	U-bends	Char digester	-	200	CS		68.3
					304 SS		0.5
					410 SS		4.4
					Monel 400	(5)	2.1
					Inconel 600		0.9
					E-Brite		0.8

Notes:

(1) No data available for TS-11 and TS-12.

(2) CS - carbon steel; SS - stainless steel.

(3) No data available due to cracking of coupon retainers and subsequent loss of coupons.

(4) Rack installed at TS-3 was broken due to mechanical damage. All specimens lost.

(5) Not removed for evaluation.

Corrosion Probes

Corrosion probes are devices measuring corrosion rates as a function of increasing electric resistance of corroding wire element. Through their quick response characterisitcs, they can flag large fluctuations in corrosion rates which would remain undetected from time-averaged weight loss measurements obtained from coupon specimens.

Two corrosion probes were installed at the PDU, respectively at Test Sites 5 and 10. Their locations in the unit are indicated in Figure 5.3-1 and Table 5.3-2. Both probes were standard Corrosometer Series 2000 fitted with 40 mil diameter wire elements.

Readings taken indicate that in both locations, the corrosion rate was minimal. The probe in the evaporator (TS-10) showed zero corrosion. The probe in the digester (TS-5) registered a corrosion rate of 2.3 mpy. This is in sharp contrast to the corrosion rack data which showed a 68.3 mpy corrosion rate on a carbon steel U-bend specimen in the digester. This is probably related to the different geometries of the two specimens.

Stream Analysis

Chemical analysis of stream samples is an important adjunct to in-situ materials testing and corrosion monitoring. Identifying the type and quantity of aggressive constituents in the process environment enables interpretation and correlation of corrosion and inspection data.

The eight PDU stream samples in this program are tabulated in Table 5.3-5, together with the species for which analyses are required. Table 5.3-6 shows a typical analyses of the eight streams. The overall low corrosion rates obtained imply that none of the chemical species were corrosive at the rack and probe locations. However, there were at least two instances where the composition of the stream played an important part in major failures. The first was the metal dusting of E/H-5 preheater coil that led to drastic thinning and failure of the tube. The carburizing tendency of the gas (74% H_2 and 26% CO) appears to be an important factor in the cause of failure. The second was the extensive cracking of the gasifier bottom and the char withdrawal line due to caustic stress corrosion cracking. The combination of potassium salts and condensed water formed a highly alkaline phase. This in combination with stress and elevated temperatures led to severe caustic cracking of the material. More details on these failures are given in the Component Examination section below.

NDT Inspection

Nondestructive testing (NDT), also called nondestructive examination (NDE), is a useful inspection technique for measuring wall thickness of equipment. Ultrasonic thickness testing (UT), the technique being employed at the PDU, may be performed during operation, within the temperature

Table 5.3-5

CATALYTIC COAL GASIFICATION PDU
STREAM SAMPLING AND ANALYSES

Location/Service	Type of Sample	Analyses(1)
Gasifier Overhead(2)	Gas	H_2S, CO_2, CO, H_2, CH_4
Sour Water Accumulator	Liquid	pH, Cl^-, CN^-, NH_3, H_2S, phenol
Filter Pot	Solid	Ash, K, Na, Ca, SO_4, SO_3, Cl
Char Pot	Slurry	Liquid: pH, K^+, Cl^-, CN^-, NH_3, H_2S Solid: ash, K, Na, Ca, S, Cl
Char Digester	Slurry	Liquid: pH, K^+, Cl^-, CN^-, NH_3, H_2S Solid: ash, K, Na, Ca, S, Cl
Char for Disposal	Solid	Ash, K, Na, Ca, SO_4, SO_3, Cl
Recycle Gas	Gas	H_2, CO, CO_2, H_2S
Evaporator (Conc. Sol'n.)	Liquid	pH, K^+, Cl^-

Notes:

(1) Sampling frequency to be once per yield period minimum unless otherwise specified.

(2) Sample taken after water scrubbing.

Table 5.3-6

TYPICAL PDU STREAM ANALYSES

Gasifier Overhead (% dry)	Sour Water Accumulator (ppm)	Filter Pot (Solid) (%)	Char Pot/ Digester (Solid) (%)	Char for Disposal (Solid) (%)	Recycle(2) Gas (% dry)	Evaporator Concentrated Solution (%)
H_2 - 56	pH - 8.35	Ash - 41.76	Ash - 38.53	Ash - 47.25	H_2 - 69	K - 11.6
CO - 9	Cl - 67	K(1) - 31.02	K - 35.12	K - 17.57	CO - 17	Cl - 1.8
CH_4 - 20	CN - 7.7	Na(1) - 1.36	Na - 1.17	Na - 0.14	CH_4 - 9	
CO_2 - 15	NH_3 - 14,300	Ca(1) - 0.02	Ca - 0.02	Ca - 0.46	N_2 - 5	
H_2S - 0.1	H_2S - 287	SO_4 - 0.15	SO_4 - 0.16	SO_4 - 0.06		
	Phenol - 19	S - 3.12	S - 1.6	S - 3.48		
		Cl - 1686 ppm	Cl - 2460 ppm	Cl - 62 ppm		

Notes:

(1) Analysis based on 16-hour reflux. Includes water soluble and acid soluble constituents.

(2) PDU operated in a once-through mode for a majority of the time during which the gas composition was 74% H_2 and 26% CO.

limitations of the transducer. The NDT program for the PDU is outlined in Table 5.3-7. Inspection of the char withdrawal lines was not pursued because of caustic cracking problems that led to replacement of the original lines. Also, the frequency of inspection for all points was reduced to reflect actual operating time.

Table 5.3-8 presents the inspection results. As expected, high metal losses ranging from 34 mpy to 86 mpy were observed in the overhead line from the gasifier to the cyclone. This is due to the fine erosive solids that are carried over from the gasifier. Losses at all other locations were minimal.

Component Examination

Failure analysis of equipment components is an important adjunct to coupon, probe, and NDT generated data for assessing materials performance in catalytic gasification applications. In addition, it is highly instructive to destructively examine critical equipment components which are still in working order after extended service exposure. Accordingly, a program was set up for the PDU, which provides for selected components to be examined in the ER&E Metallurgical Laboratory at Florham Park. This involved routine failure analysis of components to determine the cause and mode of failure. A description of the failures examined is given below.

Steam/Recycle Gas Heater Failure Analysis

Failure of the E/H-5 steam/recycle gas heater coil occurred twice, each time after approximately six months of operation. In the first case, the heater experienced an in-service coil rupture where the second tube ruptured during hydrotesting. The failure is attributed to a form of high temperature deterioration known as metal dusting. Metal dusting is effectively inhibited by sulfur compounds normally provided in the PDU by injection of H_2S upstream of the heater. However, especially in the first instance, there were periodic interruptions of H_2S injection that could have led to the coil failure.

E/H-5 is a fluidized sand bath heater preheating a mixture of steam, CO, and H_2 (6:1:3 by volume) from approximately 800°F to 1200°F at a nominal pressure of 500 psig. The single pass, 120 ft long, 1.5 ft bend radius helical coil is constructed of 3/4" OD x 0.065" wall, Type 316 stainless steel tubing. Normal operation included injection of H_2S into the gas upstream of the heater, at a target level of 300 vppm.

Visual examination of the ruptured section of tubing revealed that the failure occurred as a longitudinal split. The actual fracture surface was thinned to almost a knife edge, apparently by metal loss on the tube ID. Wall thickness measurements taken within an inch of the fracture surface revealed a minimum remaining wall thickness of 8 mils (65 mils original thickness). The failure appearance is a typical "thin lip" rupture which

Table 5.3-7

CATALYTIC COAL GASIFICATION PDU
NDT INSPECTION PROGRAM

Equipment Item	Inspection Points	Frequency
Gasifier	Opposite cyclone inlet, plus 4-6 selected spots	3 mo interval
Gasifier O/H line to cyclone	Every 3 feet and at elbows	3 mo interval
Cyclone	4-6 selected spots, including inlet area	Each turnaround
Cyclone dipleg	Every 2 feet of last 6 feet at gasifier inlet	Each turnaround
Cyclone line to filter	Every 20 feet	Each turnaround
Scrubber	Bottom 1 foot	3 mo interval
Gasifier line to char pot	Every 4 feet	Each turnaround
Char pot	Bottom head and lower shell, plus 4-6 selected spots	3 mo interval
Char digester	Body head and shell	Each turnaround

Table 5.3-8

POU ULTRASONIC THICKNESS MEASUREMENTS

Equipment	Material	Location	03/15/80 Initial Thickness (in)	07/01/81 2000-Hour Operation Thickness (in)	07/01/81 2000-Hour Operation Loss (mpy)	04/20/81 7500-Hour Operation Thickness (in)	04/20/81 7500-Hour Operation Loss (mpy)
Overhead line to cyclone	316 SS	1 ft from gasifier	0.189	0.169	86.2	-	-
		3 ft from gasifier	0.185	0.173	51.7	0.154	36.8
		5 ft from gasifier	0.189	0.177	51.7	0.145	50.6
		7 ft from gasifier	0.197	0.181	69.0	-	-
		9 ft from gasifier	0.189	0.173	69.0	-	-
		11 ft from gasifier	0.193	0.185	34.5	-	-
Cyclone	310 SS	At tangent	1.279	1.275	17.2	1.303	-
		180 from tangent	1.275	1.275	0	1.303	-
Diplet to gasifier	310 SS	5" from gasifier	0.437				
		6" above angle	0.441	(1)			
		17" from transition block	0.431				
Product gas line -- cyclone to filters	316 SS	10 ft from cyclone	0.197	-	-	0.181	18.4
		20 ft from cyclone	0.201	-	-	0.185	18.4
		30 ft from cyclone	0.201	-	-	0.193	9.2
		40 ft from cyclone	0.205	-	-	0.201	4.6
		50 ft from cyclone	0.197	-	-	0.209	-
		Before filters	0.201	-	-	-	-
Scrubber	304 SS	Beside sight glass outlet	0.366	0.366	0	0.399	31.5
		180° from first sight	0.362	0.358	17.2	0.331	31.5
Withdrawal leg #1	316 SS	24" below BV37	0.598				
		1.5" below BV36	0.602				
		5" below reactor	0.602				
		24" below BV31	0.598				
		1.5" below V830	0.598	(2)			
		5" below reactor	0.594				
Char pot #1	Inconel 625	8" below top S.E.	0.579	0.575	17.2	0.575	4.6
		9" below top N.W.	0.591	0.587	17.2	0.575	18.4
		6" below nameplate	0.575	0.567	34.5	-	-
Char pot #2	Inconel 625	8" below top N.W.	0.583	0.575	34.5	0.575	9.2
		9" below top S.E.	0.587	0.583	17.2	0.575	13.8
		6" below nameplate	0.579	0.579	34.2	-	-

Notes:

(1) Dipleg was replaced.
(2) Removed and replaced due to caustic cracking of the 316 SS tubes.

results from overstressing of a ductile material. Metal loss, rapid overheating, or overpressuring are all possible processes which cause overstressing of the material and result in such a failure. In this case, the latter two were ruled out by the PDU staff. Therefore, the failure is believed to be the result of stress rupture of the tube wall which had been extensively thinned by corrosion on the ID.

Wall thickness measurements were taken at periodic intervals from the coil inlet to the outlet. These are shown graphically in Figure 5.3-2 and show a distinct metal loss maximum near the middle of the coil. Also included in Figure 5.3-2 is a calculated tube metal temperature profile along the coil, based on active heat transfer surfaces contacting hot sand.

In addition to varying from coil inlet to outlet, metal loss also varied drastically between inner and outer bends of the coil. At a cross section close to the failure site, the remaining wall thickness on the outside radius was below 10 mils, compared to over 50 mils on the inner one. This is clearly a temperature effect, since the outer bend surface, being in direct contact with hot fluidized sand, is at a considerably higher tube metal temperature. However, there are factors other than temperature that play a significant role in their effect on metal dusting intensity. This is clearly brought out by Figure 5.3-2 which shows metal loss ranging from 10 to 55 mils at a fixed TMT of 1200°F.

Metallographic examination of the corroded coil showed generalized pitting and a carburized layer. In the second case, carburization was accompanied by some intergranular oxidation and sulfidation, associated with chromium depletion of carburized metal. However, this intergranular attack was a secondary effect and is not considered to have contributed significantly to the failure. Since sulfidation was not detected in the first coil failure, it is conjectured that there may have been sporadic overdosing of sulfide during later operations.

In order to minimize future chances of an onstream coil failure, the following recommendations were made:

- H_2S should be injected continuously in the preheater to provide protection against metal dusting.
- Sulfur levels should be cut back from 300 ppm to 150 ppm. This change will substantially reduce any chance of sulfidation and will still provide ample sulfur to be effective in preventing carburization.
- A standby coil should be fabricated utilizing Incoloy 800 at the mid-level where heavy thinning has occurred. The as-formed Incoloy 800 should be solution annealed to optimize creep strength.
- Frequent hydrotesting should be continued to forewarn of imminent failure should severe thinning occur.

Figure 5.3-2

VARIATION OF METAL LOSS AND TUBE METAL TEMPERATURE VERSUS DISTANCE FROM COIL OUTLET

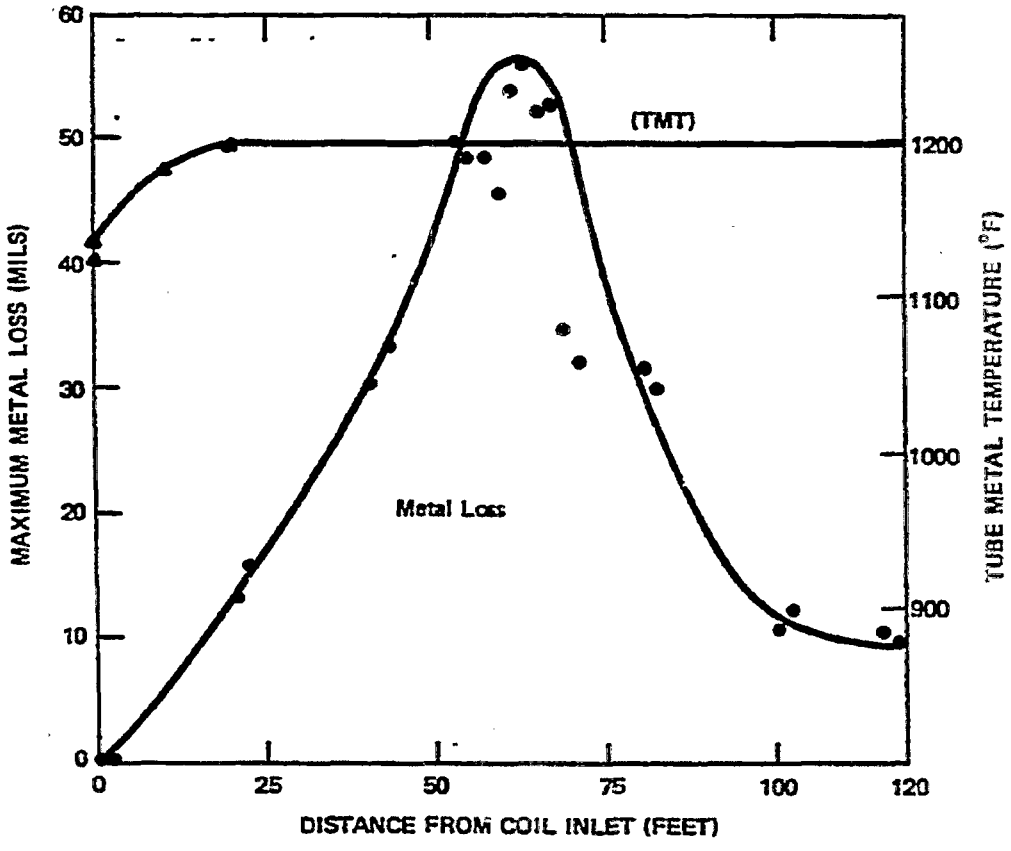

Char Withdrawal Line Failure Analysis

On October 8, 1980, one of the PDU char withdrawal lines (316 SS) developed a through-wall crack, forcing a shutdown of the unit. Removal of the line from the gasifier bottom head revealed continuation of the cracking up into the head (316 SS). Removal of the bottom head and liquid penetrant inspection of the gasifier revealed cracks extending 14-15" up into the gasifier. It is noteworthy that this cracking stopped below the weld neck (316 SS) to gasifier (HK-40) weld. The lower portion of the gasifier, where the cracking had occurred, is shown schematically in Figure 5.3-3.

Liquid penetrant inspection of the char withdrawal lines revealed extensive cracking of 316 SS, moderate cracking of Incoloy 800, and no cracking of the Inconel 625 Grayloc hubs. Inspection of the disassembled 316 SS char withdrawal valves showed extensive cracking of inlet and outlet valve necks, spool/seat assemblies, ball inside diameters, spring retainers, and spring covers.

Metallurgical examination of sections of the failed char withdrawal line, both 316 SS and Incoloy 800, revealed extensive transgranular cracking. Energy dispersive X-ray analysis (EDX) of crack surfaces detected major quantities of potassium with traces of silicon, sulfur, and chlorine. Based upon these visual and metallurgical examinations and previous failures on the PDU, cracking was concluded to be the result of caustic stress corrosion (caustic embrittlement).

Caustic stress corrosion cracking is the result of a combination of elevated temperature, tensile stress, and a strongly alkaline solution. Contacting CCG char with water produces a highly alkaline phase (pH 12); however, the ultimate sequence of events which produced the condensed water was not positively determined. Two possible causes include a lack of heat tracing on the bottom of the gasifier in combination with insufficient insulation, and the occasional loss of synthesis gas. Interruption of synthesis gas is directionally detrimental because during these outages, only steam is fed to the gasifier, thereby raising the dew point. Due to the severity of the attack, it is felt that "wet" conditions existed during operation and not just during startup and shutdown periods.

Repair procedures were recommended to ensure vessel integrity and to minimize downtime. Where possible, higher nickel alloys were utilized for increased resistance to caustic cracking. Repair of the gasifier weld neck involved machining approximately 1/2" off the I.D. to crack-free metal, followed by weld overlaying with Inconel 625 and final remachining. A similar procedure was followed for the gasifier bottom head, with the addition of Inconel 625 liners through the head to the exterior socket weld connections. Char withdrawal piping was replaced with Incoloy 800H. Three char withdrawal valves were replaced with onsite 316 SS spares, identical to the original valves. One of the cracked valves was repaired by machining and weld overlaying Inconel 625 to obtain the necessary fourth valve.

FIGURE 5.3-3

SCHEMATIC OF GASIFIER BOTTOM WELD-NECK AND FLANGE

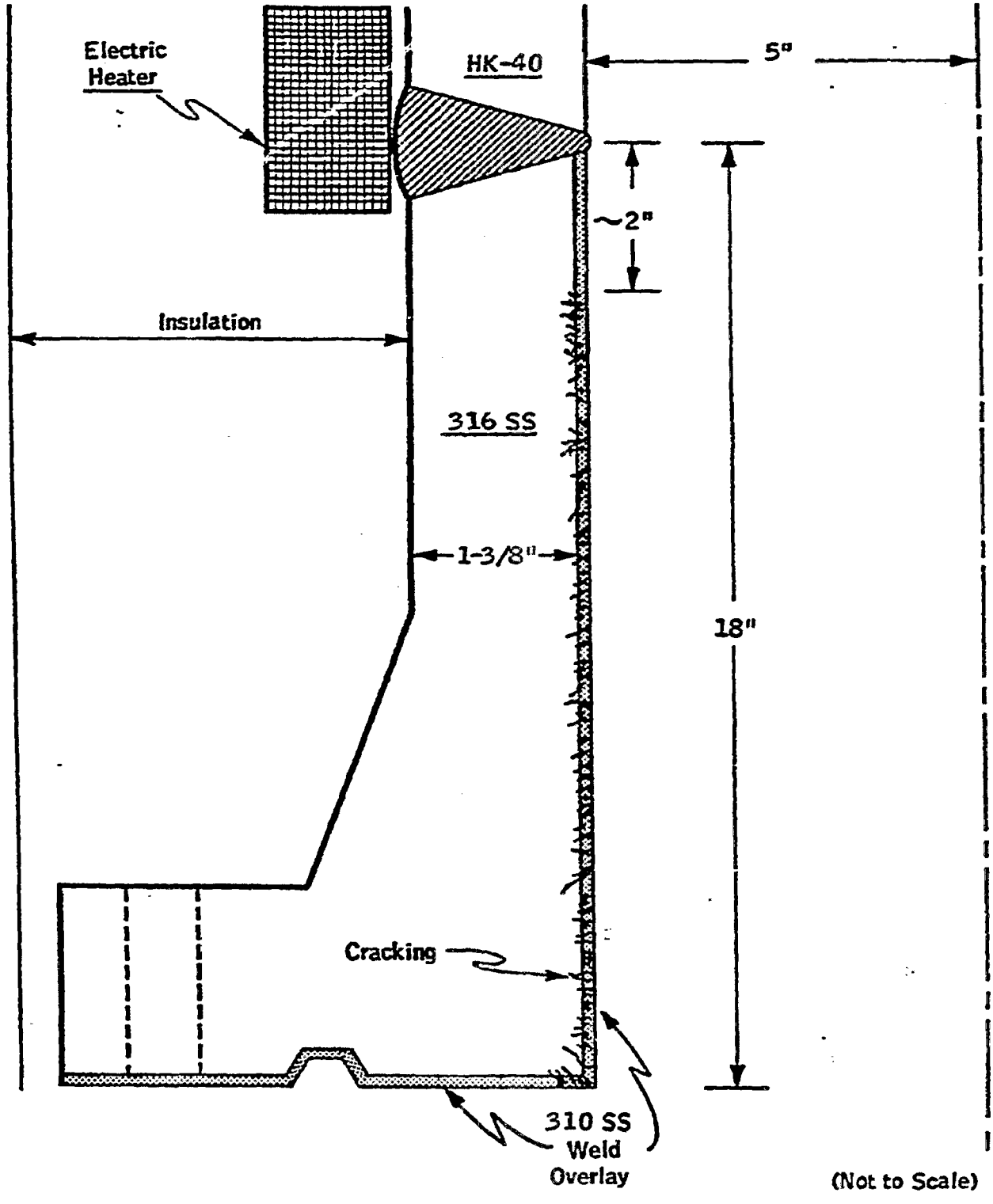

Since the system still contains 316 SS and Incoloy 800, both of which are quite sensitive to caustic stress corrosion cracking, supplemental equipment modifications and operating precautions were developed to prevent condensation. Additional heat tracing and insulation were applied to the gasifier bottom weld neck, head, char withdrawal lines, and valves. Furthermore, numerous thermocouples were installed to monitor metal temperatures in these areas.

Gasifier Bottom Char Sample Line Failure Analysis

On August 22, 1980, the 316 SS gasifier bottom char sample line cracked between the first block valve and the gasifier, forcing a shutdown of the unit. Metallographic examination revealed branched transgranular cracking; chemical analysis of the crack surface identified the presence of sulfur and potassium. This line, which is in intermittent service, was insulated but not heat-traced. It is concluded that temperature excursions below the dew point produced a highly alkaline condensate by leaching potassium from the char, which ultimately resulted in caustic stress corrosion cracking. Replacement with Inconel 600 or 625 was recommended; as an alternative, adequately heat-traced 304 or 316 SS was also considered acceptable.

Gasifier Feed Lines Failure Analysis

Two sections of failed flexible metal hoses (300 series stainless steel) from the gasifier feed lines were metallurgically examined. These hoses developed cracking onstream and, upon removal, were found to be filled with wet coal. As in the above described sample line failure, the cause of failure was identified as caustic stress corrosion cracking and similar corrective measures were recommended.

Materials Screening Tests at Tuscaloosa Metallurgy Research Center

As a result of a joint DOE/BM/ER&E meeting in March, 1979, a materials test program geared to the CCG process was conducted at the Bureau of Mines Tuscaloosa Metallurgy Research Center in University, Alabama. Funding for this program was through modification of the active Interagency Agreement EX-76A-01-2219 between DOE and the Bureau of Mines. These tests were conducted in test apparatus already built and used for similar experiments studying materials for thermal gasification processes.

The objective of the test program was to screen candidate metals and refractories in simulated CCG environments. Specifically, the intent was to evaluate the effect of potassium hydroxide (gasification catalyst) in accelerating attack on construction materials, and to elucidate the nature of such attack. Close attention was given to complex liquid phases composed of alkalis and metal sulfides. Such aggressive slags have not been encountered in CCG laboratory units, but are nevertheless possible from thermodynamic considerations. The detrimental effect of alkali contamination on refractories was demonstrated at Tuscaloosa in a series of 1978 test runs simulating thermal gasification environments at 1800°F.

Laboratory exposures of a wide variety of commercially available refractory and metallic materials to CCG environments were initiated with 100-hour screening tests. Following the short-term tests, a 2,000-hr exposure test was conducted. The candidate metal alloy selection was based primarily on testing conducted by IIT Research Institute, under the direction of the Metals Properties Council and DOE sponsorship, on gaseous corrosion of metal materials in high-Btu gasification atmospheres. The refractories chosen for inclusion in the program were those identified by the U.S. Bureau of Mines in a DOE-sponsored program directed toward selection of dry ash gasifier lining materials. The alloys and refractories tested in the CCG program are listed in Tables 5.3-9 and 5.3-10, respectively.

The simulated CCG environment was produced by continuously passing a gas stream at 500 psig having a CCG composition (32% H_2O, 22% CH_4, 21% H_2, 14% CO_2, 6% CO, 2% N_2, 2% NH_3, 1% H_2S) through a heated (1350°F) pressure vessel containing the test specimens. One specimen of each material under test was in physical contact with coal char obtained from the PDU. Specimens of each material were also exposed to the gas phase only which, in addition to the gaseous species previously mentioned, contained as equilibrium amount of alkali vapor from the CCG char.

The full results of this program are contained in process reports issued by the Tuscaloosa Research Center. A summary of these results is presented in Table 5.3-11.

Data obtained from the screening tests (50 to 100 hr exposures) indicated that refractories absorbed considerable vapor-phase-transported alkali in the simulated CCG exposures. Refractory cold crushing strength was not adversely affected; however, the gain in hot flexural strength of the low- and intermediate-alumina concretes normally occurring after exposure to similar, but alkali-free, atmospheres did not occur.

The results of cold crushing strength determinations of the vapor-exposed refractories after 2,000-hr exposure to the CCG environment are presented in Table 5.3-12. Only five refractories were included in the 2,000-hr test because of limited space. The data indicate that intermediate-alumina concrete showed significant improvements in strength whereas the strength of high-alumina concrete was reduced by this exposure. Compressive strengths of the other refractories remained unaffected by the exposure conditions. Similar trends were observed for the abrasion resistance of the exposed refractories. Chemical analyses (atomic absorption) of the 2,000-hr CCG vapor-exposed samples indicated that the K_2O content of the refractories increased by a factor of four when compared to identical, pre-exposed samples.

The refractory specimens that were exposed in the char mode by submerging them in CCG char in the environmental test chamber showed no signs of deterioration at the 500-hr inspection intervals, but showed obvious signs of degradation at the end of the 2,000-hr exposure. Examination of these refractories by means of SEM elemental analyses revealed that large amounts of potassium had migrated throughout the entire specimens.

Table 5.3-9

CHEMICAL COMPOSITION OF CATALYTIC COAL GASIFICATION TEST ALLOYS

Alloys Tested	Composition, Weight Percent									
	C	Mn	Si	Fe	Ni	Cr	Co	Al	Mo	Other
304	0.05	1.45	0.54	70.0	9.1	18.8	-	-	-	-
310	0.06	1.71	0.68	52.2	20.2	25.0	-	-	-	-
310 Aluminized										
316	0.05	1.65	0.43	65.3	13.9	17.1	-	-	2.5	-
446	0.10	0.45	0.38	74.6	0.4	24.0	-	-	-	-
Inc-800	0.03	0.80	0.33	47.1	30.8	20.6	0.10	0.32	-	0.42 Ti
Inc-800 Aluminized										
Inc-800-H	0.06	0.89	0.22	45.74	31.24	20.22	-	0.52	0	0.50 Ti, 0.61 Cu
Inc-600	0.01	0.29	0.20	9.56	76.5	15.8	-	-	-	0.35 Cu
Inc-6U1	0.03	0.24	0.19	15.62	60.33	21.88	-	1.37	-	0.34 Cu
Inc-617	0.06	0.01	0.11	0.87	53.88	22.23	12.47	1.17	9,20	-
Inc-625	0.03	0.11	0.20	3.71	60.66	22.60	-	0.26	8.57	3.44 Cb + Ta
Inc-671	0.05	0.07	0.21	0.32	52.92	46.02	-	-	-	0.41 Ti
Inc-690	0.01	0.15	0.10	10.22	61.83	27.27	-	0.17	-	0.25 Ti
Crutemp 25	0.07	1.5	0.60	47.2	24.8	25.4	-	-	0.40	-
HK-40	0.4	2.0	2,0	47.1	20.0	28.0	-	-	0.50	-
TX-47	0.38	2.0	2.0	47.0	20.0	28.0	-	-	-	-
Stellite 6B	1.0	1.4	0.5	1.9	2.8	28.1	57.1	-	1.2	4.8 W
Co-Cr-W No. 1	2.5	-	-	-	-	30.0	55.5	-	-	12.0 W
RA 333	0.05	1.5	1.4	15.5	45.0	26.2	2.5	-	3.8	2.7 W
HL-40	0.30	0.86	1.32	45.0	20.5	31.5	-	0.03	0.01	-

Table 5.3-10

REFRACTORY MATERIAL SELECTION FOR CCG TESTS

Refractory Brand Name	Refractory Type
CASTOLAST G	Calcium aluminate-bonded dense 95 wt% Al_2O_3 castable
DOE 90	Calcium aluminate-bonded dense 90 wt% Al_2O_3 castable
LOABRADE	Calcium aluminate-bonded dense 55 wt% Al_2O_3 castable
MIX 36-C	Calcium aluminate-bonded dense 50 wt% Al_2O_3 castable
H.S. BRIKCAST BF	Calcium aluminate-bonded dense 45 wt% Al_2O_3 castable
KAOCRETE D	Calcium aluminate-bonded dense 45 wt% Al_2O_3 castable
LITECAST 75-28	Calcium aluminate-bonded dense lightweighted 50 wt% Al_2O_3 insulating castable
BRIKRAM 90-R	Phosphate-bonded 90 wt% Al_2O_3 ramming mix
HW 23-75	Phosphate-bonded 60 wt% Al_2O_3 ramming mix
AA-22	Phosphate-bonded dense 90 wt% Al_2O_3 castable
ARCO 90	90 wt% Al_2O_3 brick
KX-99	45 wt% Al_2O_3 duty fire brick

Table 5.3-11

SUMMARY OF EXPERIMENTS - TUSCALOOSA RESEARCH CENTER(1)

RUN NO. (DATE)	TEST OBJECTIVES	EXPOSURE TIME (HRS)	ENVIRONMENT(2)	ALLOY SPECIMENS	REFRACTORY SPECIMENS(3)	RESULTS/CONCLUSIONS
1 (9/15/79)	1. Determine mode of introducing alkali to exposure chamber. 2. Screen materials for CCG environment.	100	CCG Gas: 1. Vapor phase with injected aqueous KOH 2. KOH/coal 3. Molten KOH	304 SS 310 SS 446 SS Incoloy 800 Incoloy 800 (aluminized)	Castolast G (C/95) H.S. BrikCast (C/45) KX-99 (B/45)	1. Vapor phase KOH caused only slight surface attack of metals. Aluminum coating subject to alkali attack from vapor transported KOH. Refractories absorbed considerable KOH from vapor phase. 2. Molten KOH/coal mixture caused severe attack of 304 and moderate attack of aluminizing. Refractories showed no obvious degradation. 3. Molten KOH caused severe attack of all metals and refractories.
2 (10/ 5/79)	Evaluate method of continuously introducing alkali by pumping aqueous alkali solution into exposure chamber.	250	CCG Gas: 1. Vapor phase with injected aqueous KOH. 2. Molten KOH (as alkali source).	None	DOE 90 (C/90) H.S. BrikCast (C/45) Lo-Abrade (C/55) 36-C (C/50)	1. Vapor phase exposure caused moderate increase in strength of low/intermediate alumina refractories. Refractories doubled in alkali content. 2. No specimens were exposed in molten KOH. 3. Aqueous injection of KOH was problematical and hence abandoned as alkali source.

Table 5.3-11 (Cont'd)

RUN NO. (DATE)	TEST OBJECTIVES	EXPOSURE TIME (HRS)	ENVIRONMENT(2)	ALLOY SPECIMENS	REFRACTORY SPECIMENS(3)	RESULTS/CONCLUSIONS
3 (10/25/79)	Determine rate of volatilization of KOH from platinum crucibles inside sample container.	250	Steam: Molten KOH (as alkali source)	None	DOE 90 (C/90) H.S. BrikCast (C/45) Lo-Abrade (C/55) 36-C (C/50) Kaocrete D (C/45)	1. Two-thirds of the KOH originally charged was vaporized. 2. Condensate levels of K_2O decreased from initial 30 ppm to less than 2 ppm after 30 hr. 3. Refractories showed up to a 4-fold increase in K_2O.
4 (1/14/80)	Determine rate of volatilization of KOH from platinum crucibles inside reactor.	60	H_2S-free CCG Gas Molten KOH (as alkali source)	None	Castolast G (C/95) Lo-Abrade (C/55) H.S. BrikCast (C/45)	1. No vapor phase transported alkali absorbed by refractories. 2. No weight change in contents of platinum crucibles. 3. Large conversion of KOH to K_2CO_3 in crucibles. 4. Very low levels of alkali in condensate.
5 (1/28/80)	Determine rate of volatilization of KOH from platinum crucibles inside reactor.	50	Steam + argon + 1.2% H_2S	None	Castolast G (C/95) Lo-Abrade (C/55) H.S. BrikCast (C/50)	1. Complete conversion of KOH to K_2S. 2. High initial alkali levels in condensate but decreasing to less than 4 ppm after 45 hr.

Table 5.3-11 (Cont'd)

RUN NO. (DATE)	TEST OBJECTIVES	EXPOSURE TIME (HRS)	ENVIRONMENT(2)	ALLOY SPECIMENS	REFRACTORY SPECIMENS(3)	RESULTS/CONCLUSIONS
6 (3/10/80)	Conduct short duration screening exposure prior to extended exposure testing of metals and refractories.	100	CCG Gas 1. Vapor phase with KOH from molten KOH in crucible. 2. KOH/coal	304 SS 310 SS, Aluminized 316 SS 446 SS Incoloy 800 Incoloy 800, Aluminized Incoloy 800H Inconel 600 Inconel 601 Inconel 617 Inconel 625 Inconel 671 Inconel 690 Crutemp 25 HK-40 TX-47 Stellite 6B Stellite No. 1	Castolast G (C/95) Lo-Abrade (C/55) H.S. BrikCast (C/50) KX-99 (B/45)	1. Refractory samples showed no evidence of chemical attack or loss of cold crushing strength in either gas phase or KOH/coal exposure. 2. In gas phase exposure, Inconel 600 was severely attacked. All other metals were slightly or moderately affected. 3. In KOH/coal exposure, severe sulfidation corrosion was suffered by Inconel 600 (complete penetration), Inconel 617, Inconel 625, and Stellite No. 1. All other metals were slightly or moderately attacked (Inconel 671 and Inconel 690 were least corroded).

Table 6.3-11 (Cont'd)

RUN NO. (DATE)	TEST OBJECTIVES	EXPOSURE TIME (HRS)	ENVIRONMENT(2)	ALLOY SPECIMENS	REFRACTORY SPECIMENS(3)	RESULTS/CONCLUSIONS
7 (7/1/80)	Conduct long-term screening exposure testing of metals and refractories.	2000 with interruption at 600 hr.	CCG Gas 1. Vapor phase with KOH from molten KOH in crucible. 2. KOH/coal	304 SS 310 SS, Aluminized 316 SS 446 SS Incoloy 800 Incoloy 800, Aluminized Incoloy 800H Inconel 601 Inconel 671 Inconel 690 Crutemp 25 HK-40 TX-47 Stellite 6B Co-Cr-W No. 1 RA-333 HL-40	Castolast G (C/95) H.S. BrikCast (C/55) H.S. BrikCast + SS fibers (C/55) KX-99 (B/45) Brickram 90-R (B/90)	1. In vapor phase, BrikCast and BrickCast + SS fibers showed strength improvements while KX-99, Castolast G, Brickram 90-R showed strength reduction. 2. Refractory specimens exposed to the char phase showed no deterioration at the 600 hr mark but showed obvious signs of degradation after 2000 hr. 3. With the exception of Inconel 671, which survived both exposures with superficial corrosion, all other alloys suffered moderate attacks in the vapor and severe attack in the char exposures.

Notes:

(1) Work performed by Tuscaloosa Research Center under Interagency Agreement Contract DE-AI05-80OR20686 (Testing and Development of Materials for Catalytic Coal Gasification Process Equipment).

(2) CCG gas composition (Mol%) - 32% H_2O, 22% CH_4, 21% H_2, 14% CO_2, 6% CO, 2% N_2, 2% NH_3, 1% H_2S. Coal - Illinois No. 6. All test runs were conducted at 730°F (1346°F), 600 psig.

(3) Refractory code: C - Castable, B - Brick. Number refers to percent alumina.

Table 5.3-12

RESULTS OF REFRACTORY EXPOSURE TO CCG VAPOR FOR 2,000 HOURS

Refractory	Compressive Strength, psi	
	Prefired in Air(1)	CCS Exposed(2)
CASTOLOAST G	9,110	4,375(3)
BRIKCAST	4,275	10,355(3)
BRIKCAST + SS fibers	4,095	12,025(3)
KX - 99	9,500	7,515
BRIKRAM 90-R	11,585	9,600

Notes:

(1) Prefired in air at 730°C for 24 hours.

(2) Exposed to CCG vapor 2,000 hours, 730°C, 500 psi.

(3) Difference significant at 99% level of confidence.

Based on the results in this study, refractories suitable for high-Btu dry ash gasifiers appear to be good candidates for high-Btu catalytic coal gasification applications.

The major observation regarding metal alloys was that aluminized coatings were very susceptible to alkali attack, in both vapor phase and char exposures. The char was much more corrosive than vapor phase exposure and, due to excessive corrosion, several alloys were not included in the long-term exposure test that followed the screening tests, as indicated in Table 5.3-13. Metallographic examination of the severely corroded metal coupons affected by the vapor and the char indicated that corrosion occurred primarily by sulfidation. This resulted in a slagging of the metal surfaces.

Of the alloys exposed to the CCG vapor, as shown in Table 5.3-13, only the aluminized Incoloy-800 showed signs of advanced corrosion after 500 hours of exposure. Metallographic examination of the metal alloy cross sections after 2,000 hours of vapor exposure revealed that an apparent passive layer was developed on the surfaces of the remaining metals. Energy dispersive analysis indicated only low concentrations of potassium on the metal surfaces and no potassium within the passive scale layer. This would appear to demonstrate that potassium, in the vapor phase, had little effect on the corrosion behavior of these alloys. The corrosion mechanism of the alloys in the vapor phase was primarily by combined oxidation-sulfidation. No significant internal corrosion was observed for any of the metal alloys remaining in the vapor at the conclusion of the 2,000-hr exposure.

It was apparent from the results of the screening tests that exposure to char is a much more severe test condition than exposure to simulated CCG vapor. Only 5 of the 21 alloys tested were exposed to char for the full 2,000 hours. The other specimens were severely corroded and removed during the test when the samples were inspected at 500-hr intervals. Significantly, even the most resistant metals suffered some corrosion damage.

Since some of the low-alloyed metals performed nearly as well or better than some of the higher alloyed metals, no general conclusion can be made with regard to metal composition. However, for the test conditions employed, it appears that alloys susceptible to rapid failure by a sulfidation-slagging mechanism will fail during or after about 100 hours of exposure; this accounts for the poor showing of high nickel alloys. The notable exception is Inconel 671 which survived both exposures with only superficial corrosion.

Table 5.3-13

CORROSION OF METAL SAMPLES EXPOSED TO CCG VAPOR-CHAR ENVIRONMENTS
(BUREAU OF MINES, TUSCALOOSA RESEARCH CENTER)

Metal Alloy	Extent of Corrosion in CCG Vapor	Time of Exposure	Extent of Corrosion in CCG Char	Time of Exposure
304 SS	Moderate	2,000 hr	Severe-surface	500 hr
310 SS	Moderate	2,000 hr	Moderate to severe	2,000 hr
310 SS Aluminized	Moderate	2,000 hr	Severe-surface	1,500 hr
316 SS	Moderate	2,000 hr	Severe-surface	500 hr
446 SS	Moderate	2,000 hr	Moderate to severe	2,000 hr
Incoloy 800	Moderate	2,000 hr	Severe-surface	500 hr
Incoloy 800 Aluminized	Severe-surface	500 hr	Severe-surface	1,000 hr
Incoloy 800H	Moderate	2,000 hr	Severe-almost complete	500 hr
Inconel 600	Severe-surface	100 hr	Severe-complete	100 hr
Inconel 601	Moderate	2,000 hr	Severe-complete	500 hr
Inconel 617	Moderate-surface	100 hr	Severe-surface	100 hr
Inconel 625	Moderate-surface	100 hr	Severe-surface	100 hr
Inconel 671	Very light	2,000 hr	Slight-surface	2,000 hr
Inconel 690	Moderate	2,000 hr	Severe-almost complete	500 hr
Crutemp 25	Moderate	2,000 hr	Moderate	2,000 hr
HK-40	Moderate	2,000 hr	Severe-surface	1,500 hr
TX-47	Moderate	2,000 hr	Severe-surface	1,000 hr
Haynes Stellite 6B	Moderate	2,000 hr	Moderate	2,000 hr
Co-Cr-W No. 1	Moderate-surface	100 hr	Severe-surface	100 hr
RA-333(1)	Moderate	1,500 hr	Severe-surface	500 hr
HL-40(2)	Moderate	1,000 hr	Severe-surface	1,000 hr

Notes:

(1) Added at the 500-hour break.

(2) Added at the 1,000-hour break.

5.3.2 Vapor-Liquid Equilibria in Sour Water/Catalyst Systems

This program's objective was to develop a vapor-liquid equilibrium (VLE) model applicable to the design of the sour water systems in the CCG Process. The systems for which such a model would be used include the wet scrubbers and condensate drums for the gasifier product gas, as well as the sour water stripping facilities.

A detailed review of the anticipated sour water streams identified the compositions, temperatures, and pressures of interest. Subsequently, a literature search was conducted to identify the available experimental data on the volatility of ammonia, carbon dioxide, and hydrogen sulfide in aqueous solutions, including solutions containing potassium compounds. Pertinent articles were obtained and analyzed. This analysis led to the conclusion that additional data on the ammonia-carbon dioxide-hydrogen sulfide-water system were needed, especially at temperatures above 100°C. Additional data on the volatility of ammonia, carbon dioxide, and hydrogen sulfide in aqueous solutions containing potassium compounds were also needed.

Wilco Research Company was contracted to obtain these additional data. Their experimental measurements are given in Table 5.3-14. Three computerized models for predicting VLE were tested with these data. The three models were: SURFIMP developed by Edwards et al. (Edwards, T. J., Maurer, G., Newman, J. and Prausnitz, J. M., "Vapor-Liquid Equilibria in Multicomponent Aqueous Solutions of Volatile Weak Electrolytes", AIChE Journal, 24(6), 966-976 (1978)), SWEQ developed for the American Petroleum Institute (American Petroleum Institute, "A New Correlation of NH_3, CO_2 and H_2S Volatility Data from Aqueous Sour Water Systems", API Publication 955, March, 1978, Washington, D.C.), and a proprietary ER&E model. The tests consisted of fixing the temperature and the liquid phase composition and letting the computer programs calculate the equilibrium vapor composition. The first conclusion of these tests was that the values reported for Run 3 are incorrect. The reported partial pressure of water is high by a factor of two. Also, for Run 3, all three models gave large errors for the other partial pressures and for the total pressure as well. The other runs reported in Table 5.3-14 are probably accurate as discussed below.

Runs 1, 2, 2R (Re-run of 2), 4, 5, and 6 do not have any potassium present. These runs were used to compare the accuracy of the three models. At the same time, the accuracy of the model predictions was used to judge the accuracy of the experimental data. The table below gives the percent errors for the calculated partial pressures for each of these runs for each of the models, with one exception. The SURFIMP computer program has a logic check to prevent calculations above a temperature of 150°C. Therefore, there are no entries for SURFIMP for Run 6. The results clearly show that ER&E's proprietary model is superior to both SURFIMP and SWEQ on these new data. As for the accuracy of the experimental data, the experimental data point usually lies between the predictions of the three models. Therefore, the data for Runs 1, 2, 2R, 4, 5, and 6 are assumed to be accurate.

Table 5.3-14

SUMMARY OF MEASURED VAPOR-LIQUID EQUILIBRIUM DATA ON NH_3-CO_2-H_2S-H_2O-KOH MIXTURES

Run No.	Temp. °C	Pressure psia	Analysis, Mole %								
			NH_3		CO_2		H_2S		H_2O		KOH
			Liq.	Vap.	Liq.	Vap.	Liq.	Vap.	Liq.	Vap.	Liq.
1	120	153.5	22.9	70.5	0	0	3.98	13.9	73.17	15.6	0
2	140	85.0	5.52	36.4	0	0	0.617	5.96	93.86	57.7	0
Re-Run 2	140	86.0	5.42	34.6	0	0	0.572	5.84	94.01	59.6	0
3	50	55.0	3.64	0.052	3.32	71.8	0.454	22.2	92.59	5.97	0
4	130	79.5	2.63	10.73	0.530	28.8	0.436	9.26	96.40	51.2	0
5	130	86.3	6.98	32.6	0.433	8.17	1.64	17.6	90.94	41.6	0
6	170	315	4.59	12.4	0.500	33.3	1.00	19.0	93.90	35.3	0
7	130	65.5	0	0	1.48	27.1	1.52	13.4	94.03	59.5	2.97
Re-Run 7	130	65.0	0	0	1.52	28.1	1.50	10.8	94.01	61.1	2.97
8	190	215	0	0	1.50	13.6	1.60	4.12	93.88	82.2	3.00
Re-Run 8	190	219.5	0	0	1.53	14.7	1.53	2.35	93.95	82.9	3.00
9	130	50.0	0.93	7.94	2.62	14.2	0	0	93.49	77.9	2.96
10	190	222.5	0.89	5.70	2.70	12.4	0	0	93.44	81.9	2.98
11	130	47.0	0.96	11.8	0	0	3.23	5.19	92.78	83.0	3.03
12	190	204	0.79	7.16	0	0	3.34	4.30	92.77	88.5	3.11

PERCENTAGE ERRORS IN CALCULATED PARTIAL PRESSURES
FOR MIXTURES CONTAINING NO POTASSIUM COMPOUNDS

	NH_3			CO_2			H_2S		
Run	SURF	SWEQ	ER&E	SURF	SWEQ	ER&E	SURF	SWEQ	ER&E
1	53	-19	9	-	-	-	226	-44	-56
2	-3	-5	3	-	-	-	35	-21	-22
2R	-1	-3	5	-	-	-	22	-31	-30
4	-8	-13	-2	13	35	1	0	14	-5
5	1	-17	-8	37	56	-18	43	41	5
6	-	0	5	-	59	-15	-	12	-20
Mean Absolute Errors	13%	10%	5%	25%	50%	11%	65%	27%	23%

For the experimental runs which contain potassium, only two of the computerized models could be tested. The SURFIMP computer program is not generalized. It cannot handle any compounds besides SO_2, HCN, NH_3, H_2S, CO_2 and water. The table below gives the comparisons of SWEQ and the proprietary ER&E model with Runs 7, 7R, 8, 8R, 9, 10, 11, and 12. The values in the table are the ratio of calculated to measure partial pressures.

RATIO OF CALCULATED TO MEASURED PARTIAL PRESSURES
FOR POTASSIUM-CONTAINING MIXTURES

	NH_3		CO_2		H_2S	
Run	SWEQ	ER&E	SWEQ	ER&E	SWEQ	ER&E
7	-	-	1.05	2.33	0.60	1.12
7R	-	-	1.56	2.70	1.10	1.59
8	-	-	2.94	3.33	1.12	1.33
8R	-	-	1.89	2.44	1.27	1.75
9	0.72	0.96	0.09	1.23	-	-
10	0.95	1.28	0.13	1.03	-	-
11	0.68	0.69	-	-	7.30	5.49
12	0.90	0.77	-	-	7.58	5.95

The CO_2 partial pressures calculated for Runs 9 and 10 by SWEQ are lower than the experimental values by a factor of 10. Wilco Research Company, which actually did the calculations with SWEQ, suggested that these large errors were due to slight inaccuracies in the measured liquid-phase composition. However, the ER&E model does a good job in predicting partial pressures for Runs 9 and 10. Therefore, the experimental data were accepted as accurate.

In general, predictions of SWEQ and the ER&E model agree with the data as well as they agree with each other. The large discrepancies between the experimental data and the predictions of the computer models are probably due to inaccuracies in the models at the high temperatures (130 or 190°C), and because of the effects of the potassium compounds. It is clear that both models give unacceptably large errors in somes cases. Adjustments to the models, or to model parameters, would be required to calculate VLE in high-temperature, potassium-containing systems typical of the CCG process. Defining the necessary adjustments should be the goal of future work in this area.

5.3.3 Physical and Thermodynamic Properties of Catalyst Recovery Solutions

The equipment in the catalyst recovery section of the CCG process may include mixing drums, solid-liquid separators, heat exchangers, pumps, evaporators, and driers. To design such equipment, physical and thermodynamic property data are needed for aqueous solutions containing electrolytes. The objectives of this program were to review representative operating conditions of the catalyst recovery system, to determine likely data needs, and then to collect and evaluate the available data. These data will be used to guide the design of the catalyst recovery system and to identify deficiencies in the available data base. These objectives were met and the results are summarized here.

A review of the catalyst recovery system identified the important properties as: density, enthalpy, viscosity, and boiling point for aqueous solutions containing up to 40 wt% dissolved potassium compounds. Temperatures of interest range from 20 to 150°C (70 to 300°F). Potassium hydroxide and potassium carbonate are the potassium compounds of primary interest. However, future tests on the PDU may identify other important compounds.

A literature search for properties of aqueous solutions containing potassium hydroxide or potassium carbonate was completed. Pertinent articles were collected and evaluated. With only two exceptions, the available data are adequate for calculating the density, enthalpy, viscosity, and boiling point of aqueous potassium hydroxide and aqueous potassium carbonate. A review of the data base, and graphs of the properties of aqueous potassium hydroxide and aqueous potassium carbonate will be presented later in this section.

Other potassium compounds are likely to be present in the process streams of the catalyst recovery section. Therefore, another literature search was made for properties of aqueous solutions containing potassium bicarbonate, potassium bisulfide, or potassium sulfide. Unfortunately, the data base for aqueous solutions of these compounds is sparse and no recommendations can be made for their properties. However, the available data are cited later in this work summary.

The process streams in the catalyst recovery section of the CCG process are likely to contain many potassium compounds. Therefore, property data on mixtures of electrolytes are important. Few experimental data exist for properties of mixtures of potassium compounds pertinent to the catalyst recovery section of the CCG process. Therefore, methods for extending data for single compounds in water to multicomponent mixtures have to be developed.

Simple methods are presented here for predicting the density, enthalpy, and viscosity of aqueous solutions containing several electrolytes. However, not enough experimental data on multicomponent mixtures exist to confirm these methods. It is recommended that the next phase of CCG development include a technology study to measure the multicomponent data needed to test the proposed prediction methods and to support the design of a commercial CCG plant. This technology study should also have an objective to develop a model for calculating vapor-liquid equilibria in highly concentrated electrolyte solutions. This model is needed to predict boiling points of multicomponent mixtures of aqueous electrolytes.

The remainder of this section provides more details on the experimental data base and the methods for predicting properties of multicomponent mixtures. Each of the four properties: density, enthalpy, viscosity, and boiling point will be discussed in turn.

Density

Mashovets et al. (17)* report extensive data for the density of aqueous potassium hydroxide from 0 to 400°C for concentrations from 0 to above 50 wt% potassium hydroxide. These data are supplemented, between 0 and 70°C, by the data of Akerlof and Bender (1). From these data (1, 17), a graph of the density of aqueous potassium hydroxide was prepared (Figure 5.3-4). For data at temperatures below 0°C, the article by Kelly et al. is useful (16).

The density of aqueous potassium carbonate has also been measured extensively. Puchkov et al. (22) report data from 25 to 300°C for concentrations up to 50 wt% potassium hydroxide. These data are supplemented by data from the International Critical Tables at 0 to 100°C (27). From these data (22, 27), Figure 5.3-5 was prepared for the density of aqueous potassium carbonate.

The densities of other aqueous potassium compounds of interest to the CCG process have not been measured as extensively as the densities of potassium hydroxide and potassium carbonate. For potassium bicarbonate, the International Critical Tables (27) tabulate data from 0 to 100°C for concentrations up to 4 wt% potassium bicarbonate. Chernen'kaya and Revenko (7) graphically and analytically present data at concentrations up to 30 wt% potassium bicarbonate for temperatures from 25 to 75°C. For aqueous potassium bisulfide and potassium sulfide, Bock (4) gives data at 18°C for concentrations up to 50 wt% of the potassium compound.

* References for Section 5.3.3 are listed at the end of the section

Figure 5.3-4

DENSITY OF AQUEOUS POTASSIUM HYDROXIDE

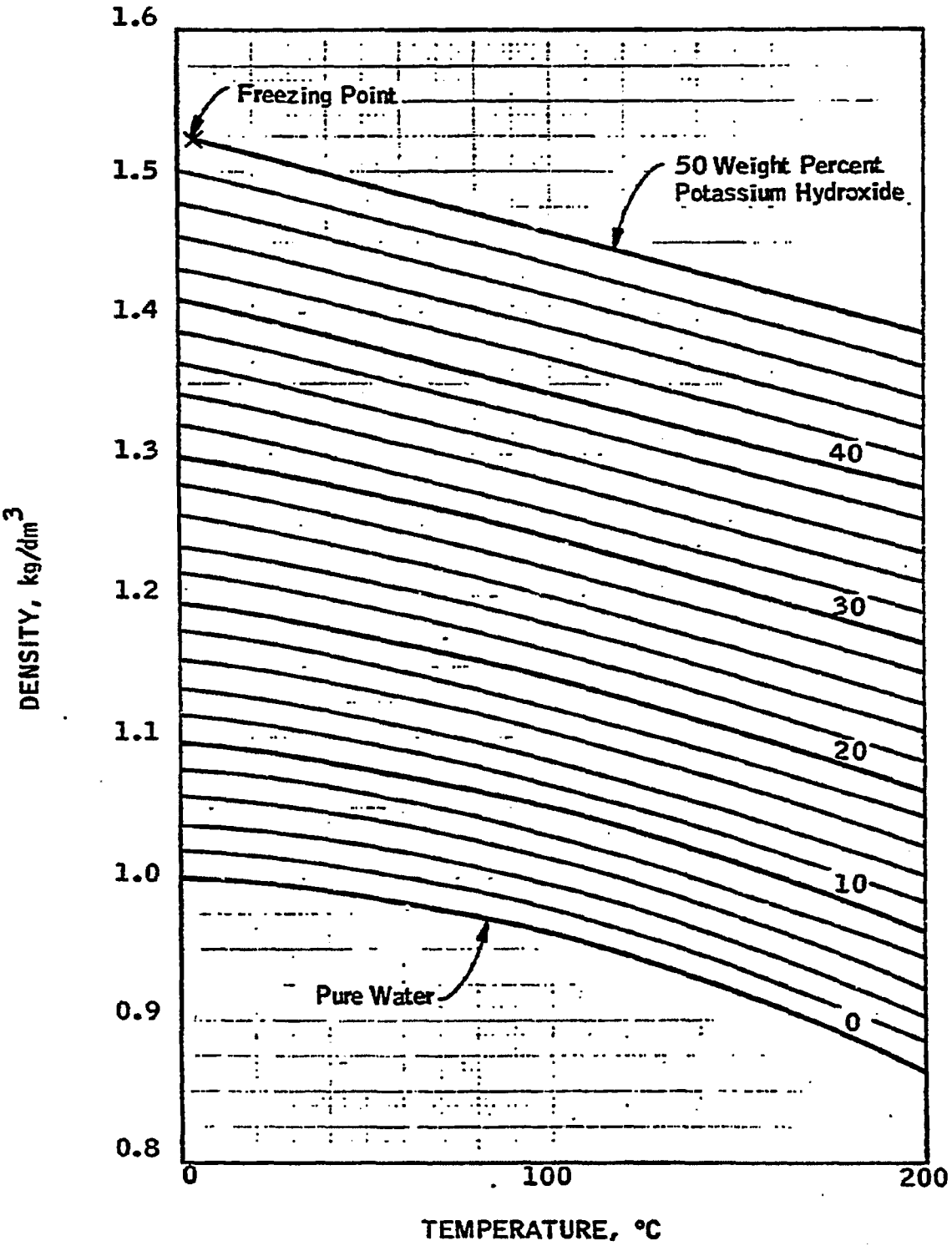

Figure 5.3-5

DENSITY OF AQUEOUS POTASSIUM CARBONATE

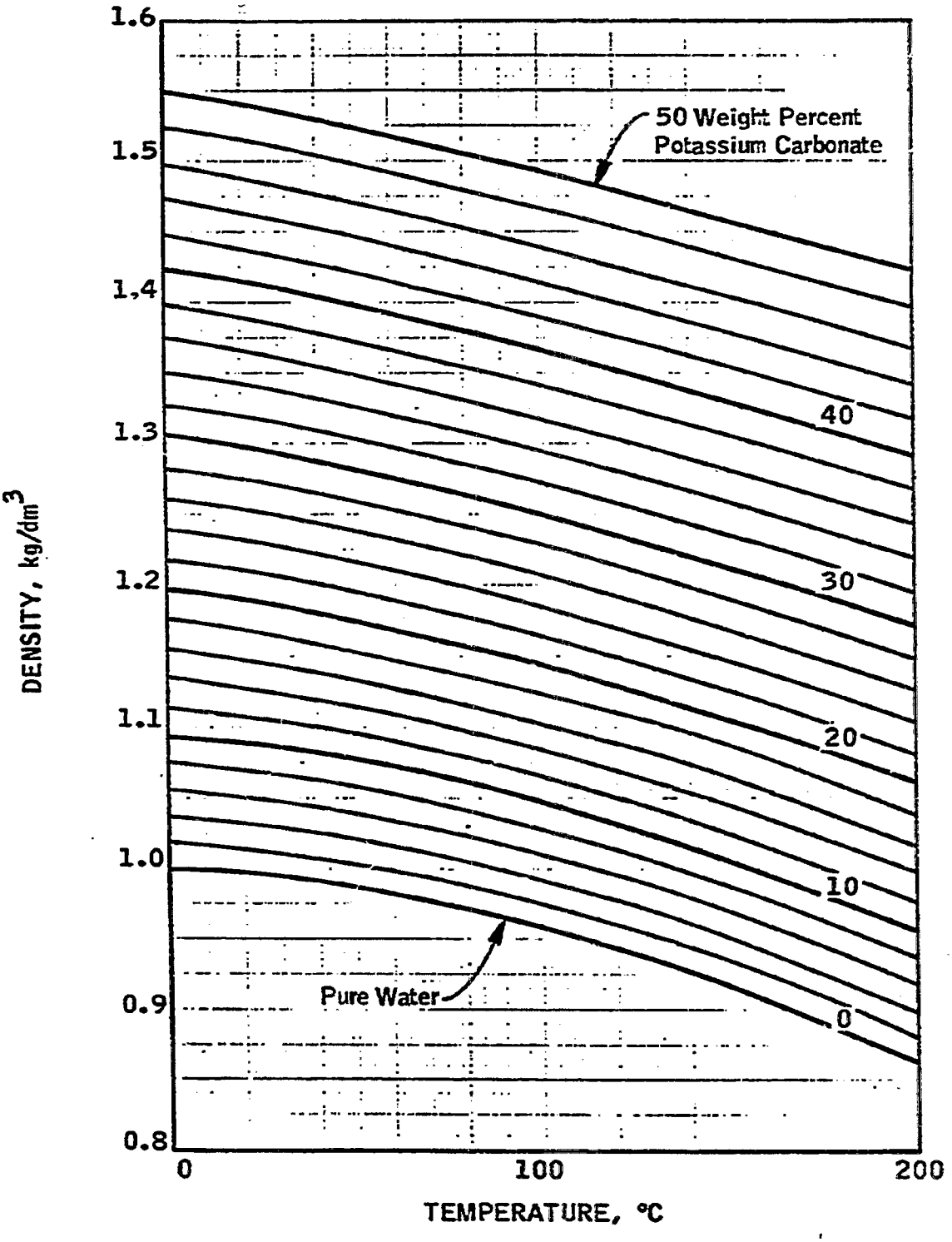

No calculation method for predicting the density of aqueous mixtures containing several potassium compounds can be recommended with confidence. Few experimental data for such mixtures exist to check the reliability of empirical methods and theoretical models are not accurate at the high electrolyte concentrations of interest in the CCG process. Therefore, a simple method was developed from two observations. First, at a given temperature and weight percent dissolved potassium compound, the density of an aqueous solution is relatively insensitive to the exact potassium compound present. For example, at 18°C and 30 wt% total dissolved electrolyte, the densities of aqueous potassium hydroxide (Figure 5.3-4), aqueous potassium carbonate (Figure 5.3-5), and aqueous potassium bisulfide (4) are 1.29, 1.30, and 1.183 kg/dm^3, respectively. The second observation is that the density of a mixture containing two electrolytes is usually between the two densities of each single elctrolyte dissolved in water at the same total weight percent. For example, at 18°C, the density of a solution containing 21 wt% potassium hydroxide and 9 wt% potassium bisulfide is 1.233 kg/dm^3 (4). This value is between the density of 1.29 kg/dm^3 for 30 wt% potassium hydroxide in water and 1.183 kg/dm^3 for 30 wt% potassium bisulfide in water. Based on these observations, it is recommended that the density of a multicomponent mixture be calculated by the following procedure:

(1) Calculate the total weight fraction, w, of electrolyte in the aqueous mixture by summing the weight fractions, w_i, of each electrolyte, i:

$$w = \Sigma\, w_i \qquad \text{(Equation 1)}$$

(2) Determine the density, d_i, of the aqueous solution that each single electrolyte would make if it were dissolved in water at the same temperature and weight fraction, w, of the mixture.

(3) Calculate the mixture density, d_{mix}, from the following equation:

$$d_{mix} = \frac{\Sigma\, w_i d_i}{\Sigma\, w} \qquad \text{(Equation 2)}$$

For example, with the potassium hydroxide/potassium bisulfide mixture mentioned earlier, the calculated density would be (0.21·1.29 + 0.09·1.183)/0.3 = 1.258. This value is 2% higher than the experimental value of 1.233 (4). Densities of aqueous mixtures of potassium hydroxide and potassium carbonate at 20°C (15) are predicted within 1% by Equation 2.

Enthalpy

Ginzburg (11) has prepared a table of the enthalpies of aqueous potassium hydroxide from 25 to 260°C for concentrations from 0 to above 50 wt% potassium hydroxide. These data were used to prepare a graph of the enthalpy of aqueous potassium hydroxide (Figure 5.3-6).

Figure 5.3-6

ENTHALPY OF AQUEOUS POTASSIUM HYDROXIDE

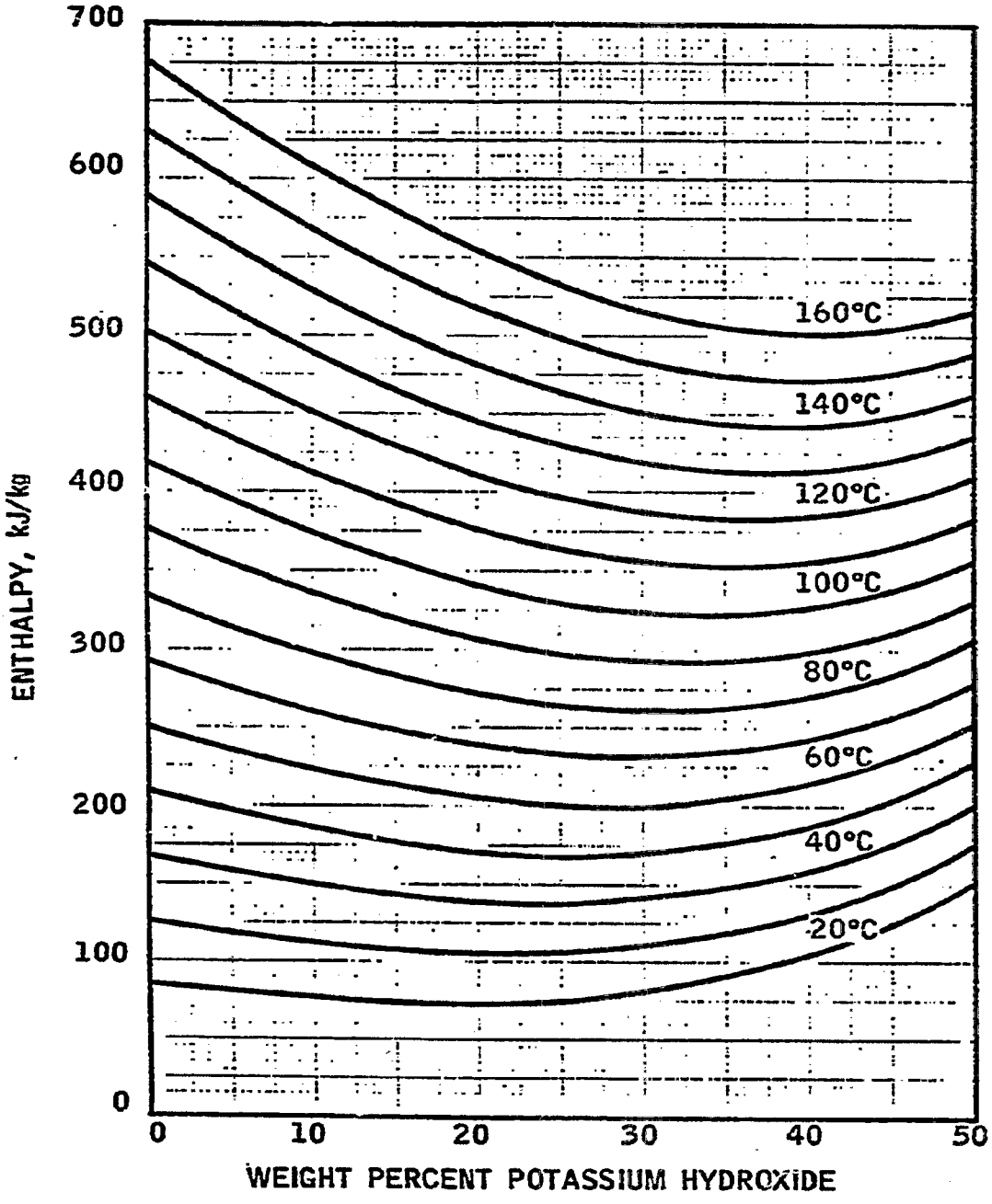

Ginzburg (12) has also prepared a table of enthalpies for aqueous potassium carbonate. This table is based on the heat capacity data of Ginzburg and Kochkaida (13) and the 1952 heat of dilution values of Rossini. Unfortunately, heat of dilution data for potassium carbonate are uncertain. For example, NBS Circular 500 (23) differs from a more recent NBS publication (26) even on the sign of the heat of dilution. Therefore, caution must be applied when doing calculations that are sensitive to the heat of dilution of aqueous potassium carbonate. Figure 5.3-7 is based on Ginzburg's tabular data (12).

Few data were found for the enthalpies of aqueous potassium bicarbonate, potassium disulfide, and potassium sulfide. Chernen'kaya and Bratash (6) give the heat capacity of potassium bicarbonate from 25 to 50°C for concentrations up to 30 wt%. NBS Circular 500 (23) provides heat of dilution data at 25°C for potassium bisulfide and potassium sulfide.

No enthalpy data were found for multicomponent mixtures of potassium compounds of interest to the CCG process. Until such data are available, it is recommended that the enthalpy of multicomponent mixtures be calculated by the following procedure:

(1) Calculate the total weight fraction, w, of electrolyte in the aqueous mixture by summing the weight fractions, w_i, of each electrolyte, i, using Equation 1.

(2) Determine the enthalpy, h_i, of the aqueous solution that each single electrolyte would make if it were dissolved in water at the same temperature and weight fraction, w, of the mixture.

(3) Calculate the mixture enthalpy, h_{mix}, from the following equation:

$$h_{mix} = \frac{\Sigma\, w_i h_i}{w} \qquad \text{(Equation 3)}$$

It is necessary that a consistent set of base enthalpies be used in these calculations.

Viscosity

Mashovets et al. (19) tabulate the viscosity of aqueous potassium hydroxide from 0 to 275°C for concentrations up to about 50 wt% potassium hydroxide. These data, along with data for pure water (3), were used to construct Figure 5.3-8. For temperatures below 0°C, the article by Kelly et al. (16) should be consulted.

For the viscosity of aqueous potassium carbonate, the data of Mostinskii et al. are the most extensive (20). However, these data only range from 30 to 90°C for concentrations of potassium carbonate up to 50 wt%. To extrapolate these data to different temperatures, a viscosity parameter, B, was calculated for each datum:

Figure 5.3-7

ENTHALPY OF AQUEOUS POTASSIUM CARBONATE

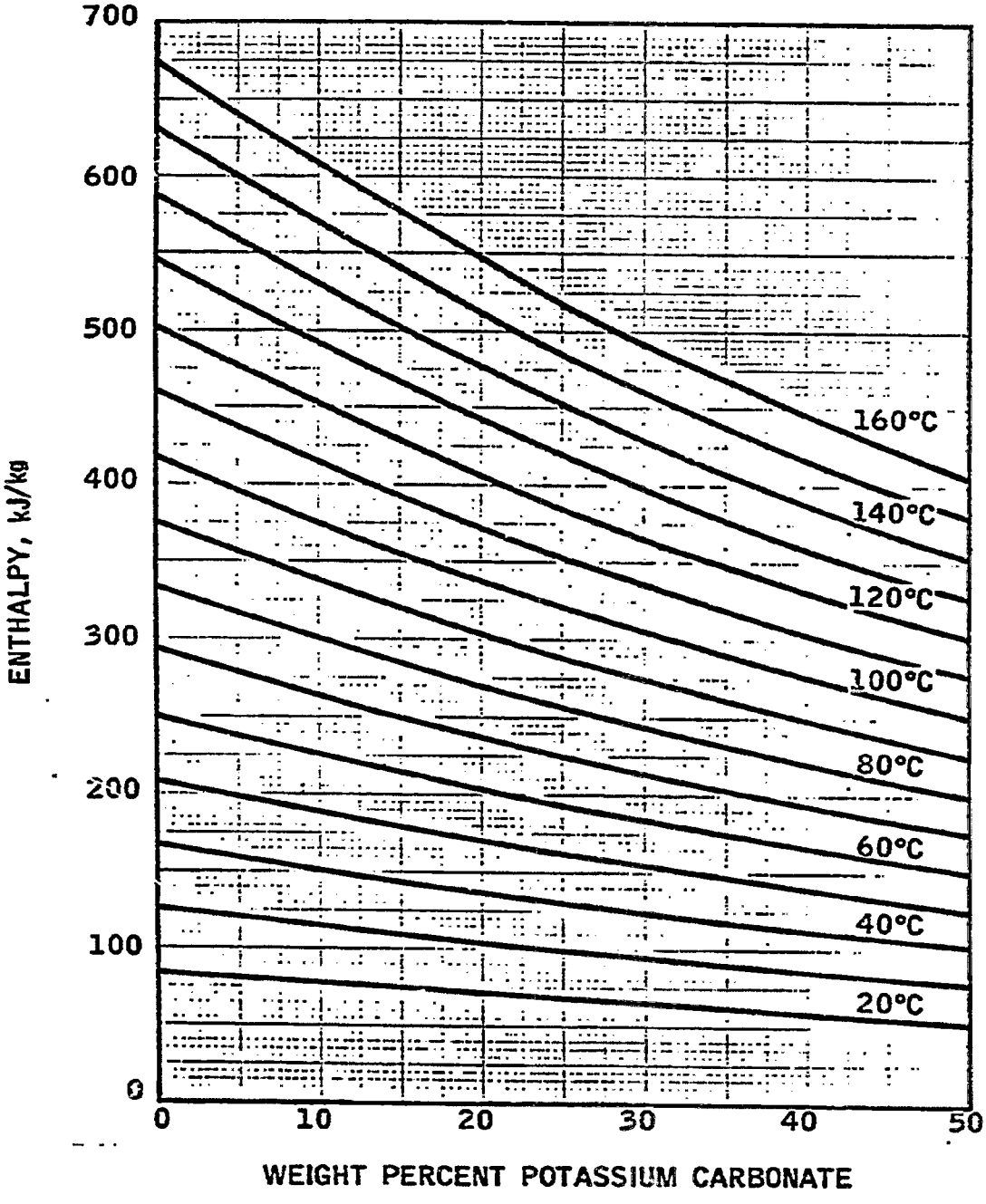

Figure 5.3-8

VISCOSITY OF AQUEOUS POTASSIUM HYDROXIDE

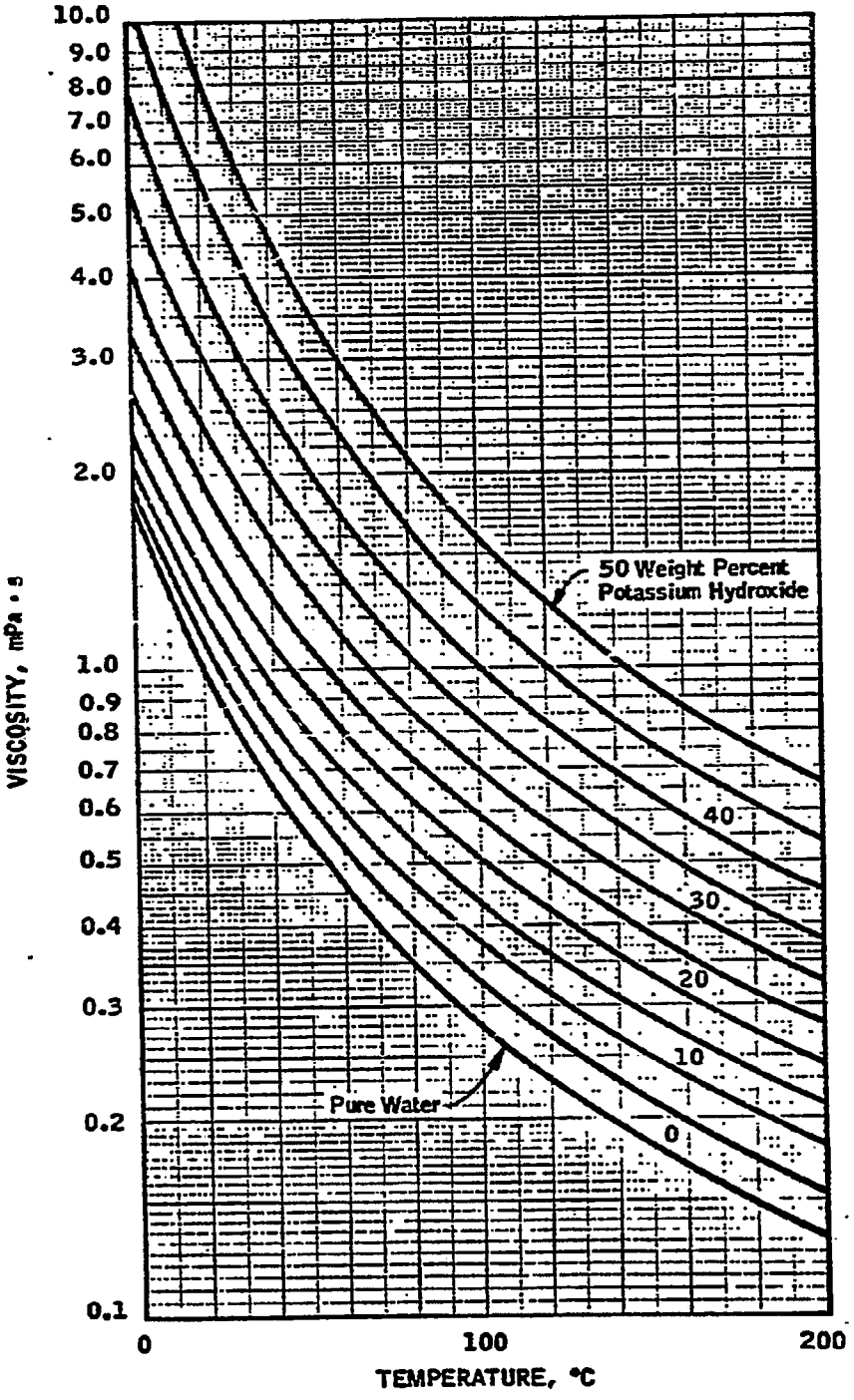

$$B = \left(\frac{v}{v_o} - 1 \right)/m \qquad \text{(Equation 4)}$$

where v is the solution viscosity at molality m and v_o is the viscosity of pure water at the same temperature as the solution. Equation 4 is similar to an equation suggested by Harned and Owen (14). The calculated viscosity parameters seemed to be linear in temperature, at a constant molality, and thus were easily extrapolated. Rearrangement of Equation 4, combined with viscosity values for pure water (3) allowed for the calculation of the viscosity of aqueous potassium carbonate from 0 to 160°C. These calculated viscosities are shown in Figure 5.3-9.

For potassium bicarbonate, only the graphical data of Chernen'kaya and Revenko were found (7). No data were found for potassium bisulfide or potassium sulfide. This is unfortunate since the aqueous viscosity of a single electrolyte is not easily predicted. One complication is the compositional dependence of viscosity. Chesnokov (8) reports that, at 20°C, the viscosities of aqueous potassium nitrate, potassium chloride and potassium bromide decrease with increasing electrolyte concentration whereas the viscosities of aqueous potassium carbonate and potassium sulfate increase with increasing electrolyte concentration. Chesnokov (8) also reports that the viscosity of aqueous potassium iodide goes through a minimum as its concentration is increased at 20°C.

For predicting the viscosity of a multicomponent aqueous mixture of electrolytes, the following procedure is recommended:

(1) Calculate the total weight fraction, w, of electrolyte in the aqueous mixture by summing the weight fractions, w_i, of each electrolyte using Equation 1.

(2) Determine the viscosity, v_i, of the aqueous solution that each single electrolyte would make if it were dissolved in water at the same temperature and weight fraction, w, as the mixture.

(3) Calculate the mixture viscosity, v_{mix}, from the following equation:

$$v_{mix} = \frac{\Sigma w_i v_i}{w} \qquad \text{(Equation 5)}$$

A test of Equation 5 with viscosity data for aqueous mixtures of potassium hydroxide and potassium carbonate, at 20°C and 40°C, showed errors of less than 5% (15). Larger errors can be anticipated for other electrolyte mixtures since aqueous potassium hydroxide and aqueous potassium carbonate have similar viscosities at the same temperature and weight fraction electrolyte.

Figure 5.3-9

VISCOSITY OF AQUEOUS POTASSIUM CARBONATE

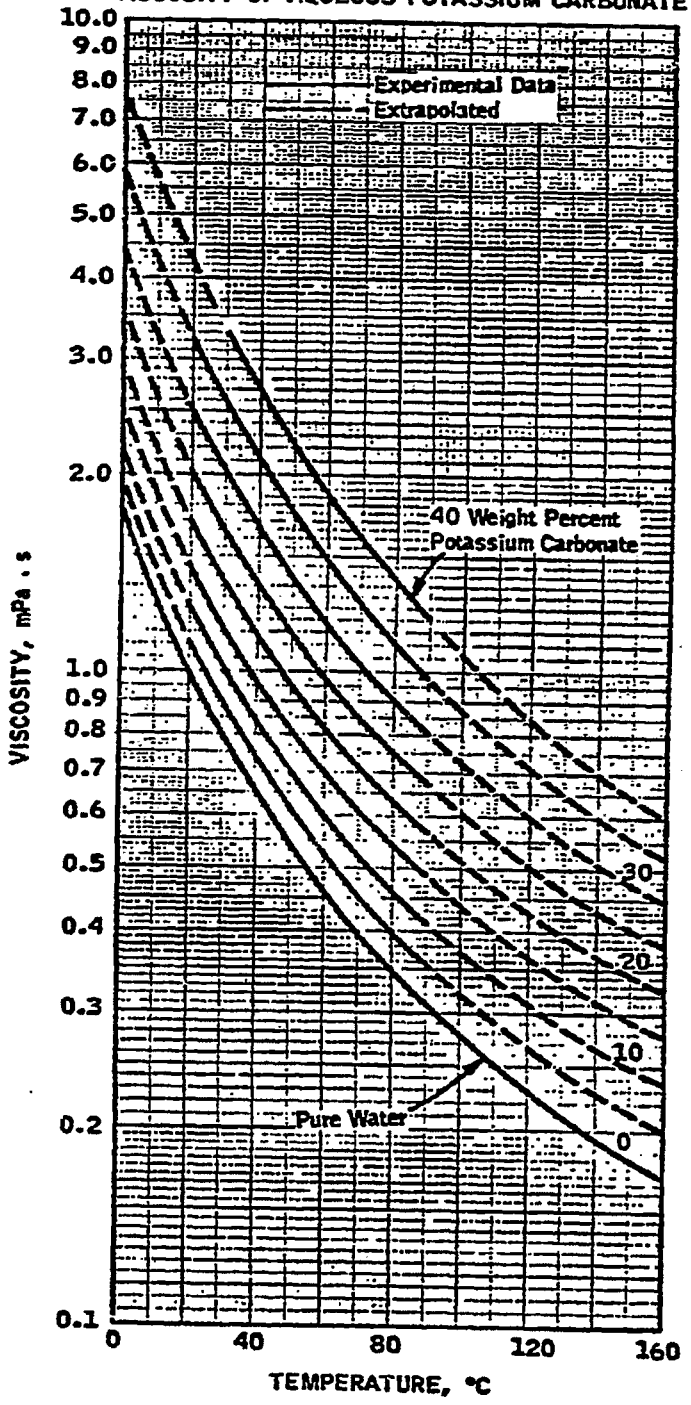

Boiling Point

Mashovets et al. (18) tabulate accurate data on the saturation pressure of aqueous solutions containing up to 49 wt% potassium hydroxide in the temperature range of 25 to 350°C. These data were used to construct Figure 5.3-10 for the boiling temperature of aqueous potassium hydroxide. For potassium carbonate, data from two articles (21, 22) were used to construct Figure 5.3-11. Puchkov and Kurochkina (21) tabulate saturation pressures of aqueous solutions containing up to 51 wt% potassium carbonate at temperatures from 25 to 90°C, while Puchkov et al. (22) tabulate data from 125 to 300°C.

No data were found for the saturation pressure of aqueous potassium bicarbonate, potassium bisulfide, and potassium sulfide. However, unlike potassium hydroxide and potassium carbonate, the saturated vapor above aqueous solutions of potassium bicarbonate and potassium bisulfide may not be essentially pure water. In the case of potassium bicarbonate, most of the vapor may be carbon dioxide (25). This can occur since potassium bicarbonate can react to form carbon dioxide ($2KHCO_3 = K_2CO_3 + CO_2 + H_2O$) and carbon dioxide is only slightly soluble in water. For mixtures of potassium carbonate, potassium bicarbonate, and potassium bisulfide, a significant fraction of the vapor can be hydrogen sulfide (24). Information about boiling temperature at a given pressure and liquid composition, such as Figures 5.3-10 and 5.3-11, will not be sufficient knowledge for such electrolytes. The composition in the vapor phase needs to be known in order to accurately calculate heat and material balances.

Four recent papers have presented models for calculating vapor-liquid equilibria in electrolyte solutions (2, 5, 9, 10). The model by Chen et al. (5) and the model by Cruz and Renon (9) are designed for high, as well as low, concentrations of electrolytes. However, these two models are too complicated for hand calculations and they contain many parameters which can only be determined from large amounts of experimental data. In general, these experimental data do not exist. The models, and computer programs, of Edwards et al. (10) and of the American Petroleum Institute (2) were evaluated in a separate program (described in the preceding section of this report). It was concluded that the computer program furnished by Edwards et al. (10) was not general enough to handle potassium-containing electrolytes. Changes in the computer code are required before conclusions can be reached about this model. The model by the American Petroleum Institute (2) can handle potassium-containing electrolytes. However, it is not accurate for predicting the partial pressure of compounds above potassium-containing solutions. Calculated partial pressures were off by as much as a factor of ten. A proprietary ER&E model also gives large errors with potassium-containing solutions.

It is recommended that the next phase of CCG development include a technology study to further develop methods for predicting the vapor-liquid equilibria of aqueous solutions containing up to 40 wt% potassium-containing electrolytes. Such a study would include the measurement of experimental

Figure 5.3-10

BOILING TEMPERATURE OF
AQUEOUS POTASSIUM HYDROXIDE

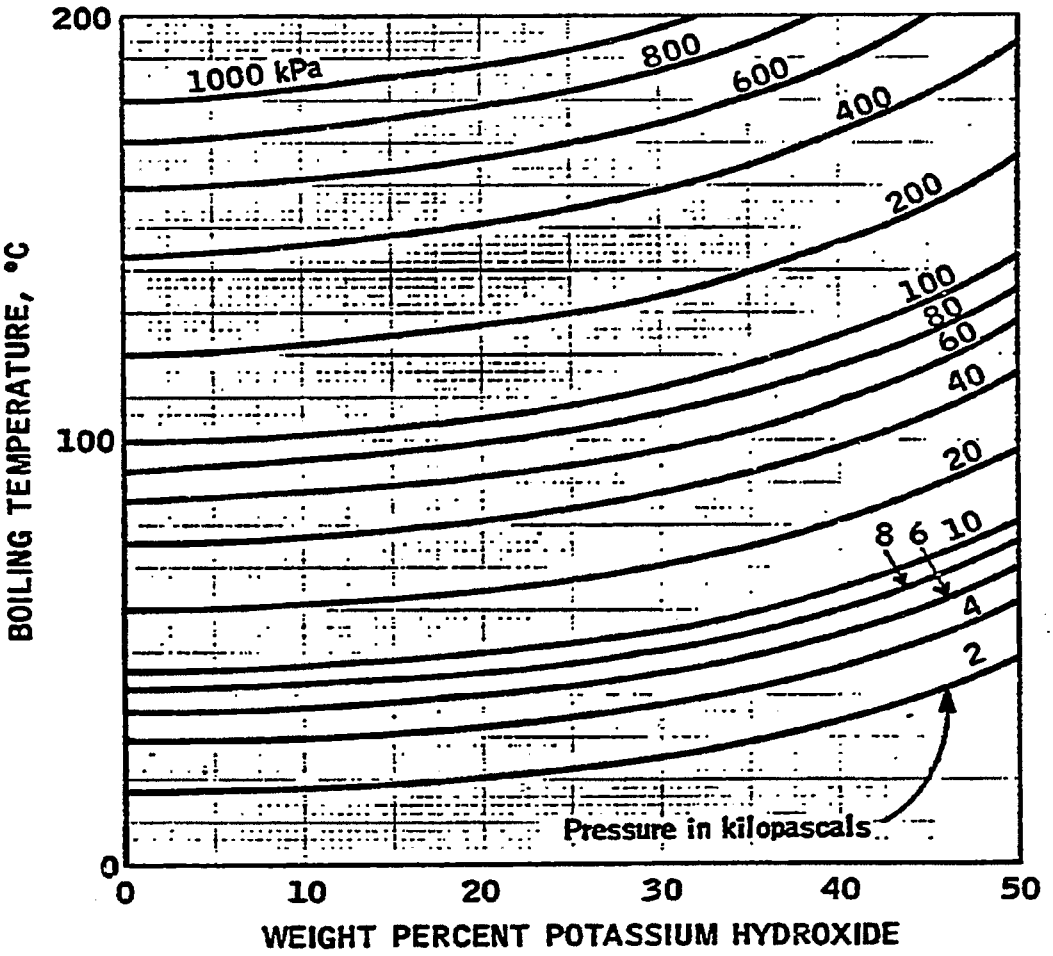

Figure 5.3-11

BOILING TEMPERATURE OF
AQUEOUS POTASSIUM CARBONATE

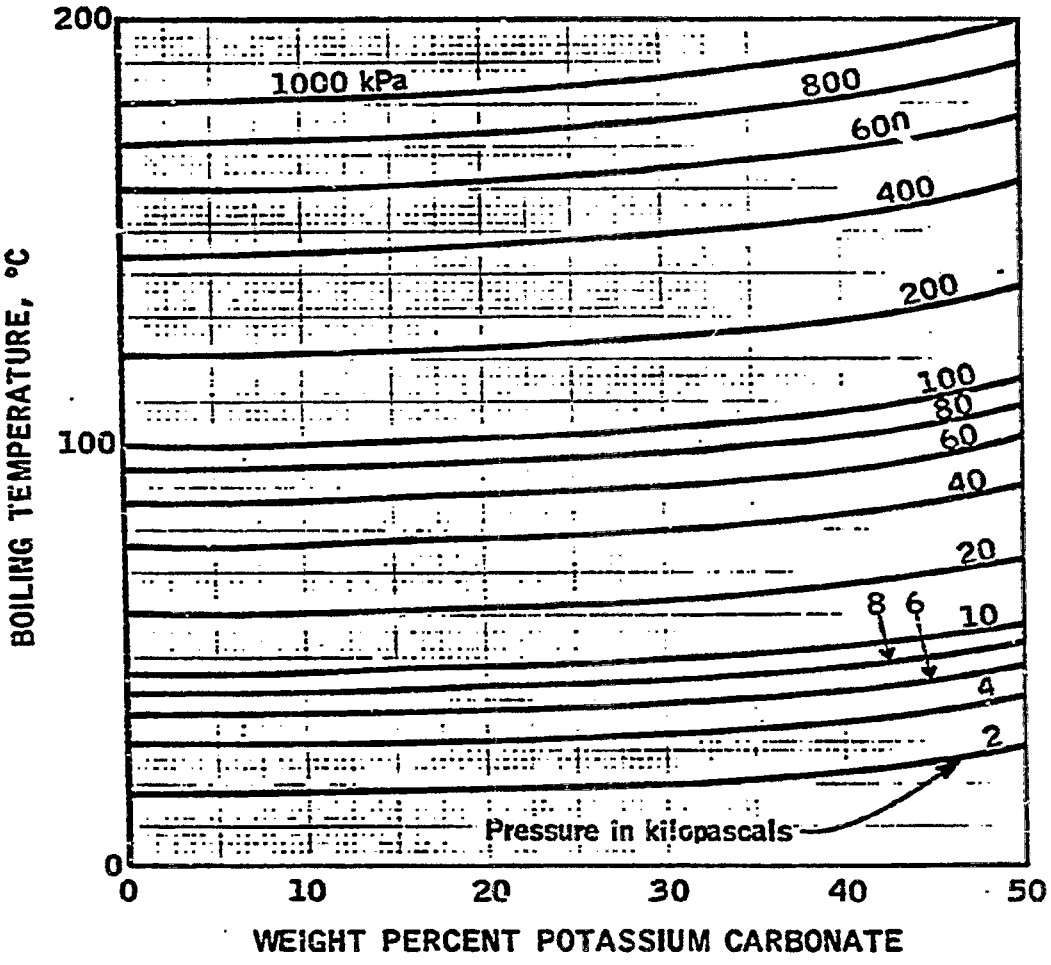

data as well as development of a computer program to calculate vapor-liquid equilibria. Until such a study is done, the vapor-liquid equilibrium data developed under the engineering technology program described previously can be used for guidance.

References for Section 5.3.3

(1) Akerlof, G., and Bender, P., "The Density of Aqueous Solutions of Potassium Hydroxide," J. Amer. Chem. Soc., 63, 1085-88 (1941).

(2) American Petroleum Institute, "A New Correlation of NH_3, CO_2, and H_2S Volatility Data from Aqueous Sour Water Systems," API Publication 955, March 1978, Washington, D.C.

(3) American Society of Mech. Eng., "ASME Steam Tables", 3rd Ed., New York, 1977.

(4) Bock, O., "The Electrical Conductivity of Compounds of Sulfur and Potassium in Solutions of Sodium Sulfide and Boric Acid", Annalen der Physik, 30, 631-638 (1887).

(5) Chen, C.-C., Britt, H. I., Boston, J. F. and Evans, L. B., "Extension and Application of the Pitzer Equation for Vapor-Liquid Equilibrium of Aqueous Electrolyte Systems with Molecular Solutes", AIChE J., 25(5), 820-831 (1979).

(6) Chernen'kaya, E. I. and Bratash, E. G., "Heat Capacities of Solutions of K_2CO_3, Na_2CO_3, $KHCO_3$, K_2SO_4 and KCl", Tr. N.-i. proekt. in-t osnovn. khimii, 34, 18-22 (1974).

(7) Chernen'kaya, E.I. and Revenko, S. S., "Viscosity and Density of K_2CO_3 and $KHCO_3$ Solutions", J. Appl. Chem. USSR, 48(1), 121-124 (1975).

(8) Chesnokov, N. A., "The Viscosity of Aqueous Solutions of Inorganic Salts", Tr. Vses. Nauchn.-Issled. Inst. Metrol., 62, 44-51 (1962).

(9) Cruz, J.-L., and Renon, H., "A New Thermodynamic Representation of Binary Electrolyte Solutions Nonideality in the Whole Range of Concentrations", AIChE J., 24(5), 817-830 (1978).

(10) Edwards, T. J., Maurer, G., Newman, J. and Prausnitz, J. M., "Vapor-Liquid Equilibria in Multicomponent Aqueous Solutions of Volatile Weak Electrolyte", AIChE J., 24(6), 966-976 (1978).

(11) Ginzburg, D. M., "Enthalpies in the Potassium Hydroxide-Water System", Tr. N.-i. proekt. in-t osnovn. khimii, 34, 35-40 (1974).

(12) Ginzburg, D. M., "Enthalpies in the Systems Na_2CO_3-H_2O and K_2CO_3-H_2O," J. Appl. Chem. USSR, 47(10), 2267-2270 (1974).

(13) Ginzburg, D. M. and Kochkalda, V. E., "Enthalpies and Specific Heats in the Potassium Carbonate-Water System", Russian J. Phys. Chem., 46(10), 1535 (1972).

(14) Harned, H. S. and Owen, B. B., "The Physical Chemistry of Electrolyte Solutions", ACS Monograph Series #137, 3rd Ed., p. 238, Reinhold Publishing Corp., New York, 1958.

(15) Hitchcock, L. B. and McIlhenny, J. S., "Viscosity and Density of Pure Alkaline Solutions and Their Mixtures", Ind. Eng. Chem., 27(4), 461-6 (1935).

(16) Kelly, W. R., Borza, P. F., and Harriger, R. D., "Densities and Viscosities of Potassium Hydroxide Solutions at Low Temperatures", J. Chem. Eng. Data, 10(3), 233-4 (1965).

(17) Mashovets, V. P., Dibrov, I. A., Krumgal'z, B. S., and Matveeva, R. P., "Density of Aqueous Solutions of KOH at High Temperatures over a Wide Range of Concentrations", J. Appl. Chem. USSR, 38(10), 2297-2299 (1965).

(18) Mashovets, V. P., Penkina, N. V., Puchkov, L. V., and Kurochkina, V. V., "Saturated Vapor Pressure Over Solutions in the System K_2O-Al_2O_3-H_2O in the 25-350°C Temperature Range", J. Appl. Chem. USSR, 44(2), 334-7 (1971).

(19) Mashovets, V. P., Puchkov, L. V., Sargaev, P. M. and Fedorov, M. K., "Viscosities of Lithium, Sodium and Potassium Hydroxide Solutions at Temperatures up to 275°C", J. Appl. Chem. USSR, 46(5), 1055-8 (1973).

(20) Mostinskii, L. L., Nekhoroshev, R. S., and Sizov, M. V., "Viscosity of Aqueous Solutions of Potassium and Cesium Carbonates", VINITI No. 1315-74, Abstract in Zh. Fiz. Khim, 48(8), 2146 (1974).

(21) Puchkov, L. V. and Kurochkina, V. V., "Vapor Pressure of Aqueous Potassium Carbonate Solutions", J. Appl. Chem. USSR, 43(1), 175-177 (1970).

(22) Puchkov, L. V., Kurochkina, V. V., and Matveeva, R. P., "Density and Pressure of the Saturated Vapor of Aqueous Solutions of Potassium Carbonate at Temperatures up to 315°C", VINITI No. 3476-76; Abstract appears in J. Appl. Chem. USSR, 50(6), 1381 (1977).

(23) Rossini, F. D., Wagman, D. D., Evans, W. H., Levine, S., and Jaffe, I., "Selected Values of Chemical Thermodynamic Properties, Part 1", NBS Circular 500, February 1, 1952. Reprinted July 20, 1961.

(24) Tosh, J. S., Field, J. H., Benson, H. E., and Anderson, R. B., "Equilibrium Pressures of Hydrogen Sulfide and Carbon Dioxide Over Solutions of Potassium Carbonate", U.S. Bureau of Mines, Report of Investigations 5622, 1960.

(25) Tosch, J. S., Field, J. H., Benson, H. E., and Haynes, W. P., "Equilibrium Study of the System Potassium Carbonate, Potassium Bicarbonate, Carbon Dioxide, and Water", U.S. Bureau of Mines, Report of Investigations 5484, 1959.

(26) Wagman, D. D., Evans, W. H., Parker, V. B., and Schumm, R. H., "Chemical Thermodynamic Properties of Compounds of Sodium, Potassium and Rubidium: An Interim Tabulation of Selected Values", NBS Interim Report 76-1034, National Technical Information Service #PB-254 460, April 1976.

(27) Washburn, E. W., (Ed.), "International Critical Tables", Vol. III, p. 90, McGraw-Hill, 1928.

5.3.4 Solid-Liquid Separations for Catalyst Recovery

The recovery of potassium catalyst from CCG gasifier char and fines is accomplished by washing the spent gasifier solids with water. The solids may be first "digested" by contacting with calcium hydroxide to increase the proportion of potassium which is water soluble. The soluble potassium is then counter-currently leached from the solids. The catalyst recovery system design depends on the solid-liquid separation efficiency between leaching stages. The prime objective of this program is to identify and evaluate alternatives for the solid-liquid separations in catalyst recovery and waste solids disposal.

Summary

This program has identified and evaluated several solid-liquid separations devices for catalyst recovery and waste solids disposal. Filters and gravity settlers are viable candidates for the separation based on laboratory studies, and larger-scale testing of these devices is recommended. Hydroclones are unlikely to be suitable because solids particle sizes were found to be too small for efficient and economical collection. Centrifuges were rejected as being too expensive.

The primary focus of the program was placed on filtration, especially on the influence of slurry pretreatment and slurry handling on filterability. Filter cake washing for potassium recovery was also studied.

Laboratory batch filtration tests on Fluid Bed Gasifier (FBG) chars showed that filtration rates for the lime "digested" solids were 4-60 gph/ft^2, far below desirable commercial rates, even with the use of flocculants and filter aids (body feeds). The water-washed, "undigested" slurry showed filtration rates of 100-230 gph/ft^2, well within the commercial range. The use of a flocculant (25 ppm D-25A) further improved the filtration rate of the undigested solids to 300-600 gph/ft^2.

Filter cake washing experiments were conducted to determine how to recover the most catalyst while using a minimum amount of wash water. Experiments on flocculated cakes indicated that 40% of the soluble potassium in the residual cake water was recovered with a wash ratio (wash water/residual cake water) of 1.0. Higher rates increased catalyst recovery but caused an undesirable dilution of the catalyst.

As slurry passes through pumps and pipes, solids can attrit. Since particle size distribution affects the behavior of filters and other solid-liquid separations devices, a laboratory program was conducted to determine the attritability of unflocculated PDU bottoms char and slurry (char plus cyclone fines). These materials were found to attrit slowly at fluid shear rates likely to be found in a commercial CCG plant. However, the rate of attrition was sufficiently slow that it would not likely adversely affect the solid-liquid separation of unflocculated char under ordinary CCG plant operating conditions. The attrition of flocculated char was not studied, nor were tests of the filterability of attrited slurry carried out. Such tests are recommended.

Filtration Studies

Laboratory batch pressure filtration experiments were run to measure the filtration rate and the cake resistance of slurries made from Fluid Bed Gasifier solids which were pretreated in different ways (e.g., digested with lime or undigested).

Filtration runs were carried out in one of two filter cells: a 320 ml cell with a 5 μm fluorocarbon coated filter medium or a 120 ml cell with a 40 μm (U.S. Filter PZ-40) screen medium. The area of the medium was the same in both cells; the volume of slurry equaled the cell volume. During a test, a slurry sample was heated to 190°F in a supply reservoir; it was forced into the heated filter cell by compressed nitrogen; the valve at the cell bottom was immediately opened to withdraw the filtrate; and the constant pressure filtration run was begun. Potassium concentration in the filtrate was measured with a specific ion electrode.

Table 5.3-15 shows the filtration rate, cake resistance, residual cake water, and other experimental data for all runs using the 320 ml filter cell. Slurry feed data are presented in Table 5.3-16.

The digested char samples D26, D39, and D44 without filter aid showed a wide variation in filtration rates, but the rates observed are generally 4-10 gph/ft^2 which is lower than the desirable threshold level of 100 gph/ft^2 for commercial filters. Though body feeds and flocculant improved the filtration rate for most samples, the rates for these digested samples were still only 20-60 gph/ft^2. Filtration rates for the water-washed (undigested) char samples D31 and D32 (100-230 gph/ft^2) are in the typical commercial range.

Table 5.3-15

LABORATORY BATCH FILTER RESULTS
(320 ml FILTER CELL)

Sample	Differential Pressure (psig)	Average Filtration Rate (4) (gph/ft²)	Cake Resistance (ft/lb x 10⁻¹⁰)(10)	Residual Cake Water (wt%)	Feed Solids (5) (wt%)	Filtrate K⁺ (6) (wt%)	Flocculant or Body Feed Type	Body Feed/ Char Ratio
D31 (1,3,8)	15	140	1.7	-	2.6	3.9	-	0
D31 "	20	197	1.7 (11)	-	2.6	3.9	-	0
D31 "	25	234	2.6	-	2.6	3.9	-	0
D32 (1,3,8)	25	103	9.0	70	3.5	0.74	-	0
D32 "	20	66	10.1 (12)	72	3.5	0.78	-	0
D32 "	15	63	9.0	69	3.5	0.69	-	0
D26 (1,3,7)	30	3.8	150	61	11.4	5.3	-	0
D26 "	50	4.6	260 (13)	68	11.4	5.7	-	0
D26 "	62	5.1	220	53	11.4	6.0	-	0
D26 "	71.5	19.9	.21	29	25.1	2.3	Body Feed A	1.0
D26 "	71.5	8.3	300	70	6.9	2.2	-	0
D26 "	71.5	6.9	120	68	13.2	5.4	Body Feed A	0.16
D26 "	71.5	8.5	310	67	7.1	3.6	-	0
D26 "	71.5	14.8	63	65	11.2	3.2	Body Feed A	0.38
D26 "	50.8	16.0	43	71	12.3	3.1	Body Feed A	0.38
D26 "	50.8	14.1	46	69	11.6	3.0	Body Feed B	0.38
D26 "	71.5	25.9	32	69	11.7	2.0	Body Feed B	0.38
D26 "	30.5	8.4	52	73	11.4	2.8	Body Feed B	0.38
D39 (2,3,7)	60	42	12	68	10.8	2.2	-	0
D39 "	50	71	5.7	68	10.1	2.3	D-25A/25 ppm	0
D39 "	60	57	6.1	68	12.9	2.6	D-25A/50 ppm	0
D39 "	60	38	10.5	67	12.1	2.3	A-1906N/10 ppm	0
D39 "	60	35	13.0	68	12.3	2.3	A-1906N/5 ppm	0
D39 "	60	59	6.2	68	12.4	2.3	D-25A/25 ppm and A-1906N/5 ppm	0
D44 (2,3,7,9)	30	5.8	350	64	6.5	5.0	-	0
D44 "	40	5.8	220	64	6.7	5.5	-	0
D44 (2,3,7)	40	3.9	260	54	16.8	9.9	-	0
D44 (2,3,7,9)	70	7.8	220	62	8.6	5.8	D-25A/25 ppm	0

Notes:

(1) Temperature = 180°F.
(2) Temperature = 190°F.
(3) All tests done using a 5 μm Fluorocarbon coated medium.
(4) Cell volume constant at 320 ml.
(5) Corrected for K⁺.
(6) By specific ion electrode.
(7) Digested char and fines plus lime.
(8) Undigested char and fines.
(9) Water added to dilute the original sample.
(10) Obtained from constant pressure filtration equations as described in Purchas, D. B., Solid/Liquid Separation Equipment Scaleup, Uplands Press Ltd., Croydon, England, 1977, p. 42 ff.
(11) Cake compressibility 0.77. See note (10).
(12) Cake compressibility 0.02. See note (10).
(13) Cake compressibility 0.65. See note (10).

Table 5.3-16

SUMMARY OF BATCH FILTRATION SAMPLES(1)

Sample	Description	Particle Size Distribution % <10μm	Particle Size Distribution % <44μm	Wt% K^+ In Solution
D26	22 lbs char, no fines, 11 lbs lime, 176 lbs of 3.29 wt% K^+ solution digested for 1 hr at 300°F using old digester and pump	71	79	4.55
D31(2)	30 lbs char, 10 lbs fines, no lime, 305 lbs 2.39 wt% K^+ solution, leached with 2.87% K^+ solution, overflow from leaching tank	5	16	Approx. 3.5
D32(2)	5 lbs char, 2 lbs fines, 160 lbs water	6	12	Approx. 1
D39	15 lbs char, 6 lbs fines, 10 lbs lime, 168 lbs 0.58 wt% K^+ solution digested for 1 hr at 300°F, no pump, new digester	12	75	2.72
D44	20 lbs char, 9.2 lbs fines, 5.3 lbs lime, 158 lbs 9.61 wt% K^+ solution digested for 1 hr at 300°F, no pump, new digester	28	57	11.58

Note:

(1) Char and fines solids used to make up these samples were obtained from the Fluid Bed Gasifier (FBG).

(2) Assumes particle size distribution is the weighted average of the particle size distributions for the char and fines used to prepare sample D44.

Flocculant and body feed generally increase the filtration rate for digested solids (Table 5.3-15). The use of D-25A (25 ppm) flocculant increased the filtration rate by a factor of 1.7 for D39 at 50 psi differential pressure. The only sample for which flocculant had no effect was D44. Body feeds had similar effects on filtration rate. However, the use of body feed is not economically attractive. Subsequent filtration runs concentrated on the effects of the D-25A flocculant.

Additional filtration studies were carried out in the 120 ml test cell on undigested char with and without flocculant (Table 5.3-17). These studies confirmed that undigested char gave much higher filtration rates than were seen with digested char. Samples filtered with and without flocculant at equal pressure differences (20.3 psi) gave filtration rates of about 300 gph/ft^2 and 120-180 gph/ft^2, respectively, for the period in which more than 90% of the filtrate volume was collected.

The 120 ml filter cell filters faster (less than 1 minute) and has smaller cake thickness (3") than the 320 ml cell (3-6 minutes and 7"). Since commercial filters usually have rates and cake thicknesses more like the 120 ml cell, the filtration rates in Table 5.3-17 are probably more typical of what a commercial filter would give.

Larger-scale tests using continuous commercial-type filters (e.g., vacuum rotary drum, pressure rotary drum, and vacuum horizontal belt filters) are recommended for confirming filtration rates under operating conditions.

Cake Washing

Additional experiments were carried out to evaluate vacuum belt filtration and cake washing to reduce the filter staging requirements. The washing was done by drawing one liter of heated distilled water through the cake immediately following cake formation with flocculant. Washing was done only in the 120 ml cell at the same pressure as the initial filtration (Table 5.3-17). During the washing experiments, the flocculated cakes showed a tendency to compress slightly. This was especially true at the higher pressure differentials.

Samples of the filtrate wash water were collected at intervals and analyzed for K^+ concentration with the specific ion electrode. These data in Figure 5.3-12 indicate that the wash filtrate concentration decreased sharply up to a wash ratio of N = 1 (N = wash water/residual cake water). At N greater than 4, the K^+ concentration leveled out at between 700 and 900 ppm, and further recovery was slow. The percent soluble K^+ recovered from the cake residual water due to washing (Figure 5.3-13) was obtained by a mass balance of the K^+ concentration in Figure 5.3-12. Figure 5.3-13 shows that 40% of the K^+ remaining in the residual cake water after filtration was recovered after only one displacement washing (N = 1). This ratio is typical of belt filter washing.

Table 5.3-17

LABORATORY BATCH FILTER RESULTS
(120 ml FILTER CELL)

Run(1)	Differential Pressure (psig)	Average Filtration Rate (gph/ft^2)	Specific Cake Resistance (3) ($ft/lb \times 10^{-10}$)	Residual Cake Moisture (wt%)	Feed Solids (wt%)	Filtrate K^+ (wt%)	Comments
FC34 (2)	10.2	324	0.8	74	11.6	5.4	D-25A/25 ppm
FC39 (2)	20.3	312	(0.2)	71	10.7	5.4	"
FC38 (2)	35.5	510	1.2	71	9.2	4.9	"
FC37	10.2	420	0.6	65	11.9	4.7	"
FC35	20.3	162	2.4	65	11.6	5.3	No Flocculant

Notes:

(1) Two undigested FBG char slurry samples, shipped from Baytown 11/28/79. One sample used for FC34 through FC39. PZ40 screen filter media used.

(2) Cake washing experiments carried out after these runs (see Figure 5.3-12).

(3) Obtained from constant pressure filtration equations as described in Purchas, D. B., Solid/Liquid Separation Equipment Scaleup, Uplands Press Ltd., Croydon, England, 1977, p. 42 ff.

Figure 5.3-12

CCG SOLIDS WASHING
FILTRATE K^+ CONCENTRATION

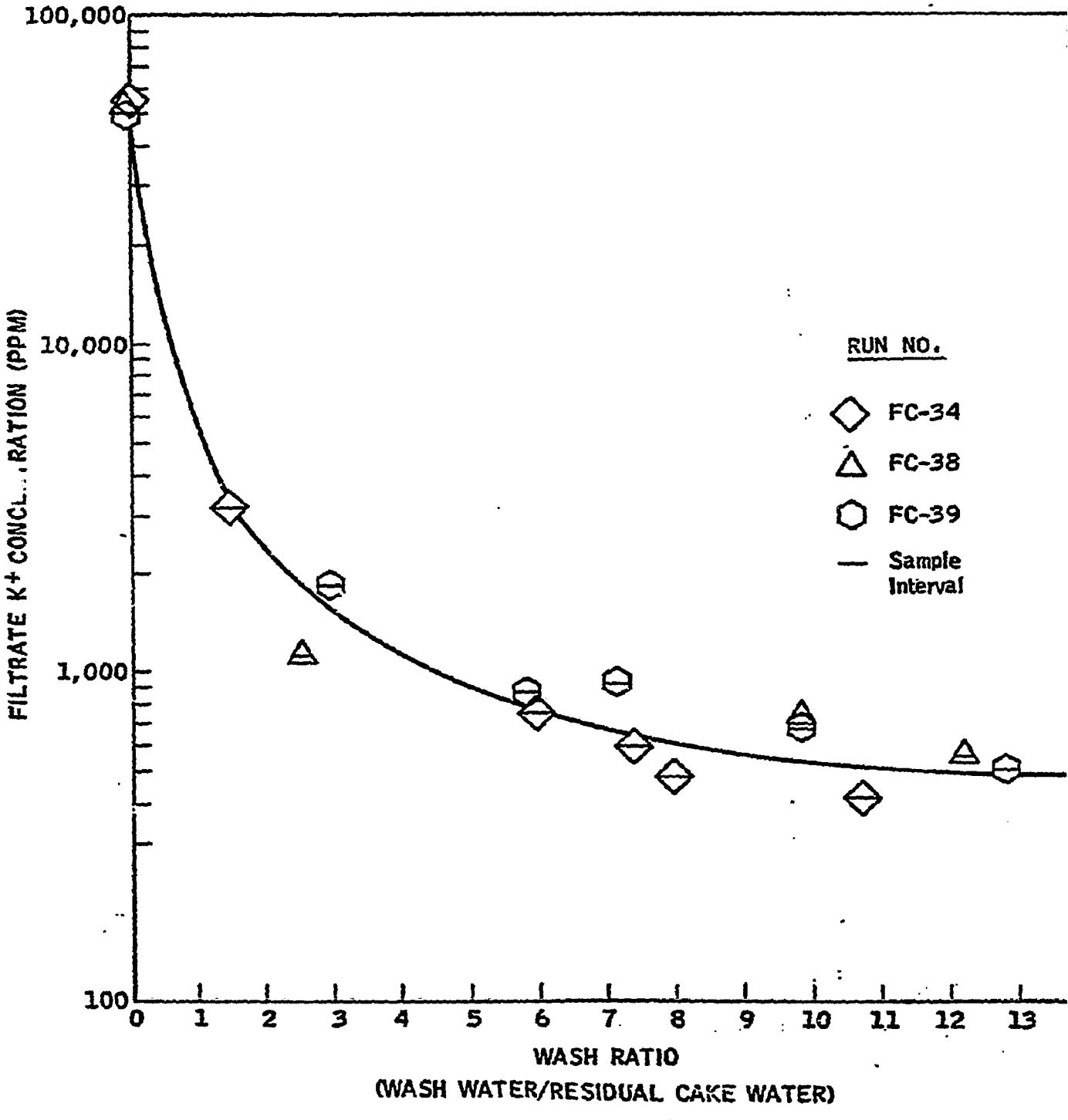

Figure 5.3-13

POTASSIUM RECOVERED FROM RESIDUAL CAKE WATER VARIES WITH WASH RATIO

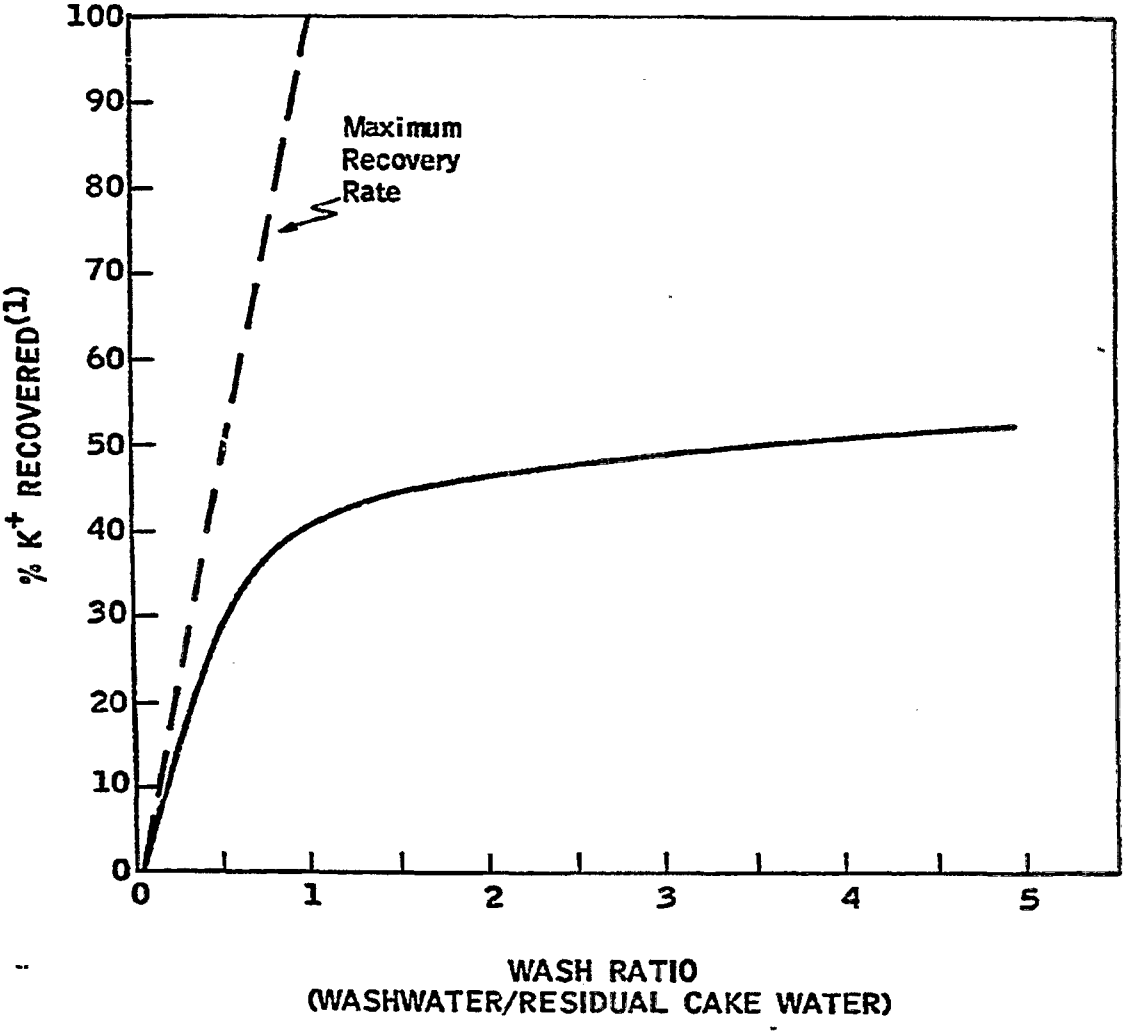

Note:

(1) Based on K^+ content of residual cake water after filtration, using distilled wash water.

These data show that filtration with a displacement wash will recover significantly more K^+ than filtration without cake washing. Cake washing should reduce the number of filtration/reslurry stages in the catalyst recovery process.

Particle Attrition

Particle size distribution has a large effect on the solid-liquid separation of a slurry. Flocculants cause particles to form agglomerates, increasing the effective particle size and making solid-liquid separation easier. On the other hand, attrition of particles due to fluid shear in pumps and pipes has the opposite effects and is undesirable. In order to quantify attrition due to fluid shear, PDU and FBG char slurries were subjected to known shear rates in a small-scale attrition rig. The particle size distributions of the slurries were measured with wet sieving and an automated stream scanning device (on the < 44 μm material) before and after attrition. Some of these size distributions were confirmed with an image analyzer.

The attrition was carried out in a couette flow viscometer in which a 3.8 cm diameter armature rotates at speeds up to 1700 RPM inside a 4.2 cm diameter cup. The narrow annulus provides a nearly uniform and known shear rate. Stagnant zones in the cup have been eliminated as much as possible. The maximum shear rate of this unit (270 sec^{-1}) corresponds to the average shear rate of low speed (low shear) centrifugal pumps. Progressive cavity and piston pumps have generally lower shear rates (about 100 to 400 sec^{-1} and 1 to 20 sec^{-1} respectively).

The results from this attrition study indicate that attrition of a PDU char and fines slurry occurs at a low and uniform rate at highest shear rate tested (270 sec^{-1}). Particles in the 300-800 μm range decreased at the rate of 12 wt%/hr; particles in the 1-10 μm range increased at the rate of 5 wt%/hr. These rates should be sufficiently low that no adverse effect on solids-liquid separation of unflocculated char is likely under ordinary CCG plant operating conditions. Slurry from the Fluid Bed Gasifier, which typically produced more dense chars than the PDU, did not attrit even after 12 hours at 270 sec^{-1}. The attrition of flocculated char was not studied, nor were tests of the filterability of attrited slurry carried out. Such tests will be needed to establish shear stability of flocculated char and to confirm that attrition does not adversely affect filterability.

Particle size measurements of the PDU slurry, made by an image analyzer did not indicate any change in particle shape or geometry, due to attrition. The particles appeared to break randomly; they did not seem to be eroded.

5.3.5 Environmental Control: Water and Solids Effluents

The overall objective of this environmental control program was to collect water and solids effluents data for an assessment of the potential

environmental impact of the CCG process on a commercial scale. The sampling programs which provided effluents data can be divided into a pre-PDU-startup program and a PDU stream sampling program.

Pre-PDU-Startup Program

Before the startup of the CCG PDU, lime-digested and undigested char samples from bench-scale catalyst recovery experiments were examined to determine the level of potential environmental hazard. Samples were first leached according to the U.S. Environmental Protection Agency (EPA) Extraction Procedure (EP). The leachates were then analyzed for phenols, halides, sulfur species, organic and inorganic nitrogen species, cyanides and carboxylic acids. As indicated by the results in Table 5.3-18, the sample leachates have low levels of contaminants. Both samples are almost identical, suggesting that lime digestion of the spent chars does not have an impact on the leachate pollutant level. Detailed metal analyses in Table 5.3-19 show that the metal contents are well below 100 times the primary drinking water standard, which is the EPA's hazardous waste criterion according to the Resource Conservation and Recovery Act (RCRA). Therefore, based on the bench-scale samples, the CCG spent chars appear to be non-hazardous and suitable for disposal in a non-hazardous waste handling facility.

PDU Stream Sampling Program

To better characterize the char waste and to begin the characterization of water effluents generated by the CCG process, a comprehensive PDU sampling program was instituted during the first quarter of 1981.

An important consideration in developing an effective PDU waste stream sampling plan was to identify the PDU waste streams that correspond to streams expected in commercial scale operation. The streams identified in this study are only the onsites process wastes which comprise about 50% of the wastewater load from a commercial plant.

In the commercial plant operation, feed coal is dried, catalyzed, and fed into the gasifier which operates at about 1300°F and 500 psia. Product gas from the gasifier is scrubbed in a product gas venturi scrubber. The scrubber slurry enters a sour slurry stripper. The stripped slurry is then filtered and the filtrate recycled to the catalyst recovery unit (CRU). The filter cake is sent to off-site disposal. Gas leaving the product gas venturi scrubber passes through a series of condensers to remove water and water-soluble components. The condenser overhead gas is subsequently treated to remove ammonia in an ammonia scrubber prior to entering the acid gas removal unit and the cryogenic methane recovery unit. All wastewaters from the condensers and the ammonia scrubber, which constitute about 95% of the total process wastewater, are sent to the sour water strippers. The stripped water is discharged at a rate of 2,000 gpm. Gasifier chars are also sent to the CRU. Solids, with 70% water content, are discharged from this unit as a filter cake at a rate of 8,000 ST/SD (wet basis), based on Catalyst Recovery Screening Study Case 2.

Table 5.3-18

CCG SPENT CHAR LEACHATE ANALYSES

(PRE-PDU-STARTUP)

	Digested Char[1] Leachate	Undigested Char Leachate
	ppm	
Phenols[2]	1.4	0.65
Fluoride	< 1	< 1
Chloride	< 10	< 10
Bromide	< 5	< 5
Nitrate	15	11
Phosphate	< 10	< 10
Sulfide[2]	< 10	< 10
Sulfate	49	29
Sulfite[2]	< 100	< 100
Thiosulfate	< 100	< 100
Cyanide (total)[2]	0.70	1.0
Cyanide (free)	0.06	0.07
Thiocyanate[3]	< 0.04	< 0.04
Ammonia[2]	< 1	< 1
Total Nitrogen (Kjeldahl)[2]	2	2
Other Carboxylic Acids[3]	< 10 each	< 10 each

Notes:

(1) Small amount of gelatinous-like material present.

(2) No special collection or preservation procedures--values are likely underestimated.

(3) n-C_3, i-C_4, n-C_4, i- and/or n-C_5.

Table 5.3-19

CCG SPENT CHAR LEACHATE METAL ANALYSES BY ICPES

(PRE-PDU-STARTUP)

	Digested Char Leachate	Undigested Char Leachate
	ppm	
Ag	.0116	< .0068
Al	.377	1.27
As	.0454	< .025
B	1.94	1.05
Ba	.5	.457
Be	.0023	.0023
Ca	2760. (3)	123.
Cd	.029	.0206
Co	.0231	.0394
Cr	< .0011	< .0011
Cu	< .0006	< .0006
Fe	.088	.1
K	38.2	220. (2)
Li	.0379	.0349
Mg	10.2	6.45
Mn	.682	.541
Mo	(.0234)	< .012
Na	.923	1.33
Ni	.168	.209
P	(.0658)	< .045
Pb	(.034)	< .017
Pt	< .24	< .24
Sb	< .023	< .023
Se	< .055	< .055
Si	43.8	39.4
Sn	(.0193)	< .016
Sr	1.78	.739
Ti	.0213	< .0005
Tl	< .026	< .026
V	< .017	< .017
Zn	.82	.963
Hg(1)	< .2 ppb	< .2 ppb

Notes:

( ) Value may not be significant.
(1) By atomic absorption.
(2) Value out of range, requires further dilution.
(3) Lime addition.

Figure 5.3-14 shows the flow diagram of the PDU. The feed coal is treated in a preoxidizer before entering the gasifier which operates at 1300°F and 500 psia. The product gas is first filtered to remove the fines and then scrubbed in a scrubber (T-2) to remove H_2S and remaining entrained solids. The scrubbed gas is then sent to the acid gas removal unit (MEA treating) and the cryogenic methane recovery unit. The scrubber purge enters a sour water stripper (T-3) at a rate of 22 gal/hr. It is stripped and then sent to the refinery wastewater treatment system.

PDU gasifier char and fines are also fed to the CRU as is done in the commercial plant. After the catalyst is extracted by water wash and filtration, the solid waste (filter cake) is shipped off-site for disposal.

Sampling Program Streams

The selection of PDU streams for the sampling program was based on their relationship to the commercial plant waste streams. Table 5.3-20 presents the commercial plant waste streams and identifies corresponding PDU streams.

The preoxidizer scrubber (T-1) purge is similar to the commercial plant's feed coal drier scrubber purge which constitutes less than 5% of the total process wastewater and has relatively little impact.

The product gas venturi scrubber purge is also of concern although it is eventually recycled back to the CRU and does not leave as wastewater. It discharges to a sour slurry stripper at a rate of 370 gpm. The design of a sour slurry stripper is not as well-developed as that for a sour water stripper. An analysis of the product gas venturi scrubber purge is necessary to provide the design information for the sour slurry stripper. Since this stream has no direct counterpart in the PDU, a sample was simulated by combining the PDU T-2 scrubber effluent and the filter fines collected upstream of the T-2 scrubber.

The PDU T-2 scrubber purge is similar to the feed to the commercial plant's sour water strippers and represents the unstripped, untreated CCG wastewater. PDU's T-3 sour water stripper effluent was selected as being the stream closest to the commercial plant sour water strippers effluent. It may have a higher pollutant level than the commercial stream because it is only steam-stripped once and at low efficiency while the commercial stream is first stripped of ammonia and then further stripped to a high level of efficiency in an H_2S stripper.

The largest solid waste stream in the commercial plant is from the Catalyst Recovery Unit (CRU). The PDU CRU filter cake should be very similar to the commercial stream.

Sampling Strategy

An efficient way of obtaining the most useful data is to follow a staged sampling and analysis approach. This approach is outlined in the U.S. EPA

Figure 5.3-14

PDU SOLID/LIQUID WASTE STREAM SAMPLING LOCATIONS

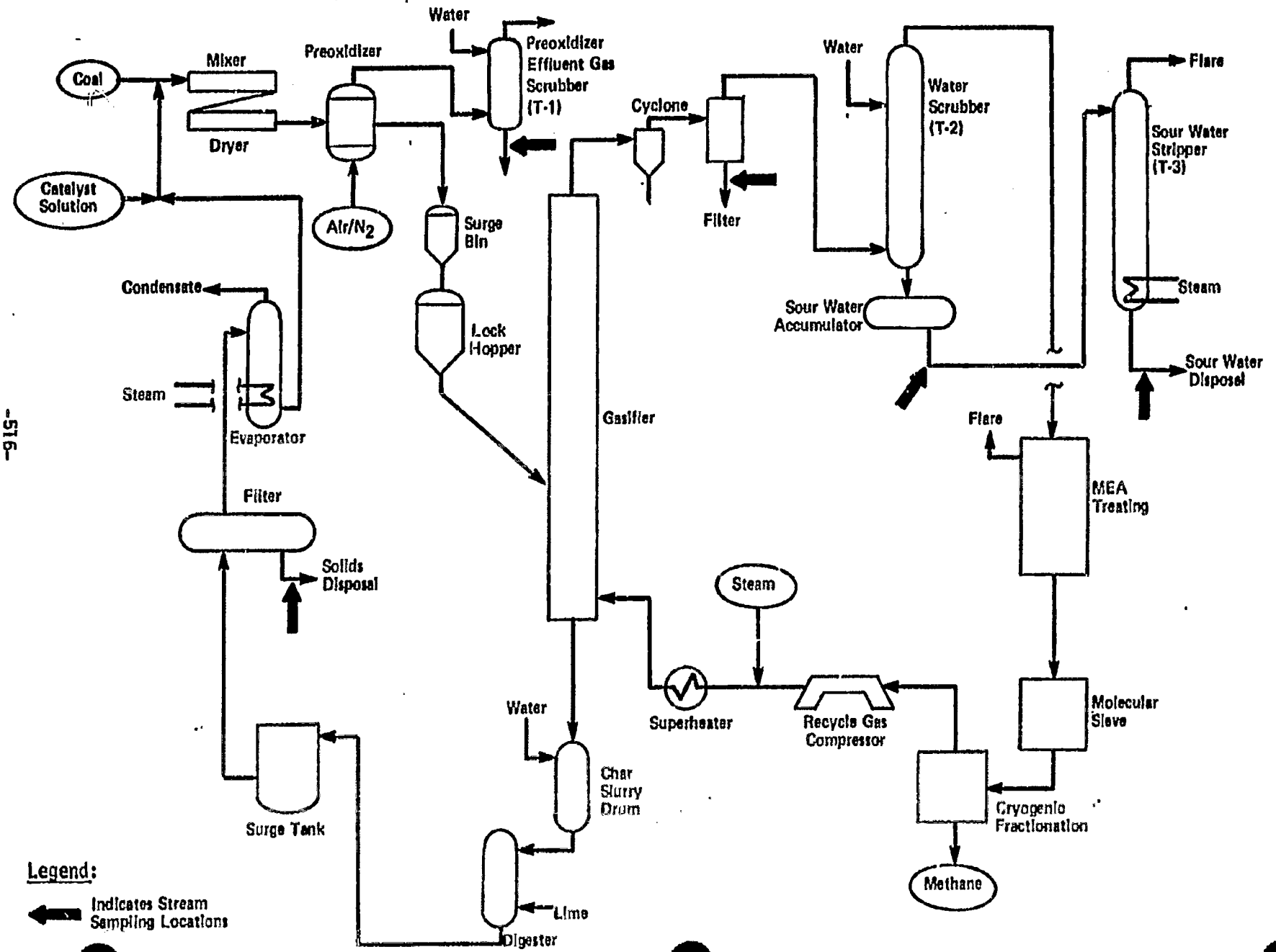

Table 5.3-20

MAJOR CCG LIQUID AND SOLID WASTE STREAMS
COMMERCIAL PLANT VS. PDU

Commercial Plant Stream	Closest Corresponding PDU Stream
• Liquid Waste Streams (% of Process Wastewater(1))	
+ Entrained Dryer Flue Gas Scrubber Purge (5%)	+ Precoxidizer Effluent Gas Scrubber (T-1) Purge
+ Product Gas Condensates(2):	+ T-2 Scrubber Water
- Intermediate Separator Sour Water (330°F)	
- Final Separator Sour Water (120°F)	
+ H_2S/NH_3 Strippers Effluent (95%)	+ T-3 Sour Water Stripper Effluent
+ Product Gas Venturi Scrubber Purge(3)	+ Mixture of:
	- Product Gas Filter Fines
	- T-2 Scrubber Water
• Solid Waste Streams (% of total solid waste)	
+ Catalyst Recovery Unit (CRU) Solids (99%)	+ Catalyst Recovery Unit (CRU) Solids

Notes:

(1) The total flow of process wastewater only comprises 50% of the entire wastewater load from a commercial plant.

(2) Enters H_2S/NH_3 Strippers.

(3) Recycles back to CRU as process water.

Industrial Environmental Research Laboratory's guide for "Level 1 Environmental Assessment" ("EPA IERL-RTP Procedural Manual: Level 1 Environmental Assessment", 2nd ed., October, 1978, EPA-600/7-78-201). The first stage consists of taking grab samples and time series samples. The grab samples are analyzed extensively to determine, within a factor of 3, the rates of pollutant production. The time series samples, however, are only analyzed for a few parameters to determine the variability of pollutant production.

Based on results of this first stage sampling and analysis program, streams containing significant levels of pollutants, and streams having the least variability, can be selected for an exhaustive analysis during the second stage sampling program. Particular types of pollutants can also be selected for a closer examination. Data from the second stage sampling program provide specific information for a quantitative assessment of the pollutants resulting from a process such as CCG. In addition, these data enable laboratory experiments to be designed to identify treatment and disposal processes.

Analytical Methods

Metals were analyzed by Inductively Coupled Plasma Emission Spectroscopy (ICPES). Detailed organic analyses were done by gas chromatography/mass spectroscopy (GC/MS). All other parameters reported herein were analyzed according to the fifteenth edition of "Standard Methods" ("Standard Methods for the Examination of Water and Wastewater", 15th ed., 1980, APHA-AWWA-WPCF).

CRU solids were extracted by both the ASTM Method A procedure and the EPA'S EP procedure. The EP leachate was only analyzed for metals as this is the regulatory compliance requirement outlined in May 19, 1981 Federal Register. The ASTM leachate was analyzed for all other parameters as it is more representative of conditions which would be anticipated at a CRU solids disposal site.

Data Analysis

The first stage sampling program was completed at the PDU. Grab samples of the selected streams were taken. Time series samples were also taken for the four liquid waste streams at two-hour intervals over a twenty-four hour period.

Comprehensive analyses of the grab samples included physical properties, inorganic-non-metal parameters, organic parameters, and metals. They are presented in Table 5.3-21.

Physical properties include pH, alkalinity, total solids (TS), suspended solids (SS), volatile solids (VS), and oil and grease. The pH of all the waste streams are on the alkaline side ranging from 8 to 9.5. Except for the preoxidizer scrubber purge, all liquid waste streams are extremely well buffered with the alkalinity values ranging from 20,000 to 90,000 ppm. The

Table 5.3-21

CHEMICAL ANALYSES OF PDU WASTE STREAM COMPOSITE SAMPLES (PPM)

	Preoxidizer Scrubber Purge	Simulated Product Gas Scrubber Purge	T-2 Scrubber Purge	T-3 Stripper Effluent	CRU Solids Leachate
Physical Properties					
pH	9.5	8.6	8.0	9.0	10.8
Alkalinity	1,100	87,400	53,500	20,000	1,550
TS	1,246	52,206	1,528	756	-
TDS	978	20,006	1,192	432	-
TSS	268	32,200	336	324	-
VS	200	22,700	118	282	-
Oil & Grease	*	*	*	26	-
Inorganic Non-Metal					
$S^=$	-	-	330	214	-
$S^=_x$	-	-	20	3	4
$SO_3^=$ as S	-	-	-	-	-
$S_2O_3^=$ as S	-	240	6	4	275
$SO_4^=$ as S	-	180	-	10	7
Total S	-	390	760	480	280
CN^-/SCN^-	3	1	1	7	2
Cl^-	540	430	280	190	110
NH_3 as N	-	6,500	7,500	7,200	-
Total N	10	7,200	7,500	7,200	-
CO_2	400	27,000	24,000	7,100	700
Organic					
BOD_5	360**	325	120	280	.12
COD	220**	8,750(8,400)	1,000**(4,400)	1,900(1,250)	-
TOC	400**	2,500(2,600)	1,000**(1,350)	760 (380)	18
Phenols	6	3	10	50	-
Naphthalene	*	567	519	255	-
Phenanthrene	*	128	68	16	-
Total Extractable Organics	*	2,790	1,470	415	-
Metals					
Ag	.0254	.0051	.0051	.0051	.0051
As	.105	.011	.228	.021	.0377
Ba	.314	.0735	.634	.0553	.848
Cd	.0474	.0098	.0095	.0095	.0119
Cr	.0618	.004	.0258	.0896	.0015
K	53.9	11,700	60	57.4	927
Pb	.105	.016	.016	.017	.0233
Se	.294	.124	.243	.145	.021
Hg	*	*	*	*	.001

-: not detectable
*: not analyzed
**: suspect values
( ): calculated value based on GC/MS analysis

alkalinity normally observed in a refinery wastewater is about 4,000 ppm. This high alkalinity would present a problem in pH adjustment if not reduced (i.e., in the sour water stripper). For example, a large acid dose would be required to bring the pH into the optimum ranges suitable for various treatment processes such as solids removal, biological oxidation, and carbon adsorption.

The suspended solids (SS) content in both the T-2 scrubber purge and the T-3 sour water stripper effluent is about 300 ppm, which is higher than the expected 50 ppm. This implies that the product gas filter upstream of the scrubber may have not been functioning properly at the time the samples were collected. About half of the suspended solids in all of the liquid waste streams are volatile solids. Therefore, removing the suspended solids would remove a considerable amount of organics. The total dissolved solids (TDS) level for T-2 and T-3 effluent is 1,200 and 400 ppm respectively. They are close to what is normally observed for refinery wastewater, which is about 1,000 ppm. CRU solids leachate has a high pH of about 11. This is due to the potassium catalyst content.

Inorganic non-metal parameters include sulfur species, chloride (Cl^-), cyanide (CN^-), and ammonia (NH_3). The preoxidizer scrubber purge has a low level of sulfur and nitrogen compounds, less than 3 ppm and 10 ppm respectively. Most of the nitrogen in the waste streams is in the form of ammonia. The ammonia level in the simulated product gas scrubber purge, as well as in T-2 and T-3 effluents is about 7,000 ppm. This level is toxic to biological activities, and ammonia stripping will be necessary prior to any biological treatment of this wastewater. The similar ammonia levels in T-2 and T-3, indicates that the PDU sour water stripper (T-3) has a poor stripping efficiency. Examination of the T-2 scrubber water analysis shows that it does not contain any species such as organic acids that would cause difficulties in stripping. Therefore, a better tower design should be able to strip the ammonia and sulfide to desirable levels. The removal of ammonia may also reduce the alkalinity and alleviate the pH adjustment problem mentioned earlier. The sulfur compounds in the CRU leachate are about 300 ppm, and the nitrogen compounds are not detectable.

Organic parameters include biochemical oxygen demand (BOD), chemical oxygen demand (COD), total organic carbons (TOC), phenols, and total extractable organics. The last item was analyzed by GC/MS, and further details of the analyses for the three streams tested are included in Tables 5.3-22, 5.3-23, and 5.3-24. The BOD_5, COD, and TOC levels of the preoxidizer scrubber purge are suspect. The BOD_5 should be lower than the COD because COD is a measurement of both the biodegradable and the non-biodegradable organics. The TOC level should be lower than the COD level because for every gram of carbon oxidized there should be at least 2.5 grams of oxygen. For the same reason, the TOC and COD levels of the T-2 scrubber purge are also suspect. The inconsistency of the data is due mainly to sample degradation caused by the long holding time which went beyond the effective period of the sample preservation methods. Although these data points are not used in the data analyses, they are presented here as the best available data based on replicate analyses.

Table 5.3-22

SIMULATED PRODUCT GAS SCRUBBER PURGE

GC Retention Time (Minutes)	Compound	Concentration in Water (ppm)
2.45	Benzene	11.4
5.23	Toluene	15.2
6.98	Ethylbenzene?	1.1
7.51	a dimethylpyridine?	8.7
9.01	Phenol	134
9.16	Aniline?	10.5
10.42	Benzofuran	4.3
11.06	o-Cresol	30.4
11.77	m+p-Cresol	53.7
12.21	5-Ethyl-2-methylpyridine or N-Ethylaniline?	2.0
13.66	a dimethylphenol?	2.9
13.78	a dimethylphenol?	9.4
13.93	a dimethylphenol?	16.8
14.62	Naphthalene	567
14.78	Benzo[b]thiophene	39.6
16.08	Quinoline	161
16.31	a C_9 phenol	3.4
16.56	Isoquinoline	43.9
17.30	2-Methylnaphthalene	54.6
17.46	Indole	66.4
17.54	a methylbenzo[b]thiophene?	0.4
17.69	2-Methylquinoline	37.8
17.76	1-Methylnaphthalene (+ a methylbenzo[b]thiophene)	37.0
17.84	8-Methylquinoline?	3.0
18.13	3-Methylquinoline?	11.8
18.39	a methylquinoline?	2.2
18.50	a methylindolizine or a methylindole? (C_9H_9N)	3.1
18.67	5-Methylquinoline?	17.0
18.81	a methylquinoline	7.4
19.03	a methylindolizine or a methylindole?	6.5
19.26	Biphenyl	24.0
19.44	4-Methylquinoline?	11.0
19.56	a methylindolizine or a methylindole?	20.6
19.61	a methylindolizine or a methylindole?	88.6
20.08	a dimethylquinoline?	4.6
20.15	a dimethylquinoline?	4.2
20.39	a dimethylnaphthalene?	3.3
20.90	Acenaphthylene	3.4
21.09	A dimethylindole or a dimethylindolizine?	1.3

Table 5.3-22 (Cont'd)

GC Retention Time (Minutes)	Compound	Concentration in Water (ppm)
21.49	Acenaphthene	32.7
22.14	Dibenzofuran	69.7
23.14	$C_{10}H_9N$?	2.5
23.60	Fluorene	75.1
23.76	$C_{13}H_{12}$?	3.9
23.87	$C_{11}H_{10}O$?	3.6
24.01	$C_{13}H_{12}$?	2.4
24.17	$C_{13}H_{12}$?	13.9
24.34	a methylbenzofuran?	15.4
24.51	Xanthene	5.3
24.78	$C_9H_{12}N$?	11.2
25.40	9,10-Dihydroxphenanthrene	13.2
25.63	3-Hydroxybiphenyl?	2.0
25.99	trans-Stilbene?	11.1
26.16	a methylfluorene?	8.3
26.83	Dibenzothiophene	27.4
27.48	Phenanthrene	128
27.60	Anthracene	27.8
27.75	Acridine?	8.5
28.17	$C_{13}H_9N$? (a benzoquinoline? phenanthridine?)	7.2
28.49	Carbazole	47.1
28.73	$C_{12}H_9N$?	8.2
28.79	1-Phenylnaphthalene?	2.9
29.39	a methylphenanthrene?	5.0
29.50	a methylphenanthrene?	6.2
29.63	a methylphenanthrene?	11.0
29.81	4H-Cyclopenta[def]phenanthrene?	18.1
29.93	a methylphenanthrene	5.4
30.42	$C_{13}H_{11}N$?	3.8
30.49	$C_{16}H_{14}$? (a tetrahydrofluoranthene?)	1.0
30.75	2-Phenylnaphthalene	7.8
31.90	4,5-Dihydropyrene?	1.3
32.34	Fluoranthene	52.5
32.79	$C_{14}H_{12}H_2$?	3.5
33.17	Pyrene	44.6
34.68	Benzo[a]fluorene?	12.8
34.95	Benzo[b]fluorene?	13.9
35.03	a methylpyrene?	1.8
35.18	2-Benzylnaphthalene	6.6

Table 5.3-22 (Cont'd)

GC Retention Time (Minutes)	Compound	Concentration in Water (ppm)
35.35	$C_{18}H_{14}$	1.6
36.47	$C_{18}H_{14}$	2.5
37.13	Benzo[b]naphtho[1.2-D]di-thiophene?	2.6
37.30	$C_{19}H_{14}$?	1.1
38.15	Benz[a]anthracene	5.6
38.34	Chrysene	13.1
42.39	a benzofluoranthene?	4.0
	$C_{20}H_{12}$ (perylene?)	2.4
	Total Amount Unidentified	512.0
	Total	2790.0

Table 5.3-23

T-2 SCRUBBER PURGE

GC Retention Time (Minutes)	Compound	Concentration in Water (ppm)
2.44	Benzene	29.4
5.30	Toluene	13.0
7.34	a dimethylpyridine?	0.9
8.90	Phenol	30.8
9.06	Indan?	4.3
10.46	Benzofuran?	6.3
10.97	o-Cresol	5.4
11.64	m & p-Cresol	23.5
13.70	a dimethylphenol?	2.2
13.80	a dimethylphenol?	2.4
14.63	Naphthalene	519
14.77	Benzo[b]thiophene	29.0
15.83	Quinoline	18.0
16.35	Isoquinoline	4.2
17.28	2-Methylnaphthalene	59.3
17.31	Indole?	5.1
17.66	1-Methylnaphthalene	28.6
18.08	3-Methylquinoline?	1.4
18.57	5-Methylquinoline?	2.7
19.24	Biphenyl	17.0
19.51	a methylindole or a methylinodlizine?	3.9
19.75	a dimethylnaphthalene	10.8
20.08	a dimethylnaphthalene	6.6
20.14	a dimethylnaphthalene	4.7
20.69	Acenaphthylene	8.4
21.46	Acenaphthene	16.9
22.11	Dibenzofuran	13.0
23.53	Fluorene	31.3
25.36	9,10-Dihydrophenanthrene	5.8
26.78	Dibenzothiophene	13.8
27.39	Phenanthrene	68.1
27.53	Anthracene	16.2
28.37	Carbazole	10.2
29.37	a methylphenanthrene	4.0
29.55	a methylphenanthrene	6.0
30.72	a methylbenzothiophene	4.2
32.26	Fluoranthene	26.6
33.12	Pyrene	29.6
34.64	Benzo[a]fluoranthene?	8.0
34.91	Benzo[b]fluoranthene?	8.1
38.14	Benzo[a]anthracene	5.5
38.32	Chrysene	11.1
42.37	$C_{20}H_{12}$	3.3
43.31	$C_{20}H_{12}$	3.2
	Total Amount Unidentified	338.3
	Total	1470.0

Table 5.3-24

T-3 STRIPPER EFFLUENT

GC Retention Time (Minutes)	Compound	Concentration in Water (ppm)
8.74	Phenol	0.8
10.93	o-Cresol	0.1
11.56	m & p-Cresol	0.6
14.48	Naphthalene	259
14.64	Benzo[b]thiophene	8.9
17.25	2-Methylnaphthalene	8.3
17.66	1-Methylnaphthalene	3.5
19.29	Biphenyl	4.6
21.51	Acenaphthene	2.2
22.17	Dibenzofuran	1.0
23.55	Fluorene	7.1
27.38	Phenanthrene	15.6
28.41	Carbazole	0.2
32.31	Fluoranthene	0.1
33.13	Pyrene	0.2
	Total Amount Unidentified	33.6
	Total	415

The GC/MS results indicate that naphthalene constitutes about 20% of the total organics for the simulated product gas scrubber purge, 30% for the T-2 scrubber purge, and 65% for the T-3 sour stripper effluent. The second highest organic compound is phenanthrene which constitutes about 5% of the total organics for all three waste streams. The theoretical COD and TOC for these three waste streams are also calculated based on the GC/MS analyses. They are close to the measured values for the simulated product scrubber purge. For the critical T-3 stripper effluent, the theoretical values are from 50% to 65% of the measured values. It should be noted that the level of organic compounds as measured by GC/MS in T-3 is considerably lower than that of T-2. This may be due to process variability and not due to stripping. Therefore, the stripped effluent in the commercial plant could contain higher organic level than indicated by the analysis. Additional verification of the organic components will be obtained from the second stage sampling program.

The BOD_5 to TOC ratios of the waste streams range from 0.12 to 0.37, while the typical values observed for refinery wastewaters are about 2.75 (Eckenfelder, W. W., "Water Quality Engineering for Practicing Engineers," Barnes and Noble, New York (1970)). This suggests that the portion of non-biodegradable organics is higher in the PDU wastewater than a typical refinery wastewater. This may be due largely to the non-biodegradability of naphthalene although the toxic effect of ammonia may also contribute to the low BOD. Naphthalene has been shown to be biodegradable at low concentrations of up to 5 ppm (Tabak, H. H., et al., "Biodegradability Studies with Organic Priority Pollutant Compounds" (draft), U. S. EPA MERL Water Research Div.; and Treatability of Carcinogenic and Other Hazardous Organic Compounds, August, 1979, EPA-600/2-79-097), but its biodegradability at higher concentration is not well known. The influent to the commercial plant's wastewater treatment facility, however, may be more biodegradable because the gasifier wastewater will have been stripped of ammonia and will not contain the inhibitory level of ammonia found in the PDU wastewater. In addition, the process wastewater can be diluted by non-process water such as cooling tower blowdown, boiler blowdown, and storm water run-off, making it more biodegradable. Further BOD analyses during the next sampling program and the future treatability study will be conducted to clarify this issue. The BOD analyses will impact on the level of stripping required for the sour water stripper. For example, at the currently reported wastewater BOD level, very little ammonia will be converted in the biox unit. Therefore, the sour water stripper will have to strip the ammonia down to about 20 ppm so that the biox unit discharge will meet the effluent standard. On the other hand, if a higher wastewater BOD can be obtained, then a higher ammonia level in the biox unit influent will be acceptable.

The COD to TOC ratios of the waste streams are from 2.5 to 3.5, while refinery wastewaters are typically around 5.4 (Eckenfelder). This may be because the inorganic oxygen-demanding refinery wastewater compounds such as those from sulfur processing are not found in the PDU wastewater.

The CRU solids leachate has a very low level of organics which were not detectable by the GC/MS method.

The metals content of all the liquid streams are below the levels inhibitory to biological oxidation, except for the simulated product gas venturi scrubber purge (Wastewater Engineering Treatment/Disposal/Reuse, Metcalf and Eddy, Inc., 2nd ed. (1979)). The potassium level in the simulated sample is toxic to biological life. However, since this stream will be recycled back to the CRU, its potassium level is not a concern for the wastewater treatment design. The metal content of the CRU solids leachate is below the EPA hazardous waste standard which is 100 times primary drinking water standard (PDWS). If a more stringent standard of 10 times PDWS is applied, which might be proposed by EPA in the future, the CRU solids would still be classified as non-hazardous. Detailed metal analyses are included in Table 5.3-25.

Waste Load Variability

Parameters measured for the time series samples were pH, total suspended solids (TSS), total organic carbon (TOC), total Kjeldahl nitrogen (TKN), and total sulfur (TOT S). The variability data indicated that aside from pH, most parameters have log normal distributions. The peak load to a treatment facility is defined as the 95% upper confidence limit (UCL). Table 5.3-26 presents the peaking factor of each stream in terms of the UCL to mean (M) ratio (Table 5.3-27 contains more of the variability information). However, these factors are based on 24 hour data, and represent only the 24 hour fluctuation. To design treatment processes to function properly under varying loading conditions, additional data over a longer period must be obtained to calculate the sustained peak mass loadings.

Considerable variability of all five parameters was observed for the preoxidizer scrubber purge. The peaking factor of both the TOC and total sulfur was close to 2.0. The TKN peaking factor was 4.0. Since this stream constitutes a relatively small portion of the CCG wastewater, its variability, although high, should have little impact on the wastewater treatment system.

The variability of the simulated product gas scrubber purge was similar to the T-2 effluent which makes up 90% of the sample. The total sulfur content peaking factor of the T-2 scrubber purge is 1.6, which is about the same as the T-3 stripper effluent.

Normalized CCG PDU Wastewater Pollutant Load

Table 5.3-28 compares the predicted PDU wastewater pollutant load with literature values for wastewater from other gasification processes. All wastewater pollutant levels are normalized to lb/ton of coal feed and represent the unstripped, untreated gasifier wastewater. The PDU pollutant load is based on the analyses of the T-2 scrubber purge.

Since accurate waste stream flow measurements as well as gas stream data were not available at the time of sampling, a complete material balance could not be obtained. Because of the material balance problem and the large scale

Table 5.3-25

DETAILED PDU WASTE SAMPLE METAL ANALYSES (PPM)

	Preoxidizer Scrubber Purge	Simulated Product Gas Scrubber Purge	T-2 Scrubber Purge	T-3 Effluent	CRU Solids Leachate
Ag	< .0254	< .0051	< .0051	< .0051	< .0051
Al	3.06	< .011	< .011	.0829	.0745
As	< .105	.262	.228	< .021	(.0377)
B	.539	28.8	17.9	8.58	3.67
Ba	.0314	.0735	.0634	.0553	.848
Be	< .006	(.0033)	< .0012	< .0012	< .0012
Ca	2.35	6.18	.186	2.85	123.
Cd	< .0474	(.0098)	< .0095	< .0095	(.0119)
Co	(.0294)	.0041	< .0041	< .0041	.109
Cr	.0618	(.004)	.0258	.0896	< .0015
Cu	.918	< .0004	< .0004	< .0004	.0248
Fe	2.63	10.4	< .0023	.0378	.0593
K	53.9	11,700	60.	57.4	927.
Li	< .0015	.164	< .0003	.0013	.0356
Mg	.382	2.42	.082	.195	2.07
Mn	.0176	.0237	.0314	.0032	.527
Mo	(.0424)	.554	.0262	(.244)	< .0083
Na	41.6	93.8	1.74	1.72	11.3
Ni	(.194)	(.0358)	< .013	.0533	3.02
P	1.21	2.94	.188	.994	.244
Pb	< .105	< .016	< .016	(.017)	(.0233)
Pt	< .379	< .076	< .076	< .076	< .076
Sb	(.239)	< .031	< .031	< .031	< .031
Se	(.294)	.124	.243	.145	< .021
Si	2.72	24.	2.86	7.48	25.
Sn	< .0798	< .016	< .016	< .016	< .016
Sr	.011	.287	.0362	.0499	1.55
Ti	.0393	2.82	.248	.132	< .0011
Tl	< .0489	< .0098	< .0098	.237	< .0098
U	(.413)	< .029	< .029	< .029	(.0837)
V	< .0454	.751	.0091	.111	< .0091
W	< .299	.309	< .06	< .06	< .06
Zn	.919	.164	.11	.136	1.38
Hg**	*	*	*	*	1 ppb

( ): value may not be significant
*: not analyzed
**: by atomic absorption

Table 5.3-26

PEAKING FACTORS (UCL/M) OF PDU WASTE LOAD

Stream	pH	SS	TOC	TKN	TOT S
Preoxidizer Scrubber Purge	1.1	6.9	1.7	4.0	1.9
Simulated Product Gas Scrubber Purge	1.08	1.7	2.0	1.3	1.5
T-2 Scrubber Purge	1.08	3.3	2.8	1.2	1.6
T-3 Sour Water Stripper Effluent	1.08	4.9	1.6	2.5	1.5

Definition of Terms:

UCL: 95% upper confidence limit
M: mean
SS: suspended solids
TOC: total organic carbon
TKN: total kjeldahl nitrogen
TOT S: total sulfur

Table 5.3-27

PDU WASTE LOAD VARIABILITY

Stream	pH	SS	TOC	TKN	TOT S
Preoxidizer Scrubber Purge	M=7.6 20=0.75	M=304 UCL=2,085 LCL=44	M=13 UCL=20 LCL=8	M=3 UCL=12 LCL=0	M=25 UCL=46 LCL=13
Simulated Product Gas Scrubber Purge	M=9.3 20=1.5	M=60,500 UCL= 99,950 LCL= 35,900	M=38 UCL=74 LCL=19	M=7,500 UCL=9,500 LCL=5,900	M=380 UCL=580 LCL=250
T-2 Scrubber Purge	M=7.9 20=0.6	M=15* UCL=50* LCL=0*	M=16 UCL=44 LCL=6	M=8,290 UCL= 10,200 LCL=6,380	M=415 UCL=650 LCL=180
T-3 Sour Water Stripper Effluent	M=9.8 20=0.8	M=7 UCL=34 LCL=0	M=12 UCL=19 LCL=8	M=1,760 UCL=4,340 LCL=25	M=20 UCL=30 LCL=15

Definition of Terms:

M: mean
UCL: 95% upper confidence limit
LCL: 95% lower confidence limit
SS: suspended solids
TOC: total organic carbon
TKN: total kjeldahl nitrogen
TOT S: total sulfur

Note:

*Data do not show any distribution pattern; arithmetic mean is used for M, highest and lowest values are used as UCL and LCL respectively.

Table 5.3-28

COMPARISON OF COAL GASIFIER WASTEWATER POLLUTANT(1) (LB/ST COAL)

Coal	Montana Rosebud		Illinois
Gasification Process	Source A(2)	Source B	CCG
BOD	27.1 + 34%	66.5	.42
COD	55.5 + 64%	103	4.2
TOC	22.1 + 69%	N.A.(4)	.1
Phenol	8.7 + 79%	21.8	.04
Oil & Tar	1.8 + 44%	3.2	.1
Thiocyanate	.067 + 105%	.08	.004(3)
Total Sulfur	.449 + 22%	1.31	3.2
NH_3	14.0 + 29%	72.1	31.7
Alkalinity	3.95 + 33%	219	222.0

Notes:

(1) Raw-unstripped, unextracted.

(2) Neufield, R. D. and L. Matson, "Thiocyanate Bio-oxidation Kinetics", 35th Purdue Industrial Waste Conference, May 1980.

(3) Sum of cyanides and thiocyanates.

(4) N.A. = not available.

difference between PDU and the commercial plant (1 T/D vs. 15,000 T/D), the normalized PDU data are at best a qualitative indication of the CCG pollutant load. In general, however, CCG wastewater pollutant levels as shown in the table are lower than those of the other two processes.

Underestimation of Solid Waste Pollutant Load

Based on the PDU data, the CRU solids are non-hazardous and are suitable for land disposal in a non-hazardous facility. However, the commercial plant solid waste may have a higher pollutant load than estimated. During the time the CRU solids were sampled, the PDU product gas fines were not sent to the CRU, while in the commercial plant, the product gas fines would be handled by the CRU. Since the filter fines are believed to act as an adsorbent for organics, their absence in the PDU solid waste may result in lower pollutant levels. However, since RCRA, as currently written, is not concerned with organics, the CCG solid waste would still be classified as non-hazardous.

Conclusions

As a result of the PDU waste sampling and analyses program, the following conclusions were drawn:

- Because of the large throughput difference between the PDU and the commercial plant, as well as the incompleteness of the data validation, results from the first stage PDU sampling program gave only qualitative indication of the pollutant load to be expected from the CCG process.

- The pollutant load of the CCG wastewater is generally less than other gasification processes, according to data found in the literature.

- The PDU wastewater contains a high level of ammonia due to the poor stripping efficiency of the T-3 sour water stripper. In a commercial design, the ammonia level should be lower.

- The level of organic compounds as measured by GC/MS was considerably lower in the sour water stripper effluent than that of the scrubber water. This may be due to process variability and not due to stripping. Therefore, the stripped effluent in the commercial scale could contain a higher level of organic compounds than indicated by the analysis.

- Naphthalene is the predominant organic specie identified in the process wastewater.

- The PDU wastewater exhibits low biodegradability which may be caused by the high proportion of refractory organics as well as the toxic level of ammonia. The biodegradability of the CCG wastewater is not well defined.

- The hazardous metal content in the leachate of the CCG PDU solid waste was below the 100 times primary drinking water standard specified by RCRA. The organic level of the leachate was also low. Based on these results, the solid waste is non-hazardous and should be suitable for land disposal in a non-hazardous facility. However, the solid waste pollutant load of the PDU was probably underestimated due to the absence of filter fines in the CRU solids.

- There was considerable 24-hour variability of the suspended solids (SS), the total organic carbon (TOC), and the nitrogen content of the CCG PDU wastewater. Additional variability data covering a longer period are necessary to better define the peak load to the waste water treatment facility.

- Additional data will be needed to further characterize PDU waste streams for biotreatability studies.

Recommendations

The following recommendations were made:

- Additional time series samples covering a period of two weeks should be conducted to better define the waste load variability.

- Since the PDU has started sending product gas fines to the CRU, the CRU waste stream should be resampled to upgrade the waste load estimation.

- A second stage sampling program should be conducted in the near future to provide additional information of the CCG wastewater quality and to provide the basis for the design of a bench-scale treatability experiment. Data to be collected during the sampling program include:

  + Operational data for the feed and effluent of T-1, T-2, and T-3 (flow rate, temperature, pressure)

  + Gasifier operational data (steam to coal ratio, temperature, pressure)

  + Gas stream data (composition of product gas at the outlet of the gasifier, composition of vapor leaving the T-3 stripper)

  + Analytical data (physical properties, inorganic analyses, organic analyses, metal analyses)

- A biotreatability study should be conducted to better define the biodegradability of the CCG waste water. In addition, other treatability experiments (e.g., activated carbon adsorption, etc.) should also be conducted to define effluent treatability and waste water treatment parameters.

5.3.6 Environmental Control: Atmospheric Emissions

The atmospheric environmental control program for the CCG Process Development Program identified and quantified potential atmospheric emission sources for a conceptual commercial CCG plant. The results are presented below as a preliminary emissions inventory. This completes the environmental air control efforts for two objectives: identify potential emission sources and estimate their emissions quantity. A third objective, assess the air quality impact and identify control alternatives for a commercial plant, was not completed.

Preliminary CCG Commercial Plant Emissions Inventory

The estimated emissions inventory, summarized in Table 5.3-29, was based on the best available process information from the CCG Predevelopment Program Final Report (FE-2369-24), and on anticipated U.S. regulatory requirements. The process and regulatory information is described in Table 5.3-30. Tables 5.3-31, 5.3-32, and 5.3-33 summarize, in order, expected emissions from the offsite boiler and coal dryers, expected emissions from the steam/recycle gas preheat fired heaters, and expected fugitive particulate matter emissions. Expected sulfur dioxide emissions from the sulfur recovery units are described in Table 5.3-34. Particulate and hydrocarbon emissions from the coal/catalyst preoxidizer exhaust and the low pressure coal lockhopper vents could not be estimated since emissions data were not available. Information about these process emissions should be obtained from tests at the PDU.

Noncriteria Pollutant Emissions

Based on tests conducted by the EPA on other coal gasification operations, some trace releases are expected of noncriteria pollutants such as H_2S, COS, mercaptans, polynuclear organic matter (POM) and heavy metals from process-related CCG operations. However, since the CCG process converts heavy organics to methane more efficiently than other processes, the quantities of noncriteria pollutants emitted per ton of coal should be less than emitted by other gasification processes.

The major sources in a CCG commercial plant which potentially can release these pollutants are: flared transient releases due to start-up and process upsets, flared releases from the low pressure gasifier lockhopper vents, fugitive emission from flanges, valves, pump seals, and liquid product storage tanks, vented emissions from the coal/catalyst preoxidizer, and emissions associated with spent char from the catalyst recovery unit.

The degree of concern that should be associated with these sources in the CCG process will be determined through tests planned at the PDU. To develop accurate estimates of noncriteria pollutant emissions for a commercial plant will require testing at a larger scal

Table 5.3-29

PRELIMINARY CCG EMISSIONS INVENTORY

SUMMARY OF ESTIMATED EMISSIONS FROM A CCG COMMERCIAL PLANT

Basis: Illinois No. 6 Coal
See Table 5.3-30 for assumptions and operating conditions

Contributing[1] Sources	Particulate[2] Matter ST/SD	SO_2[2] ST/SD	NO_x[2] ST/SD	Hydrocarbons ST/SD	CO ST/SD
Steam Generation	0.95	19.0	16.0	0.45	1.5
Coal Dryers	0.2	4.2	3.7	0.1	0.4
Coal Handling (Fugitive Emissions)	0.5	none	none	negligible	none
Lime Handling (Fugitive Emissions)	<0.1	none	none	none	none
Waste Solids (Fugitive Emissions)	<0.1	none	none	negligible	negligible
Coal/Catalyst[3] Preoxidizer	?	0.5	?	?	?
Lockhopper Vent[3] and Transient Emissions	?	negligible	?	?	?
Sulfur Recovery Units	negligible	7.2	?	negligible	negligible
Steam/Recycle Gas Preheat Fired Heaters	negligible	negligible	2.0	negligible	negligible
Fugitive Gaseous[3] Vapor Sources	none	negligible	negligible	?	?

Notes:

(1) Assumptions and operating conditions are presented in Table 5.3-30.
(2) Where pollutants and sources are likely to be subject to emission regulations such as the New Source Performance Standards (40 CFR, Part 60, 6-11-79), the specified emission limits were applied. Otherwise Best Available Control Technology (BACT) is assumed to be employed. BACT for each process is described in the following Tables 5.3-30 through 5.3-34.
(3) No data are currently available describing transient emissions from these sources. Sampling tests planned for the CCG PDU should indicate what pollutants can be expected.

Table 5.3-30

CCG COMMERCIAL PLANT OPERATING ASSUMPTIONS

Operating assumptions are based on the CCG Predevelopment Program Final Report (FE-2369-24).

Coal Quantity, Handling and Use

- Normal coal rate of 18,160 ST/SD of which 2,960 ST/SD is for boilers, 710 ST/SD is for dryers, and 14,490 ST/SD is for process.
- 400,000 ST storage in open pile.
- 14,000 ST storage in each of two silos.
- Conveying operations move coal to silos, dryers (fuel and process coal), and offsite boilers.
- Coal composition is as described in Table 4.2-1 of FE-2369-24.

Lime Quantity, Handling and Use

- 1,000 ST/SD used in catalyst recovery.
- 21,000 ST covered storage.
- Conveying moves the lime to catalyst recovery.

Waste Solids for Disposal

- 7,520 ST/SD (wet basis) total waste solids (includes solids from catalyst recovery, sour water stripping, lime softening sludge, and boiler ash).
- Ultimate waste disposal is offsite.

Emission Factors Developed from Process Information and Regulatory Standards

- Emission factors used are developed from AP-42 and FE-2369-24.
- Best Available Control Technology (BACT) is applied. These are process-specific and are referenced in the individual tables.
- Boiler emissions will comply with proposed New Source Performance Standards (NSPS) for utility boilers.

Table 5.3-31

PRELIMINARY EMISSION ESTIMATES FOR OFFSITE BOILERS AND COAL DRYING

Pollutant	Calculated Pollutant Emission Factor[1] lb/ST coal	CCG Uncontrolled Pollutant Emission Rate lb/SD	CCG Maximum Allowable Emission Rate[2] NSPS x Firing Rate, $\frac{MBtu}{hr}$ x 24 hr/day lb/SD	Control Reduction Required to Meet NSPS %	Expected Emissions with Controls ST/SD
Offsite Boilers					
Boiler Size = 2,960 ST/SD Coal Fired (2,639 MBtu/hr)					
Particulates	128.0	380,000	1,900	99.5	0.95
SO_2	133.0	390,000	38,000	90.0	19
NO_X	18.0	53,000	32,000	40.4	16
CO	1.0	3,000	3,000	n/a	1.5
Hydrocarbons	0.3	900	900	n/a	0.45
Coal Drying					
Dryer Size = 710 ST/SD Coal Fired (632 MBtu/hr)					
Particulates	128.0	90,000	455	99.5	0.2
SO_2	133.0	95,000	9,500	90.0	4.2
NO_X	18.0	13,000	7,500	40.4	3.7
CO	1.0	710	710	n/a	0.4
Hydrocarbons	0.3	213	213	n/a	0.1

Notes:

(1) Emission Factors are from AP-42. Particulates, 16 x (% ash in coal) lb/ST; SO_2, 38 x (% sulfur in coal) lb/ST; NO_X, 18.0 lb/ST; CO, 1.0 lb/ST; hydrocarbons, 0.3 lb/ST.

(2) 40 CFR Part 60, 6-11-79, Proposed New Source Performance Standards (NSPS) for utility boilers. Particulates, 0.03 lb/MBtu; SO_2 0.6 lb/MBtu or 90% reduction; NO_X, 0.5 lb/MBtu; CO and hydrocarbons are not regulated under NSPS.

Table 5.3-32

PRELIMINARY EMISSIONS ESTIMATES
FOR STEAM/RECYCLE GAS PREHEAT FIRED HEATERS

Basis: The total firing rate for the four preheat fired heaters is expected to be about 5% of the product SNG or about 13.5 GBtu/SD (1.35×10^4 MSCF/SD).(1) Nitrogen oxides (NO_x) are the only pollutants of concern. Other criteria pollutants should not be emitted in significant quantities since the fuel is pipeline-quality gas. About 300 lb NO_x/MSCF can be expected with conventional tangently fired boiler designs.(2) The resulting NO_x emissions estimate follows.

Pollutant	Emission(2) Factor lb/MSCF	Emission Factor lb/MBtu	Feed MBtu/SD	Emission Estimate ST/SD	Control Standard NSPS(3) lb/MBtu	Control Reduction Required to meet NSPS(3)	Expected Emissions ST/SD
NO_x	300	0.3	13,500	2.0	5.0	None	2.0

Notes:

(1) Assume 1 MBtu/1000 SCF.

(2) Emission factor from AP-42, 1974.

(3) 40 CFR Part 60, 6-11-79, proposed New Source Performance Standards for utility boilers.

Table 5.3-33

PRELIMINARY EMISSION ESTIMATES FOR FUGITIVE PARTICULATE MATTER

Processing Area	Estimated(1) Average Number of Transfer Points	Emission Factors(2)	Material Transferred ST/SD	Material Stored ST	Control(3) Reduction %	Estimated Fugitive Particulate Emissions ST/SD
Coal Receipt	8	0.0034 lb/ST-transfer point	18,000	-	75	< 0.1
Coal Storage	-	5.8 lb/ST-yr	-	40,000	90	0.4
Coal Preparation	8	0.0034 lb/ST-transfer point	18,000	-	75	< 0.1
Lime Receipts Preparation	6	0.0034 lb/ST-transfer point	1,000	-	75	negligible
Waste Solids	6	0.0034 lb/ST-transfer point	7,500	(4)	75	< 0.1
					Total Fugitive Particulate Matter	< 0.7 ST/SD

Notes:

(1) The number of transfer points is assumed based on an integrated terminalling/coal preparation area using conveyors.

(2) Blackwood, et al, federal contract 68-02-1974.

(3) Emissions can be reduced 75-90% using Best Available Control Technology including water sprays on coal storage piles and enclosures vented to baghouses at transfer points.

(4) Waste disposal is not considered to be onsite and is not included in the fugitive particulate estimate.

Table 5.3-34

PRELIMINARY EMISSIONS ESTIMATES
FOR THE SULFUR RECOVERY UNITS (SRU)

Basis:

- Only SO_2 is expected to be a major pollutant from this area. (Other criteria pollutants may be present in trace quantities but should have a negligible effect on overall plant emission rate.)
- 99% overall efficiency for H_2S to elemental sulfur conversion.(1)
- Remaining 1.0% H_2S and trace COS is emitted as SO_2.

Resulting Sulfur Balance(2):

$$324 \frac{LT}{SD} \text{ sulfur produced} = 356.4 \frac{ST}{SD} \text{ sulfur produced}$$

$$356.4 \frac{ST}{SD} \text{ recovered} \times \frac{100}{99} = 360.0 \frac{ST}{SD} \text{ S to SRU and}$$

$$3.6 \frac{ST}{SD} \text{ S to atm} = 7.2 \frac{ST}{SD} SO_2 \text{ to atm}$$

Notes:

(1) Achievable efficiency for multi-stage Claus plant with tail gas clean-up.

(2) CCG Predevelopment Program Final Report (FE-2369-24).

Fugitive Hydrocarbon Emissions

Fugitive hydrocarbon emissions can occur from flanges, valves, pump seals, and tank seals that are in non-methane hydrocarbon stream service. It is assumed that at a commerical CCG plant Best Available Control Technology will be employed for fugitive hydrocarbon control. This should reduce fugitive hydrocarbon emissions by 75% from uncontrolled fugitive emissions.

To complete a fugitive emissions estimate the number of valves, pumps, flanges and tanks should be known and the appropriate emission factors applied. At this time, estimating the number of these for a commercial CCG plant would be purely speculative. Further study should be conducted when the process design is more clearly defined.

Future Work

Future CCG development work should include estimating emissions from the coal/catalyst preoxidizer, the low pressure coal lockhopper vents, and the plant's fugitive emission sources, estimating noncriteria pollutant emissions, and updating the emissions inventory.

5.3.7 Dynamic Simulation of the CCG Reactor System

The objective of this program was to study the dynamic response, stability and control requirements for the gasifier reactor and associated recycle gas system.

The presence of both endothermic and exothermic reactions in the CCG gasification reactor makes determination of gasifier stability to temperature and composition upsets difficult. One cause of upsets to the gasifier could be operating problems in the recycle loop such as fouling of heat exchangers, pump failure, or recycle gas compressor failure. In addition, the dynamics of the methane recovery section are not fully understood.

Dynamic models of the CCG gasification reactor and recycle loop (Fig. 5.3-15) were developed to gain an understanding of CCG plant dynamics. These models were programmed in FORTRAN and were tested separately before linking them. After the models are linked, case studies of specific plant upsets can be run to determine stability and controllability of the plant.

The gasifier model consists of portions describing the reactor concentration profiles in the emulsion and bubble phases involved integration over the reactor length of material balance equations containing bulk flow, reaction, and interphase mass transfer terms. Correlations for diffusivity, viscosity, bubble diameter, minimum fluidization velocity, and bubble velocity are used to calculate mass transfer coefficients and the fraction

Figure 5.3-15

SYSTEM STUDY
FLOWPLAN FOR RECYCLE GAS LOOP

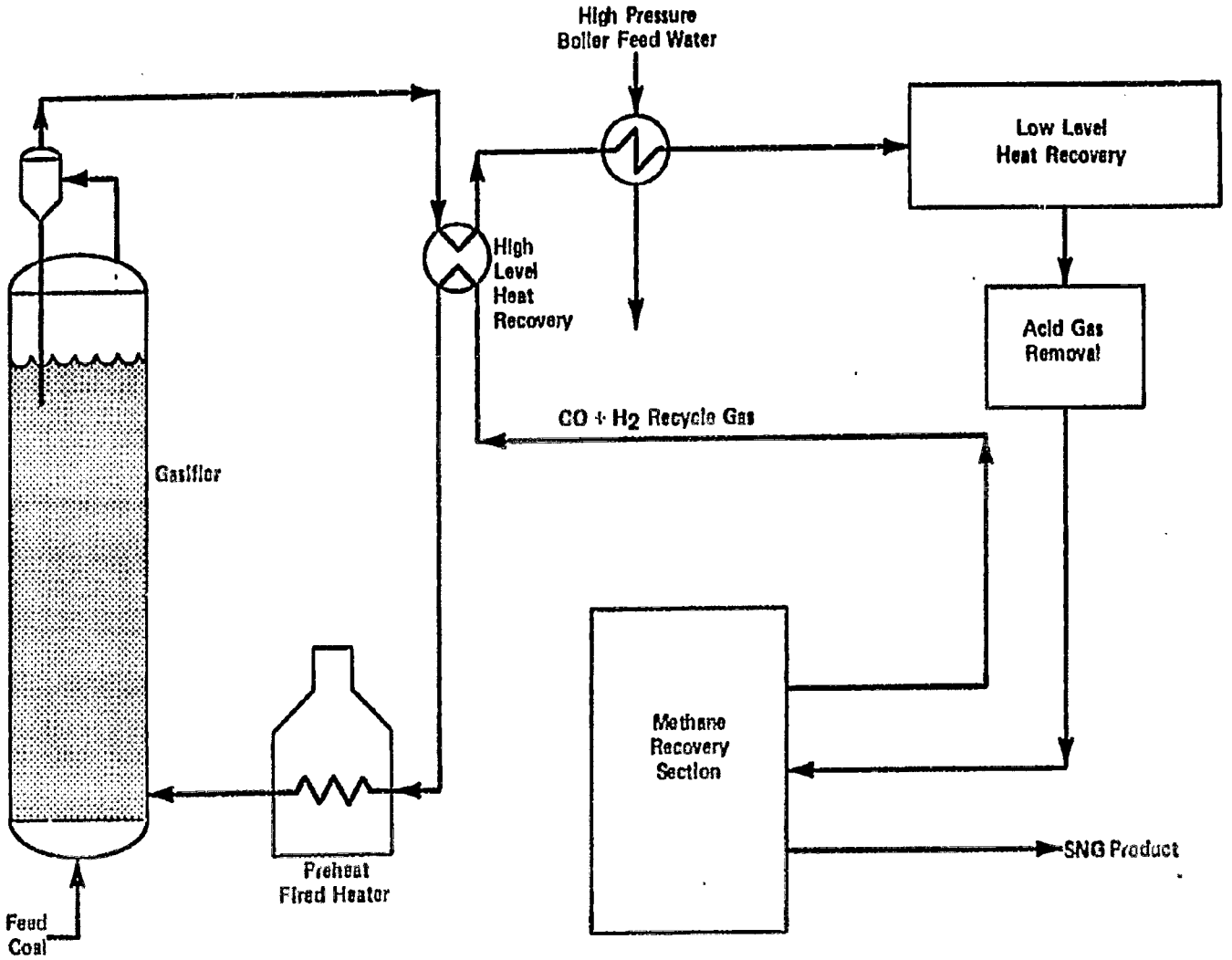

of gas in the bubble phase. Devolatilization of feed coal is calculated as a function of feed composition and hydrogen partial pressure and is assumed to occur instantaneously at the feed entry point.

Reaction rates are calculated from existing steady-state kinetic relationships. Methanation, gasification, and shift rates are calculated for the emulsion phase as is the shift reaction rate for the bubble phase. As the gas holdup in the reactor is much smaller than the solids holdup, the accumulation term in the gas phase material balance is ignored.

Dynamic solid material balance equations are used to calculate the concentration of char and fines leaving the reactor. Catalyst coal reactions are assumed to occur instantaneously before the feed enters the gasifier and the extent of each reaction is determined from the amount of the limiting species in the feed. The unreacted feed and catalyst reaction products comprise the solid feed to the reactor. Each component (carbon, hydrogen, oxygen, nitrogen, sulfur, ash, and six catalyst species) is followed using a dynamic material balance. The amounts of ash and organics lost in the gas phase and the solids level are also determined. An overall gasifier energy balance is used to compute the bed temperature. Existing correlations for the sensible and chemical enthalpy of organic, ash, mineral matter, moisture, and various catalyst compounds in the solids phase are employed. Correlations are also used for the enthalpies of the gas phase streams.

The kinetic, solids material balance, and overall enthalpy balance modules just described allow the calculation of the composition of all streams leaving the reactor, the reactor temperature, and the reactor level.

Figure 5.3-16 shows the relationships between the various modules which comprise the solids heat and material balances, and the kinetic model. Module A analyzes the various catalyst reactions and computes gases evolved and an adjusted solids composition. Differential equations describing the dynamic solids, heat, and material balances are solved in Module B to obtain the char and fines composition and the reactor temperature. In Module C, correlations are used to calculate the devolatilization of coal organics. Finally, Module D passes the gases liberated by catalyst reactions and devolatilization, the carbon content of the char, and the catalyst activity to the gasifier kinetic model which computes the reactor product gas composition.

The recycle loop model comprises high and low level heat recovery, acid gas removal, and methane recovery sections as well as the recycle gas preheat fired heater. An existing preheat fired heater model, modified to include two convection sections, is used to simulate the preheat fired heater. High level heat recovery is modeled using an existing heat exchanger routine for the two gas-gas exchangers and high pressure waste heat boiler. Low level heat recovery, including the ammonia scrubber, is assumed to work

Figure 5.3-16

SCHEMATIC DIAGRAM OF SOLIDS BALANCE IN GASIFIER

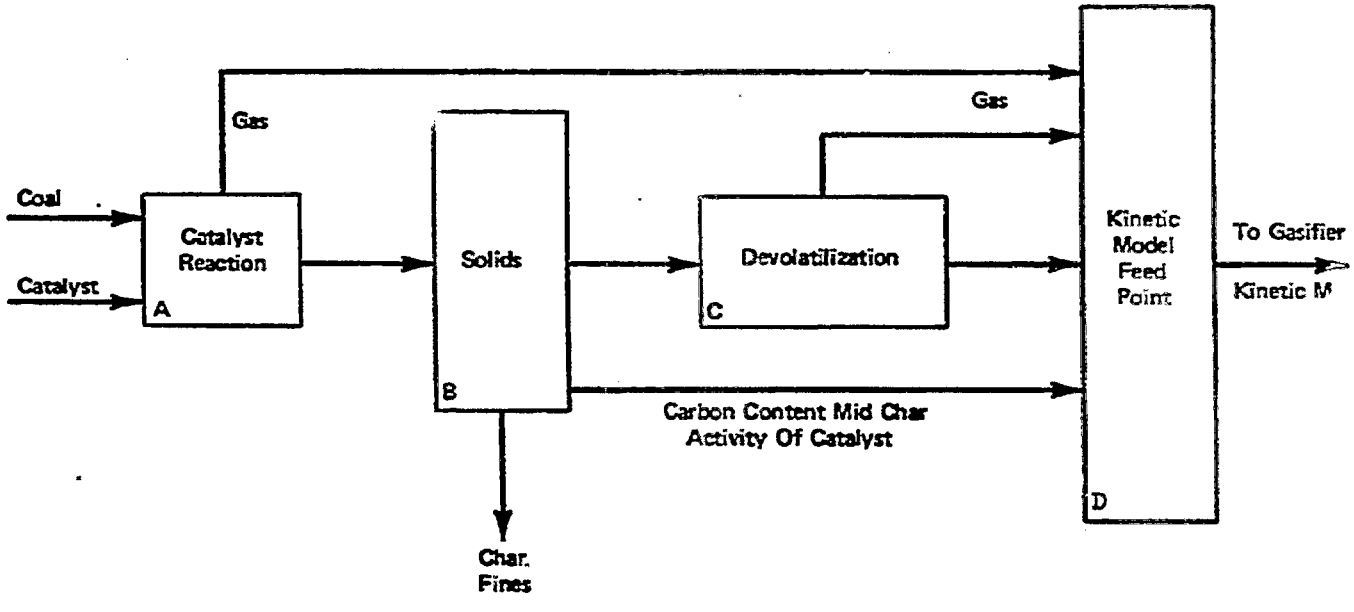

properly and is modeled very simply. The outlet temperature of this section is assumed to be the design value. Since the heavy glycol solvent acid gas removal system is proprietary, that section was also modeled very simply using assumed absorption functionalities based on solvent regenerator performance.

The majority of time was spent modeling the cryogenic methane recovery section. An existing tower model was modified to account for non-constant molal overflow in order to simulate the carbon monoxide (CO) stripper. A new heat exchanger model was developed to meet the more rigorous simulation requirements of the cold box. A large amount of testing indicated the lumped parameter heat exchanger model first developed was inadequate due to the presence of incorrect inverse responses to temperature upsets. The improved model developed to simulate the cold box is a distributed parameter model, capable of handling up to five multi-component, two-phase streams. The stripper reboiler is also modeled using the new exchanger model in conjunction with a dynamic material balance on the boilup stream.

Vapor-liquid equilibrium calculations are performed by a generalized flash routine developed for this simulation. Equilibrium constants (K values) were obtained and correlated as functions of temperature and pressure by the Exxon Data Library, an extensive proprietary thermodynamics package. The above approach was used instead of directly linking the Exxon Data Library with the recycle loop model because the latter approach was too costly, required too much computer time, and the correlations are accurate enough.

Preliminary results were obtained for the recycle loop model. The following results are preliminary because the recycle loop model was run independently of the gasifier model, which is essentially completed except for the solids material balance.

Figures 5.3-17 through 5.3-21 show three variables characteristic of the methane recovery section plotted as functions of time. Figure 5.3-22 is a schematic diagram of the methane recovery section. The three variables plotted in Figures 5.3-17 through 5.3-21 are the feed stream temperature at points A and B, and the percent methane (CH_4) in the product stream at point C in Figure 5.3-22. These three variables were chosen because the stream at point C is the CCG plant product, the temperatures at points A and B directly influence product purity, and the methane recovery section exhibits the most interesting dynamics in the recycle loop.

Figure 5.3-17 is the base case computer run which shows the methane recovery section going to steady state from the design point initialization. This run is included to show that the model's steady state is not exactly equivalent to the design steady state. All inputs to the model were held constant in the run that generated the data for Figure 5.3-17. When the recycle loop and gasifier models are run together, the most frequent disturbances introduced into the recycle loop model will be fluctuations in the gasifier model's output. Therefore, three of the computer runs chosen for

FIGURE 5.3-17

BASE CASE RUN METHANE RECOVERY SECTION

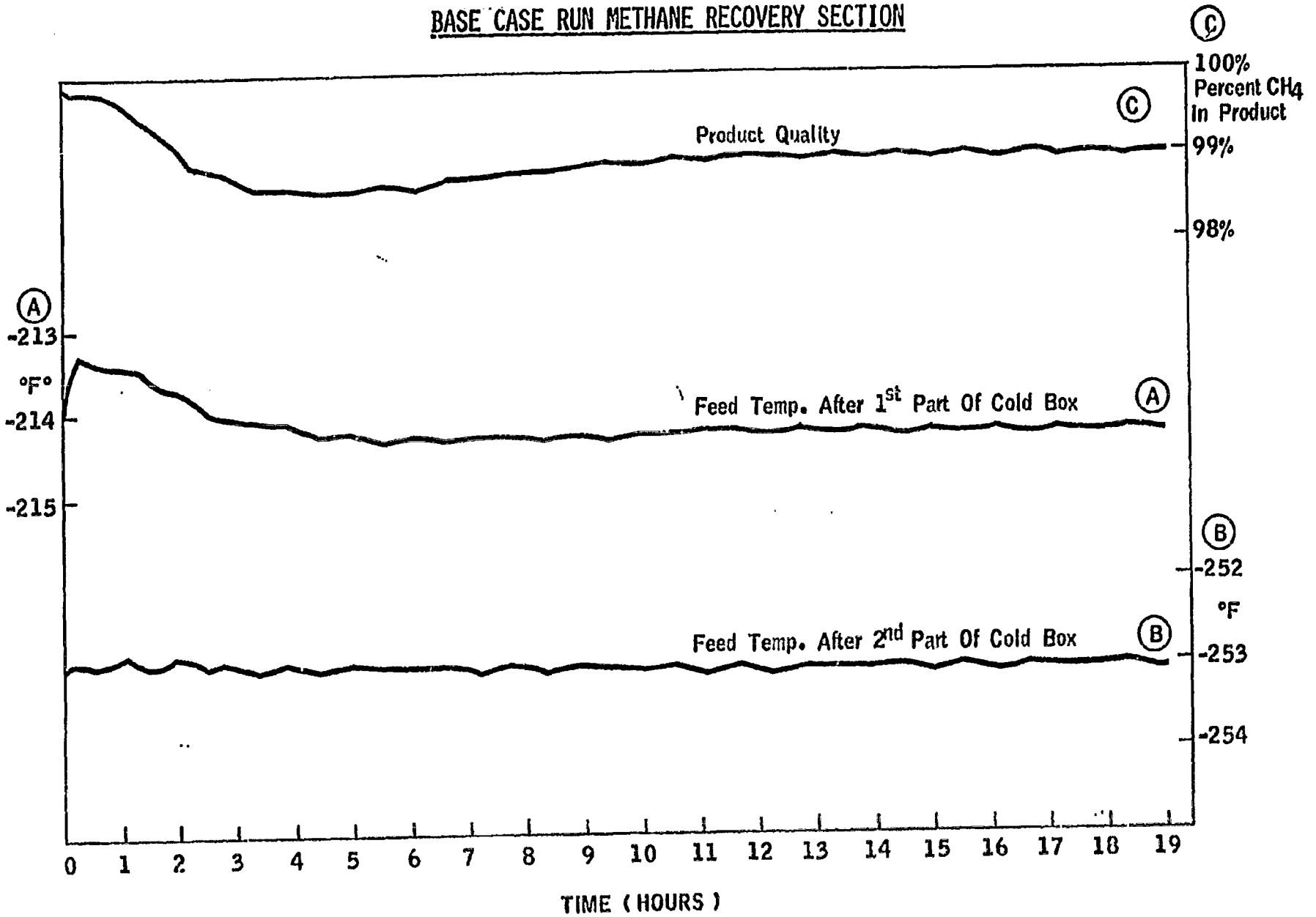

FIGURE 5.3-18

METHANE RECOVERY FEED TEMP. CHANGE (10° - 50°F)
METHANE RECOVERY SECTION RESPONSE

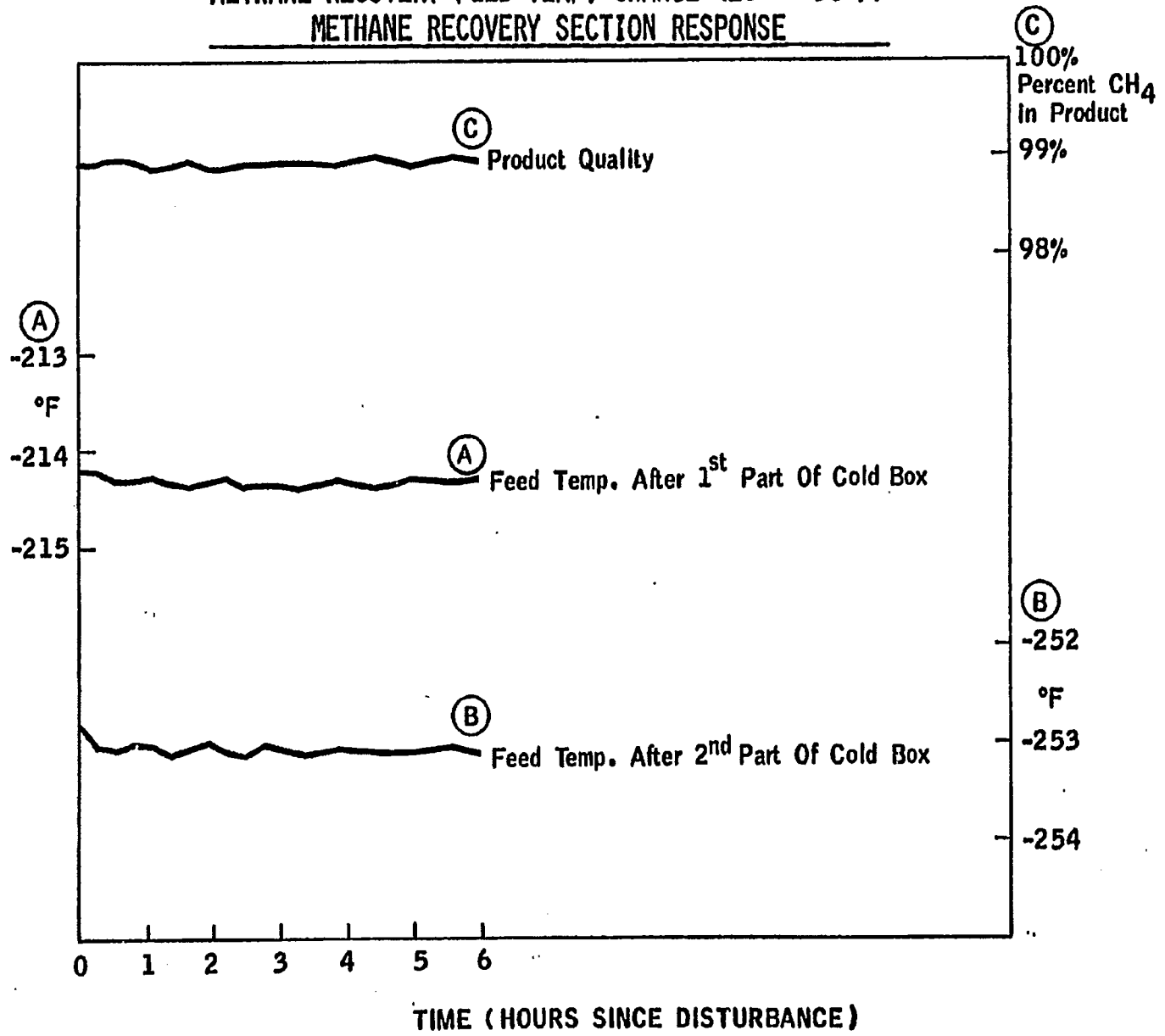

FIGURE 5.3-19

REACTOR EFFLUENT RATE CHANGE (39768 - 45000 $\frac{\text{LB. - MOLES}}{\text{HR}}$)
METHANE RECOVERY SECTION RESPONSE

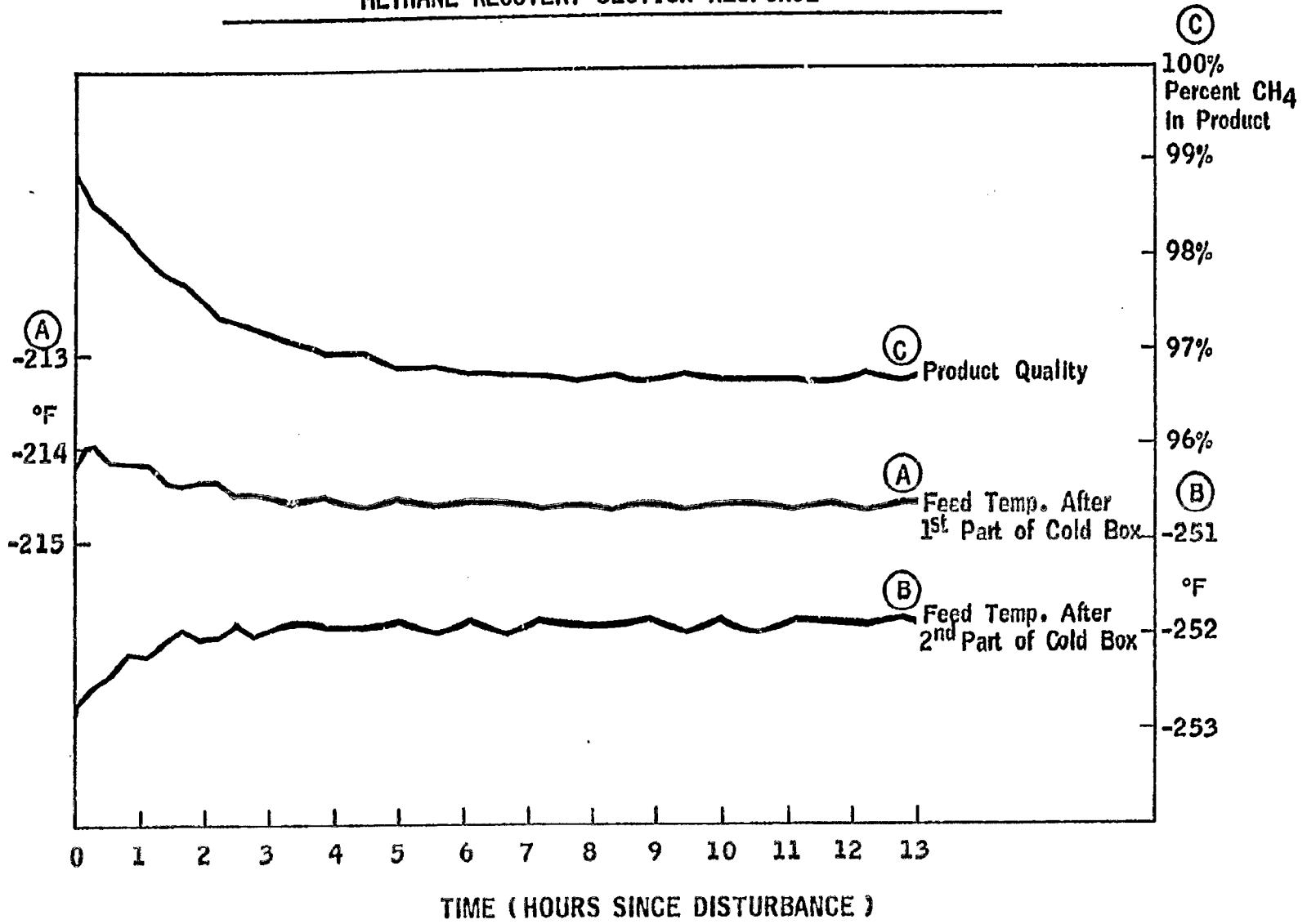

FIGURE 5.5-20

REACTOR EFFLUENT COMPOSITION CHANGE CO (6% - 4%)
METHANE RECOVERY SECTION RESPONSE

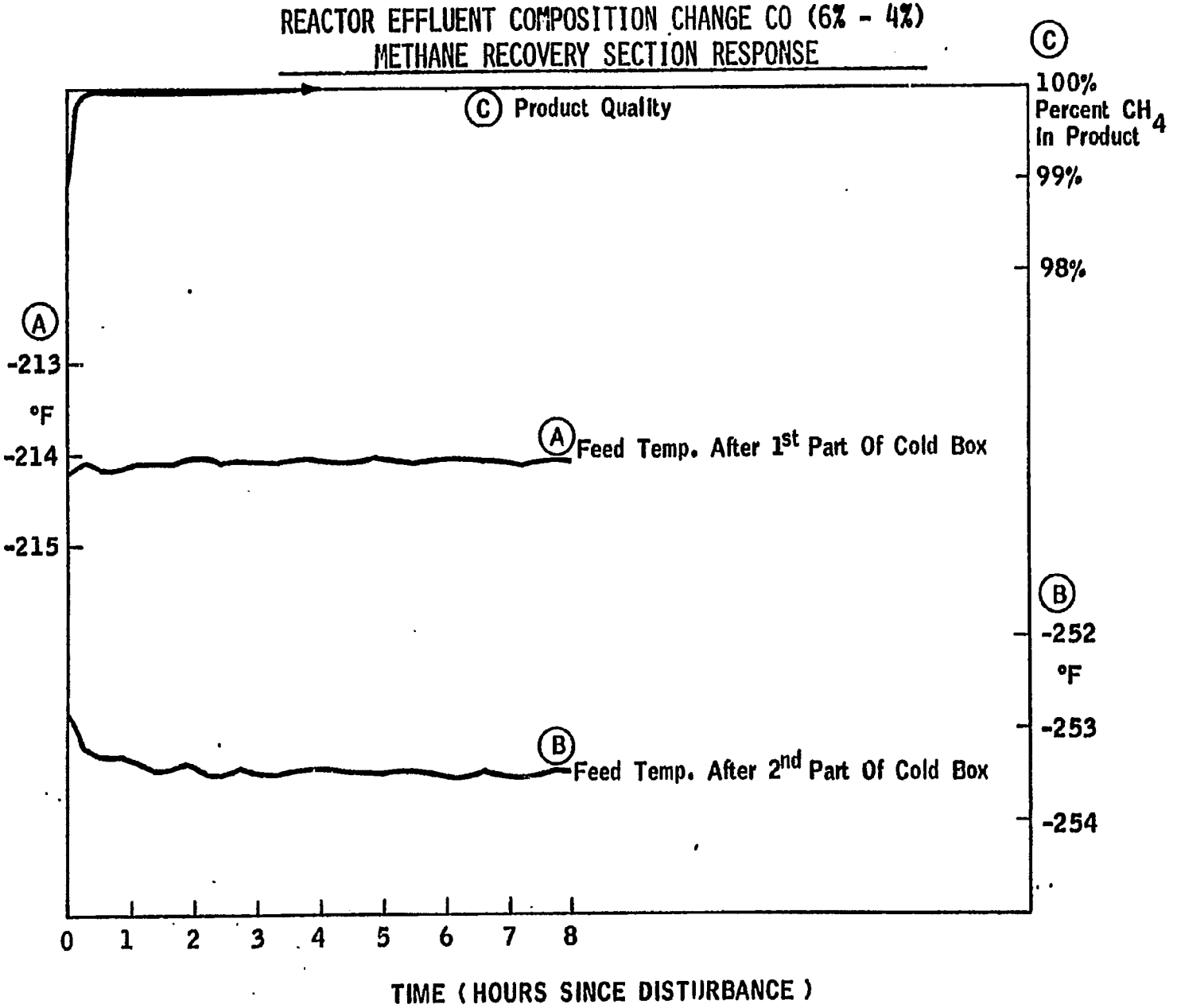

FIGURE 5.3-21

REACTOR EFFLUENT COMPOSITION CHANGE CO (6% - 8%)
METHANE RECOVERY SECTION RESPONSE

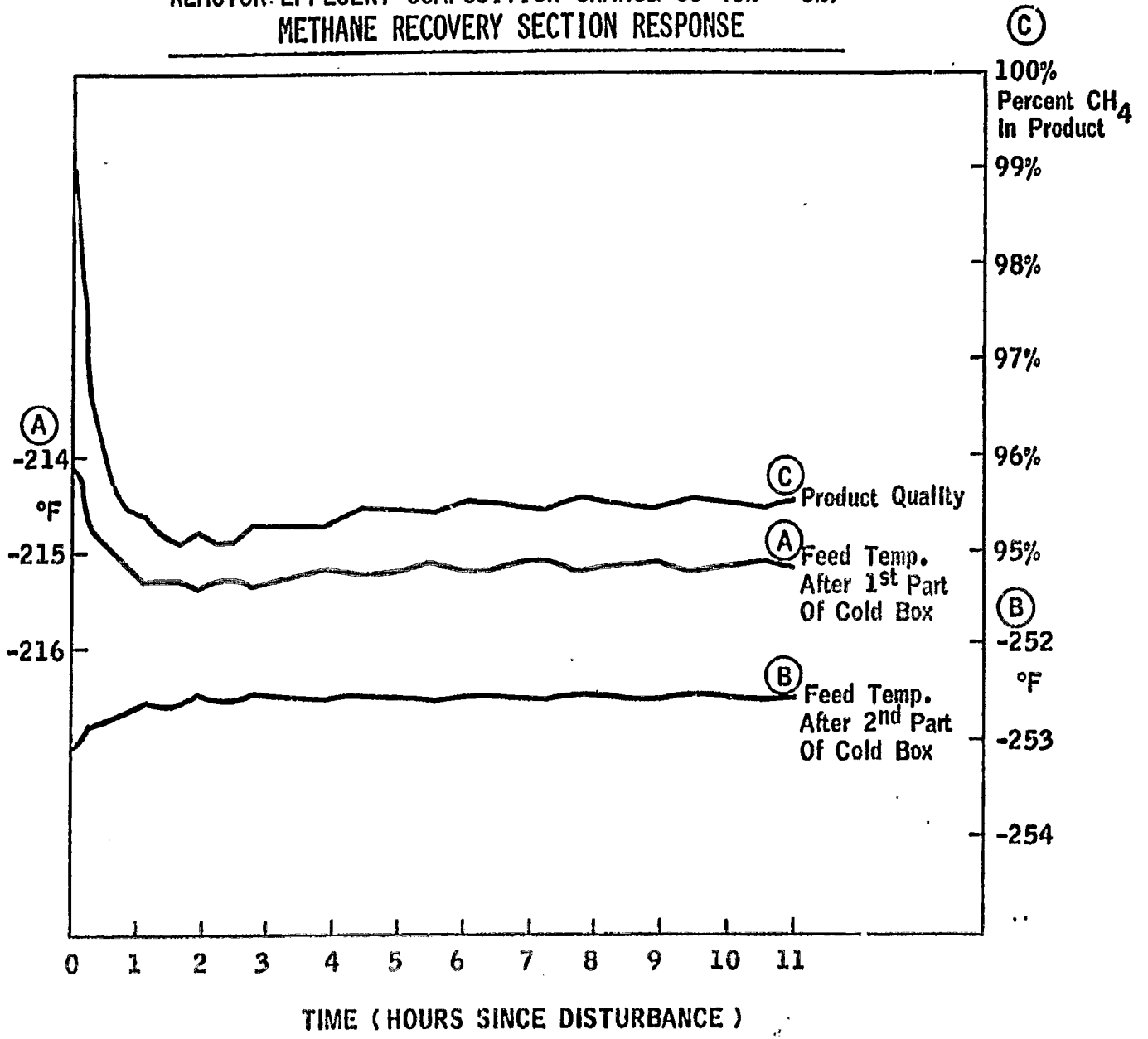

FIGURE 5.3-22

METHANE RECOVERY VIA LOW PRESSURE CO STRIPPING

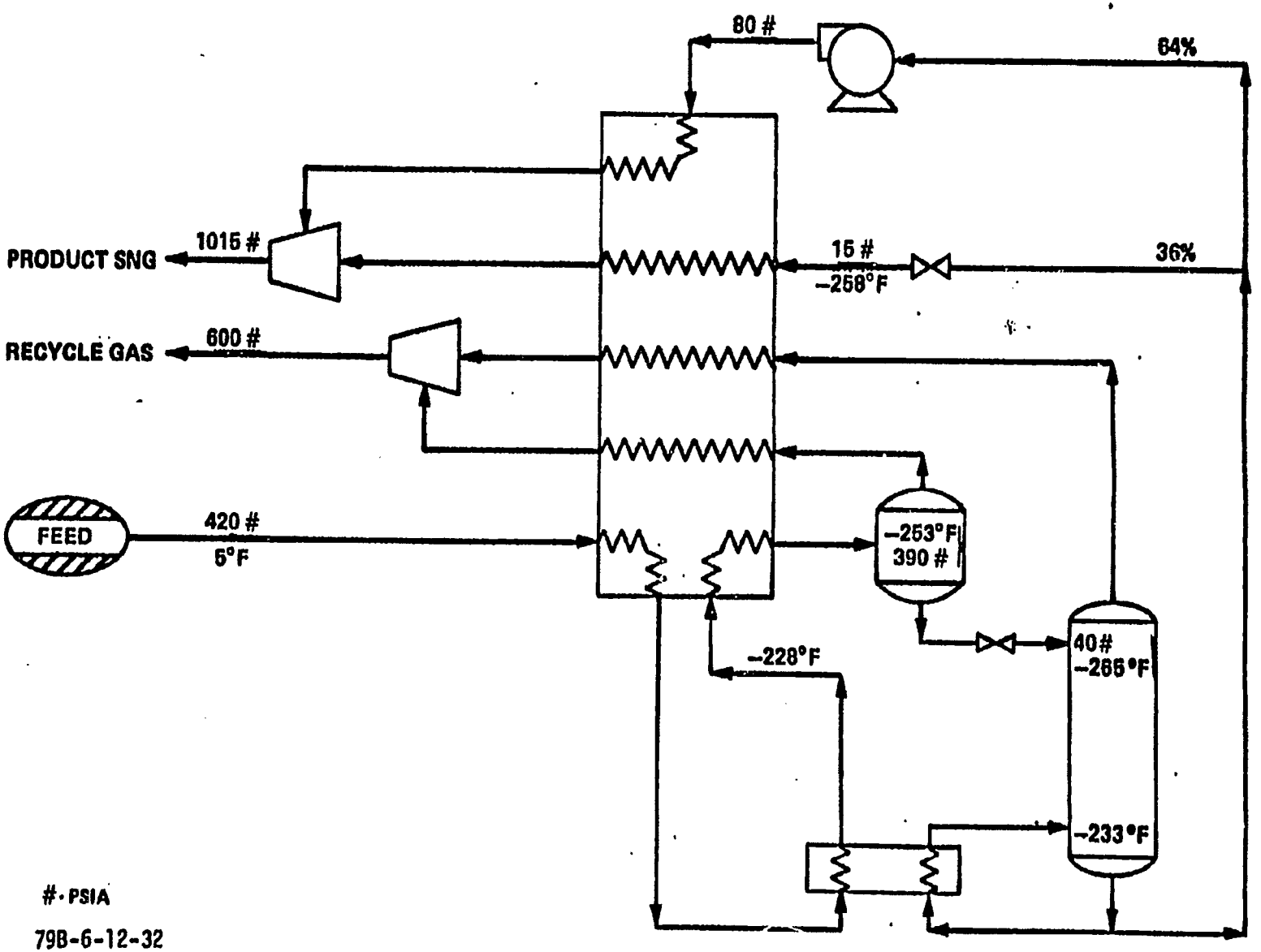

#·PSIA

79B-6-12-32

presentation show the results of disturbances in the gasifier effluent stream introduced into the recycle loop model. Figures 5.3-18 through 5.3-21 show results generated in response to the following disturbances respectively: 1) feed stream temperature change to the methane recovery section from 10° to 50°F, 2) gasifier effluent flow rate change from 39,768 to 45,000 lb. moles/hr., 3) gasifier effluent carbon monoxide (CO) composition change from 6% to 4%, and 4) gasifier effluent CO composition change from 6% to 8%. Disturbances are introduced into the model after steady state is reached, 16 hours and 40 minutes after initialization. The point at which disturbances are introduced is taken as zero time in Figures 5.3-18 through 5.3-21.

Virtually no change in the recorded variables is seen in Figure 5.3-18, the feed temperature change. Product quality remains at 99% CH_4 and both recorded temperatures do not change.

The gasifier effluent flow rate change resulted in a change in feed rate to the methane recovery section from 43,532 to 49,054 lb.-moles/hr. Figure 5.3-19 shows that in response product quality decreased from 99% to about 96.5% CH_4.

A CO composition change from 6% to 4% in the gasifier effluent stream leads to a CO composition change from 12% to 8.5% in the methane recovery section feed stream. Figure 5.3-20 shows that product quality quickly approached 100% CH_4.

A CO composition change in the gasifier effluent from 6% to 8% leads to a CO composition change in the methane recovery section feed from 12% to 15.3%. Figure 5.3-21 shows that product quality decreased rapidly from 99% to 95% CH_4 and leveled out at about 95.5% CH_4.

Figure 5.3-18 demonstrates that the cold box in the methane recovery section is substantially oversized to absorb temperature disturbances. The recycle loop is stable to temperature, flow rate and composition upsets. Recycle loop stability depends on the inclusion of "base level" controllers to maintain constant pressures and levels.

In the results shown and in other computer runs not presented, a strong dependency exists of product quality at point C on the temperatures at points A and B in Figure 5.3-22. This dependence indicates that a control strategy to maintain product quality should include controlling the temperatures at points A and B. Manipulating the pressures of the SNG streams flowing into the cold box should make it possible to control the temperatures at points A and B in Figure 5.3-22.

5.3.8 Catalytic Gasifier Solids Balance Model

The objective of this program was to adapt DYNAMOD, a proprietary solids balance computer model developed and validated for other Exxon fluid-solids processes, to simulate the steady-state loss rates and particle size

distributions both in the catalytic gasifier and in all streams leaving the vessel. These simulations are needed to provide a base for more definitive process designs through improved specifications of fines recovery and catalyst recovery systems and reliable assessments of design and process limitations imposed by solids balance and fines losses.

A single species gasifier solids balance model was developed for a first pass assessment of the effects of variables such as solids attrition, particle density and gasification on equilibrium bed size distributions and fines losses. Validation of the model was carried out using preliminary data for the Process Development Unit (PDU). A good match of predicted and measured PDU gasifier distributions and fines losses for the first two yield periods was obtained by adjusting the char attrition rate constants and using a tentative entrainment correlation for low superficial velocities. Simulations of PDU operations with cyclone underflow return predicted finer bed size distributions and lower bed densities than with no cyclone return as the PDU currently operates.

A two-solids species model for distinguishing between char and high conversion "ash" particles was then developed.

Initially, a uniform char particle density was assumed in adapting DYNAMOD to the CCG process. Fluidized bed parameters for the gasifier and process characteristics were first reviewed to define modifications required for simulating both pilot plant and commercial unit operations. Data from Fluid Bed Gasifier (FBG) operations during the predevelopment research phase were used to develop a solids attrition model and assess the effects of char/ash density differences on their relative entrainment rates.

The single species DYNAMOD model was used to simulate the CCG Commercial Study Design case. For this case, the char attrition rate was assumed to be five times that of coke produced from petroleum. Gasification was assumed to proceed according to the shrinking core model and a conventional two-stage cyclone design was considered for the gasifier. Predicted losses from the gasifier were eight times lower than estimated in the Study Design. In order to match the Study Design losses, the equilibrium bed size distribution would have to be much finer than assumed in the Study Design. Predicted losses remained about the same when the more realistic reaction model of homogeneous reaction throughout the char was employed.

The data base used to validate DYNAMOD for other Exxon fluid solids processes falls outside the operating superficial velocities (< 0.6 ft/sec) and pressures (500 psia) of the PDU. Limited entrainment data at lower than 1 ft/sec superficial velocities and ambient conditions for glass beads and cat cracking catalysts, available from the Particulate Solids Research Institute (PSRI) were used to develop a tentative correlation for low velocity entrainment. DYNAMOD predictions with the revised entrainment correlation matched measured PDU fines losses by assuming a char density of 42 lb/ft^3, equal to the density of the FBG char, and adjusting the attrition rate constants.

The PDU operations corresponding to yield period runs one and two were simulated with and without a single stage cyclone for assessing the affect of cyclone underflow return to the gasifier on equilibrium bed size distributions. In these and subsequent runs the gasifier cyclone did not return fines to the bed due to dipleg plugging. These simulations are shown in Figure 5.3-23. The measured surface/volume average particle size for the Gasifier Mid Char was about 90 μm vs. 80 μm predicted with no cyclone underflow return. Including a single cyclone in the simulation reduced the average size to 55 μm, and resulted in a lower bed density (about 90% of the gasifier density without a cyclone).

The basis for a two species model which solid balances both char and high conversion ash components was developed. The aim was to account for the separate char and ash attrition in the gasifier bed and cyclones and to consider particle residence times for different size particles in calculating char to ash conversion. An efficient integration algorithm based on the GEAR method was used to solve the large set of simultaneous differential equations representing transient material balances for size ranges of each species.

Limiting test cases were used to check consistency in results between the single and two species models. The results of these cases showed the bed ash concentration to be sensitive to the specification of gasification level at which ash is formed and to the relative char/ash densities and attritabilities. Validation of the two species model was performed using early PDU data, assumed char and ash attrition rates, and particle densities from the FBG operations.

FIGURE 5.3-23

DYNAMOD PREDICTIONS OF PDU GASIFIER PARTICLE DISTRIBUTIONS